

UNIVERSITY OF CALGARY

Sand Control in Steam Assisted Gravity Drainage (SAGD) Wellbores and Process of
Slotted Liner Design and Manufacture

by

Brent Fermaniuk

A THESIS

SUBMITTED TO THE FACULTY OF GRADUATE STUDIES
IN PARTIAL FULFILMENT OF THE REQUIREMENTS FOR THE
DEGREE OF MASTER OF ENGINEERING

DEPARTMENT OF PETROLEUM & CHEMICAL ENGINEERING
CALGARY, ALBERTA

May 2013

© Brent Fermaniuk 2013

Abstract

Steam Assisted Gravity Drainage (SAGD) is a thermal recovery technology used to produce heavy oil and high viscosity bitumen from Alberta oil sands. The oil sands of Alberta are unconsolidated sands which require sand control within the horizontal wellbores to reduce the erosive power of the sand and plugging of sand control screens. Slotted liners have been extensively used in Alberta's SAGD wells to provide sand control. Slotted liner slot width specifications can be effectively designed based on the particle size distribution of the in-situ reservoir sands and coupled reservoir parameters. Modified laser particle size analysis can simulate a sieve analysis to determine slot width sand control requirements and provide a means to estimate the particle size for stable arching of sand around a slot during production. The slot must be designed to allow free flow of fines and clays through the slot and near well pore space without plugging. Based on the findings of research documented in this thesis, the minimum slot width for the majority of slotted liners used for sand control in clastic heavy oil and bitumen formations is 0.012" (~300 μm). The results also reveal that a seamed slot, which provides a "keystone" profile, provides anti-plugging characteristics. Slotted liner manufacturing is a complex process of metal-to-metal slotting of an interrupted cut. Pipe grades, process of manufacture, chemical composition and physical properties can dramatically affect the machinability tool-life and sand control. The results of the research also show that machinability of the pipe is largely controlled by the combination of optimal microstructure (manufacture) and chemical composition (specifically sulfur content). Sulphur content has been widely known to improve machinability but too high

of a sulphur content can have dramatic effects on the performance of a slotted liner when H₂S is present. Tool-life tests proved that the carbon content of the pipe cannot be used as a predictor of the pipe's machinability. Taylor's tool-life equation can be successfully applied to blade slotting and a metric developed here, called the Relative Material Machinability Index, has can be used to relate slot manufacturing performance of differing grades of pipe, microstructure, and chemical composition.

Acknowledgements

I would like to thank God for my family and for all the blessings he has provided. I would like send my deepest thanks to my wife Tina and my children Paige, Brooke and Cole for their overwhelming love, support and inspiration.

I would like to extend a big thanks and appreciation to Regent Energy Group Ltd. for providing continued support and encouragement, and for providing me with the tools and help in completing my Master's thesis and program.

I would also like to extend my thanks and appreciation to my supervisor Dr. Ian D. Gates for his continued support, patience and knowledge.

Table of Contents

Approval Page.....	ii
Abstract.....	1
Acknowledgements.....	3
Table of Contents.....	4
List of Tables.....	6
List of Figures.....	7
List of Symbols, Abbreviations and Nomenclature.....	12
CHAPTER 1: INTRODUCTION.....	15
1.1 Horizontal Well Technology.....	20
1.2 Reservoir Characterization.....	21
1.3 Steam-Assisted Gravity Drainage.....	21
1.4 Problem Statement.....	24
1.5 Organization of Thesis.....	24
CHAPTER 2: LITERATURE REVIEW – SAND CONTROL TYPES.....	26
2.1 Barefoot Completion.....	26
2.2 Gravel Pack.....	27
2.3 Stand Alone Screens – Wire Wrap.....	29
2.4 Slotted Liners.....	31
CHAPTER 3: CHARACTERISTICS OF RESERVOIRS UNDERGOING SAGD.....	34
3.1 Wettability.....	34
3.2 Permeability.....	38
3.3 Capillary Pressure.....	39
3.4 Plugging.....	40
3.5 Superficial and Interstitial Velocity.....	41
3.6 Unconfined Compressive Strength (UCS).....	43
3.7 Mohr-Coulomb Circle.....	45
3.8 Flow Rate.....	47
3.9 Sand Screen Open Area.....	48
3.10 Clay Content.....	49
3.11 Problematic Clay Content.....	53
CHAPTER 4: SAND CONTROL ANALYSIS.....	55
4.1 Introduction.....	55
4.2 Procedure.....	56
4.3 Particle Size Distributions.....	58
4.4 Model Development.....	61
4.5 Pore Space Calculation.....	64
4.6 In-situ Particle Arching.....	65
4.7 Near Wellbore Flow Velocity and Slot Density Calculation.....	68

4.8 Results and Discussion	69
4.9 Conclusions.....	77
CHAPTER 5: SLOTTED LINER MANUFACTURING	79
5.1 Introduction.....	79
5.1.1 Laser Slotting.....	79
5.1.2 Electric Discharge Machining.....	80
5.1.3 Water-jet Slotting.....	81
5.1.4 Metal-metal Slotting / Slot Milling.....	82
5.1.5 Slotted Liner Geometry and Simple Slot Mathematics	84
5.1.6 Straight and Seamed Slot	86
5.1.7 Slot Surface Finish.....	89
5.1.8 Slotting Blade Nomenclature.....	90
5.2 Experimental Apparatus.....	92
5.3 Results.....	93
5.3.1 Slotting Blades Up Milling and Down Milling.....	93
5.3.2 Cutting Geometry and Shear Cutting Angle.....	96
5.3.3 Cutting Process - Chips and Form	100
5.3.4 Built-up Edge	103
5.3.5 Blade Wear.....	106
5.3.6 Blade Material and Coatings.....	113
5.4 Conclusions.....	121
CHAPTER 6: TOOL-LIFE AND MACHINABILITY	125
6.1 Introduction.....	125
6.2 Experimental Apparatus.....	127
6.3 Results.....	128
6.3.1 Taylor's Tool-life Equation	128
6.3.2 Coolant/Cutting Fluid	136
6.3.3 Machinability	147
6.3.4 Relative Material Machinability Index	151
6.3.5 OTCG Pipe Process and Manufacture	156
6.3.6 OTCG Hardness.....	158
6.3.7 OTCG Chemistry and Carbon Content.....	160
6.3.8 OTCG Microstructure and Chemical Composition	162
6.3.9 New OTCG Chemical Tolerance.....	175
6.4 Discussion.....	182
6.5 Conclusions.....	186
CHAPTER 7: CONCLUSIONS AND RECOMMENDATIONS.....	189
BIBLIOGRAPHY.....	195

List of Tables

Table 1 - Gravel Pack Sizing according to sieve sizes and the frequency distribution of each size of sand (Cameuseis 2011).	29
Table 2 - Experimental results - sieve/screen size and category for retained fraction and cumulative fraction with accordance to the particle size.	58
Table 3 - Experimental results - particle size analysis table of results of the five samples or depths for the oil sands reservoir.	61
Table 4 - The grade scale that has traditionally been used to classify sediments, called the Wentworth scale (Wentworth 1922).	63
Table 5 - Slot width modeling results.	72
Table 7 - Blade coatings and representative properties enhancement and their indication of best-to-worst tool-life response (How Metals Are Cut 1976).	114
Table 8 - Experimental results - cutting fluid and coolant testing.	138
Table 9 - Experimental results - Relative Material Machinability Index.	154
Table 10 - Experimental results - Relative Machinability Ranking by Carbon Equivalent - K-55.	161
Table 11 - Experimental results - Relative Machinability ranking by Carbon Equivalent - L-80.	162
Table 12 - Experimental results - RMMI by pipe grade, carbon content and hardness.	166
Table 13 - Experimental results - blade, pipe, grade and machinability ranking. Note: there is insufficient data for machinability ranking based on blade widths for any other blades tested.	169
Table 14 - New K-55 pipe chemical composition.	176

List of Figures

Figure 1 - Alberta oil sands deposits showing significant areal extent and net pay thickness (ERCB 2011).....	16
Figure 2 - Grosmont bitumen-bearing carbonate platform under laying the Wabasca and Peace River oil sands and further, which provides another challenging resource source for exploitation (ERCB 2008).....	17
Figure 3 - Conventional versus unconventional oil geographic distribution of hydrocarbon resources worldwide.	17
Figure 4 - Conventional and unconventional world oil resources in accordance to the top oil and gas production countries (ERCB 2009).	19
Figure 5 - SAGD well pair schematic showing continuous steam injection in the upper well and continuous production of heated bitumen from the lower producer well.	23
Figure 6 - Direct wrap - wire wrap screen showing the longitudinal ribs which provide the support for the wire which is wrapped around the perforated base pipe (Halliburton 2004, used with permission).	31
Figure 7 - Slotted liner configuration depicting the staggered offset pattern from column to column, the slot length differences from the outside to inside of the pipe due to the arc of the slotting blade and the small slot width required for sand control (Regent Energy Group Ltd. 2006).	32
Figure 8 - Mobility of fines due to mobility of the wetting phase (Bennion 2002, used with permission).....	36
Figure 9 - Non-plugged seamed slot under simulated reservoir core flowing conditions in the laboratory setting (HYCAL/Weatherford Labs 2004, used with permission).....	37
Figure 10 - Plugged straight slot under similar reservoir core with similar reservoir simulated flowing conditions in the laboratory setting (HYCAL/Weatherford Labs 2003, used with permission).	37
Figure 11 - Plugged slot due to clays present in the reservoir core becoming mobile (HYCAL/Weatherford Labs 2003, used with permission).	38
Figure 12 - Uniaxial compressive stress-strain curve (Fairhurst et. al 1999).	44

Figure 13 - Rock strength envelope - Mohr-Coulomb failure (Core Labs 2000, used with permission).....	45
Figure 14 - Flow convergence effects due to slot density (Kaiser et al. 2000).....	49
Figure 15 - Clay deflocculation due to anionic charge of clay particles and the unstable valent bonding of clays which are easily affected by salinity and pH (Bennion 2002, used with permission).	51
Figure 16 - Kaolinite clay (vermicular) under 1500x magnification showing the booklet stacked configuration, white bar is 10 μ m long (Bennion 2009, used with permission).....	52
Figure 17 - Smectite Clays (swelling) under 2000x magnification, white bar is 10 m long (Bennion 2009, used with permission).	53
Figure 18 - Series of stacked sieves with progressively smaller sieve sizes below each stacked sieve allowing for the smaller particles to fall through to their respective sieve screen size-to-particle size while the system is being agitated (Introduction to Sieve Analysis University of Memphis 2008).	57
Figure 19 - Experimental results - particle size distribution graph for Depth 1 for the oil sands reservoir.	60
Figure 20 - Experimental results - cumulative particle size distributions of samples obtained at five depths for the oil sands reservoir.	60
Figure 21 - Arched in-situ particles from actual core flow tested under simulated reservoir conditions, 50 μ m scale (HYCAL/Weatherford Labs 2003, used with permission).....	67
Figure 22 - Example of slot width modeling program displaying the analyzed sieve results with optimal slot width specifications and zones of shales.	77
Figure 23 - Laser cut slots with intermittent slots created, heat affected zones and low quality slots (Roscoe moss Company 2006).	80
Figure 24 - Blade slotting configuration showing the 6-inch on center slotting and depicting the staggered offset per column and an uncut column between slots so as to provide axial pipe strength (Regent Energy Group Ltd. 2010).	85
Figure 25 - A typical straight slot profile of a blade created slot (Regent Energy Group Ltd. 2003).	88
Figure 26 - A typical seamed slot profile showing the differential slot widths from O.D. to I.D. with the larger aperture opening on the I.D. of the pipe (base slot) (Regent Energy Group Ltd. 2003).	88

Figure 27 - Slotting blade nomenclature, geometry and cutter surface (www.steelcuttingtoolspeedsandfeeds.com 2010).....	91
Figure 28 - Slitting saw blade nomenclature, geometry and helix angle for chip formation relief (Mechlook 2010).....	91
Figure 29 - Schematics of down milling and up milling, respectively, depicting the milling orientation and table feed direction, which depict that down milling starts the cut with a high tooth load (Fundamentals of Machining and Machine Tools 2005).	95
Figure 30 - Experimental results - up milling and down milling laboratory test torque results on a single material and under similar machining conditions.	95
Figure 31 - The primary shear cutting angle gives rise to the chips thickness and the secondary shear cutting zone generates heat into the chip and the tool's tooth during the cutting process.	97
Figure 32 - Shear cutting angles and chip form from an actual cut slot.	97
Figure 33 - Cutting nomenclature showing the relief angle, blade tooth, rake angle and chip formation.	98
Figure 34 - Cutting force and impact zone causing tooth breakage due to impact forces.	98
Figure 35 - Triangular and curvilinear tooth formed blades with DIN standardization quality configuration. DIN stands for Deutsches Institut fur Normung, meaning German Institute for Standardization.	100
Figure 36 - Experimental results - chip form and thickness of an actual slot created with a blade.	101
Figure 37 - Illustration of built-up edge of a portion of the primary shear cutting zone with overheated work piece material, which becomes "welded" onto the rake face of the tooth during the slotting process.	104
Figure 38 - Experimental results - BUE depiction theoretical drawing and actual picture of a chip welded to the rake face of a tooth during the cutting process.....	105
Figure 39 - Experimental results - BUE on the rake face of a blade during the slotting process.....	105
Figure 40 - Experimental results - BUE and flank welding of work piece material to the flanks of the blade from overheating in the cutting zone and flank zones of the blade slotting process.	105

Figure 41 - Experimental results - slotting blade flank wear.....	107
Figure 42 - Experimental results - slotting blade crater wear caused by heat and vibration during the slotting process.....	107
Figure 43 - Experimental results - slotting blade notch wear shown on the flank of the blade due to excess heat generated during the slotting process and due to impact forces.....	108
Figure 44 - Experimental results - slotting blade tooth showing rounded wear on the tip of the blades tooth also called nose radius wear.....	108
Figure 45 - Experimental results - cutting speed vs. tool wear rate and the relationship of the summation of both types of wear with the point of optimum speed-to-wear rate combination.....	109
Figure 46 - Experimental results - tool-life and blade matrix material and/or coating material and their respective blade material response recorded as tool-life increase.	118
Figure 47– Experimental results - actual tool-life graph showing the break-in region, the steady-state region and the inflection point for the unstable region or failure region of the slotting process.	127
Figure 48 – Taylor’s (1937) tool-life equation presented on a log-log scale of tool-life.	129
Figure 49 - Experimental results - calculated Taylor’s tool-life equation with revolutions per minute and tool-life response slotting a specific pipe material.....	133
Figure 50 – Experimental results - revolutions per minute versus tool-life response for various pipe grade materials, slotting under the same parameters and conditions.	134
Figure 51 – Illustration showing the theoretical fluid, tooth and chip optimal interface interaction where the cutting fluid is optimally placed between the slotting blades tooth performing the cut and the pipe material being cut which forms the chip and helps reduce friction and particularly heat generation.	141
Figure 52 – Experimental results - water-based coolant test and tool-life response.	144
Figure 53 – Experimental results - water-based coolant test and tool-life testing results with similar pipe grade and slotting parameters.....	145
Figure 54 – Experimental results - coolant concentration tool-life tests showing that a higher additive concentration performs better than a lower additive, giving rise to the notion that the slotting process requires lubricant more than heat extraction and this can be due to the fact that the intermittent slotting process has a difficult	

time allowing for optimal displacement of coolant between the blade tooth and the work piece or pipe.....	145
Figure 55 – Experimental results - coolant concentration tool-life tests with one pipe material grade cut.....	146
Figure 56 – The ease of material grade/pipe machinability and the pipe’s hardness and ductility (Machinability of OTCG, 1998).	149
Figure 57 - Experimental results - relative machinability index graph.	152
Figure 58 – Experimental results - RMMI and pipe material response with torque rating during the slotting process.....	153
Figure 59 – Experimental results - torque graph of an individual slot and the distance into the slot creation on a pipe showing the point the blade has broken through the pipe wall thickness as the torque requirement to complete the slot is reduced.	154
Figure 60 – Experimental results - maximum torque required per pipe material grade.	155
Figure 61 – Experimental results - relative machinability index according to torque or current draw during the slotting process.	155
Figure 62 – A graphical representation of an iron-carbon phase diagram with changes in microstructure according to temperature and duration of heating or cooling (Subtech 2010).	157
Figure 63 – Experimental results - Tool-life of a slotting blade and the machinability response.....	169

List of Symbols, Abbreviations and Nomenclature

<u>Symbol</u>	<u>Definition</u>
A	Area (m ²)
A	Cross Sectional Area (m ²); (Equation 5)
AISI	American Iron & Steel Institute
API	American Petroleum Institute
AWJ	Abrasive Water Jet
BBI	Broken Blade Indicator
B _L	Blank Liner Length (m)
Blade O.D.	Outside Diameter of Blade (inches)
Blade. P.D.	Blade Plunge Depth (inches)
BS	British Standards
BUE	Built Up Edge
C	Constant (0.275-0.300)
CBM	Coal Bed Methane
C _f	Conversion Factor
CHOPS	Cold Heavy Oil Production with Sand
Cos	Cosine Function
CSS	Cyclic Steam Stimulation
CVD	Chemical Vapour Deposit
CVI	Cutting Volume Indicator (inches)
D10	Sand Diameter @ 90% smaller and 10% larger
D30	Sand Diameter @ 70% smaller and 30% larger
d30	Sand Diameter @ 30% smaller (m)
D40	Sand Diameter @ 60% smaller and 40% larger
D50	Sand Diameter @ 50% smaller and 50% larger
D70	Sand Diameter @ 30% smaller and 70% larger
D90	Sand Diameter @ 10% smaller and 90% larger
DBI	Dull Blade Indicator
DIN	Deutsches Institut für Normung (German)
DM	Down Milling
E	Young's Modulus for Compression
EDM	Electric Discharge Machining
EIA	Energy Information Association
ENCH	Chemical Engineering
EOR	Enhanced Oil Recovery
EP	Extreme Pressure
ERCB	Energy Resources Conservation Board
F	Force, Load Applied (N)
FEA	Finite Element Analysis
FPT	Feed Per Tooth
HRc	Rockwell Scale "C" Hardness Measure
HSS	High Speed Steel

<u>Symbol</u>	<u>Definition</u>
ID	Inside Diameter
IPM	Inch Per Minute
J_L	Slotted Liner Joint Length (m)
JIS	Japanese Industrial Standards
k	Permeability (m^2)
k (abs)	Absolute Permeability (m^2)
k_h	Horizontal Permeability
k_i (si)	Measured Permeability @ Saturation (m^2)
k_{ri}	Relative Permeability @ Saturation Level 'I'
k_v	Vertical Permeability
L	Length of Bed Pack (m); (Equation 1)
L	Horizontal Wellbore Length (m); (Equation 12)
M2	High Speed Steel Material
M35	High Speed Steel with 5% Cobalt Content
M5	High Speed Steel with 5% Molybdenum
MRR	Metal Removal Rate
NAIT	Northern Alberta Institute of Technology
NBT	Natural Bridging Tendency
OD	Outside Diameter
O.D. Slot Length	Outside Diameter Slot Length (inches)
OTCG	Oil Country Tubular Goods
P_c	Capillary Pressure
P_{nw}	Non-wetting Phase Pressure
P_w	Wetting Phase Pressure
Pipe. W.T.	Pipe Wall Thickness (inches)
PSD	Particle Size Distribution
PSI	Pounds Per Square Inch
q	Liquid Flow Rate (bbls/d)
Q	Total Discharge (m^3/s); (Equation 5)
Q	Localized Flow Rate of the Phase (m^3/s)
r	Radius of Curvature of Wetting Phase
R	Ratio of Blank-to-Slotted Liner
Re	Reynolds Number (dimensionless)
RMMI	Relative Material Machinability Index
RPM	Revolutions Per Minute
R&D	Research & Development
SAGD	Steam Assisted Gravity Drainage
SC	Sorting Coefficient
SFPM	Surface Feet Per Minute
S_L	Total Slotted Length per Joint (m)
SPC	Slots Per Column
SPE	Society of Petroleum Engineers
SPP	Number of Slots Per Pipe
SSCC	Sulphide Stress Corrosion Cracking

<u>Symbol</u>	<u>Definition</u>
SS	Svensk Standard (Swedish Standard)
T	Tool-life Time (sec); (Equation 10)
T	Tool-life (min); (Equations 11 & 12)
TRS	Transverse Rolled Slot
UC	Uniformity Coefficient
UCS	Unconfined Compressive Strength
u_s	Superficial Velocity of a Given Phase (m/s)
UM	Up Milling
v	Advection Velocity (m/s)
v	Specific Discharge (m/s); (Equation 9)
v	Cutting Speed (RPM); (Equation 10)
V	Volumetric Flux per Slot (L/slot/hr)
V	Cutting Speed (ft/min); (Equation 12)
μ	Viscosity of Water or Mixture (kg/s m)
μ	Dynamic Viscosity (Pa s)
ΔP	Applied Pressure Difference (Pa)
ΔP	Differential Pressure
σ	Surface Tension
σ	Stress (N/m ²)
θ	Theta Angle (degrees)
ϕ	Porosity (dimensionless, fraction)
ϵ	Strain (% of Elongation)
ρ	Density of Water or Phase Mixture (kg/m ³)
π	Pie (3.1415)

CHAPTER 1: INTRODUCTION

Geographically, oil sands and heavy oil are found throughout the world with the greatest potential resources identified in Canada, Venezuela, and the former Soviet Union. Globally, heavy oil and oil sands reservoirs are estimated to contain approximately 6 trillion barrels of oil; however the true resource base could be much larger because heavy oil resources have not traditionally been documented unless they are economically viable under current market conditions (Center for Energy 2011). Heavy oil, with viscosities typically lower than 100,000 cP, in Canada is mostly situated near the Alberta-Saskatchewan border near the city of Lloydminster. Oil sands deposits, which typically refer to bitumen bearing unconsolidated reservoir sands with viscosities typically greater than 100,000 cP, are located primarily in Alberta and within three specified regions called the Athabasca, Peace River, and Cold Lake regions. These three specific regions cover a total of nearly 141,000 square kilometers as shown in Figure 1 and Figure 2, which would cover the size of the province of New Brunswick. The “Carbonate Triangle” region of Alberta, mostly hosted in the Grosmont carbonate deposit, displayed in Figure 2, also contains significant bitumen reserves, but typically these reserves are deeply buried and are currently considered uneconomic to develop although there has been recent pilot activities in this resource (Laricina 2012).

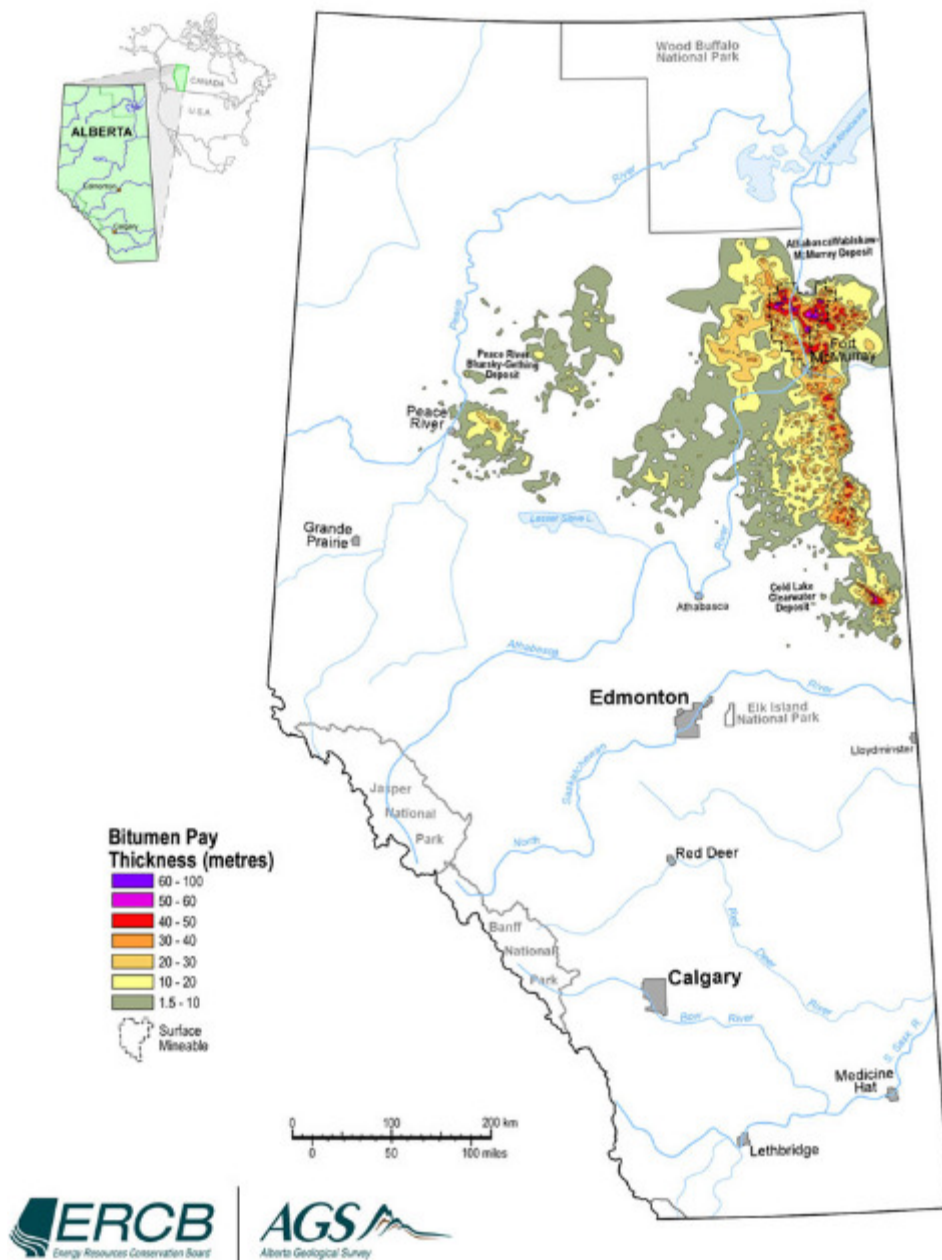


Figure 1 - Alberta oil sands deposits showing significant areal extent and net pay thickness (ERCB 2011).

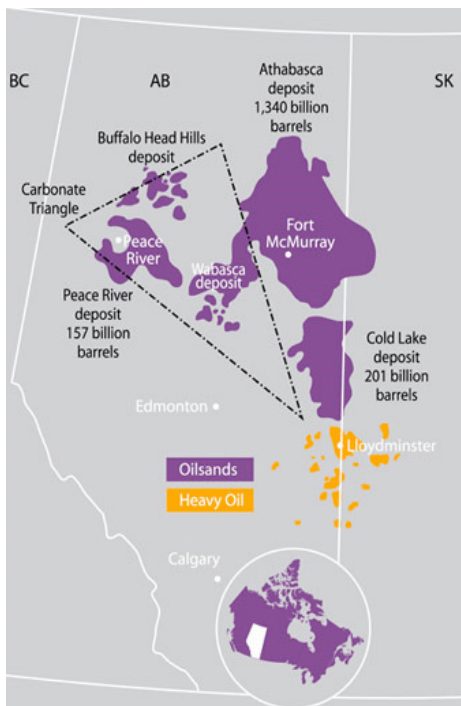


Figure 2 - Grosmont bitumen-bearing carbonate platform under laying the Wabasca and Peace River oil sands and further, which provides another challenging resource source for exploitation (ERCB 2008).

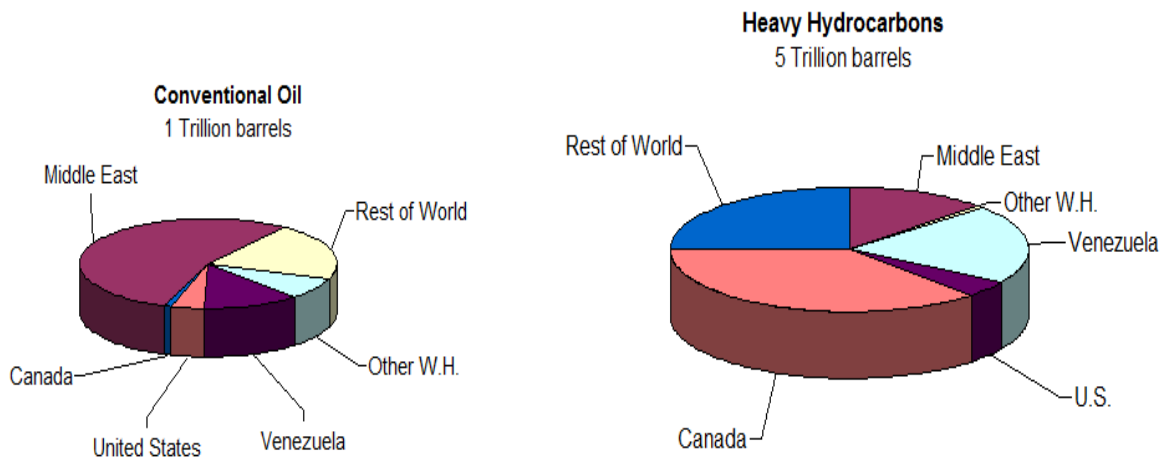


Figure 3 - Conventional versus unconventional oil geographic distribution of hydrocarbon resources worldwide.

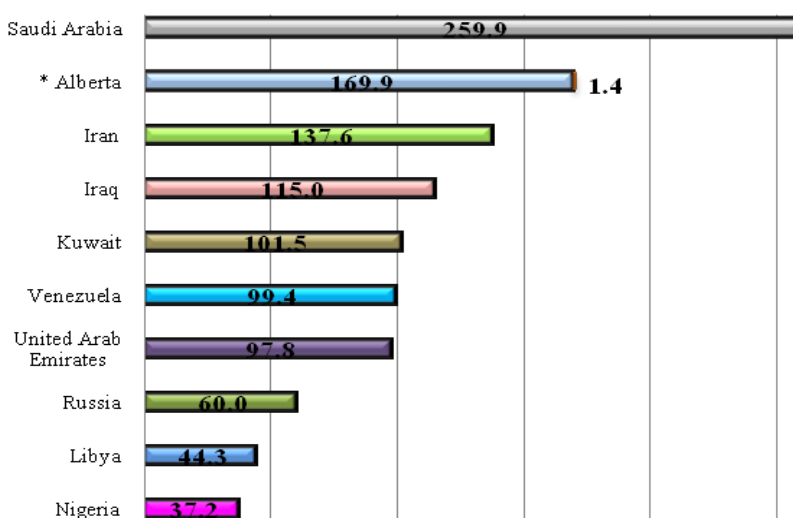
The oil sands deposits of Canada have proven reserves equal to about 1.75 trillion barrels ($280 \times 10^9 \text{ m}^3$) of bitumen in place (Datalog Technology Inc. 2012). The Alberta Energy

and Utilities Board estimates that the remaining established reserves of crude bitumen is about 170.8 billion barrels ($27.0 \times 10^9 \text{ m}^3$) of which about 10.8 billion barrels are within areas of active development (Datalog Technology Inc. 2012). All heavy oil, bitumen and oil sands of the world are biodegraded conventional oil over geological timescales. Biodegradation of crude oil in reservoirs is an important alteration process with major economic consequences. It raises the viscosity and density of the oil, increases the sulphur content of the oil, and enlarges the asphaltene content of the oil. This makes in-situ exploitation of the biodegraded oil much more challenging with technologies centered on thermal recovery methods, used to reduce the viscosity of the oil, being most important. In other words, biodegradation lowers the value of the oil (Larter et al. 2006).

Approximately, 3.6 trillion barrels ($570 \times 10^9 \text{ m}^3$) of recoverable heavy oil is contained in Canada and Venezuela reservoirs, as compared to 1.75 trillion barrels ($280 \times 10^9 \text{ m}^3$) of conventional oil worldwide. Thus, on a global scale, the value of Canada's oil sands is immense. Alberta bitumen production is expected to reach 3 million barrels per day by 2018 from approximately 1.31 million barrels per day today (Government of Alberta 2011). Approximately 80% of oil sands reservoirs are recoverable through in-situ production with the remainder being recoverable by surface mining.

Depending on the recovery mechanism or method of extraction chosen, variable rates of recovery can be expected. Recovery factors between 5 and 10% are expected for primary recovery of conventional heavy oil, which can be improved by up to 20% recovery factor by using enhanced recovery methods such as water flood or polymer flood. Recovery

factor of up to 50 to 60% of the original bitumen in place can be expected by employing thermal recovery methods such as Steam Assisted Gravity Drainage (SAGD) and 25 to 35% recovery factor by using Cyclic Steam Stimulation (CSS). In surface mining, since all of the oil sand is taken to extraction vessels, up to 90% of the bitumen in place can be recovered in mining operations.



* Alberta's total oil reserves were 171.3 billion barrels, of which oil sands reserves accounted for 169.9 billion barrels and conventional crude oil reserves for 1.4 billion barrels.

Figure 4 - Conventional and unconventional world oil resources in accordance to the top oil and gas production countries (ERCB 2009).

North American crude oil consumption is expected to rise significantly in the next 10 years to approximately 31 million bbls/d. Production is expected to be of the order of approximately 12.5 million bbls/d leaving a shortfall of about 19 million bbls/d. The Alberta oil sands are a significant source of oil for North America and more specifically the United States of America. Proper exploitation of the Alberta oil sands and worldwide heavy oil and oil sands deposits is critical to offset the shortfall and the impending

economic impacts of the shortfall and a relative rise in oil prices, which would create a cascading effect on the world economy. The use and development of horizontal wellbores and new technology to drill safely, efficiently and effectively will be necessary to properly exploit most of the heavy oil and oil sands deposits Worldwide.

1.1 Horizontal Well Technology

Horizontal drilling provides an improved economic option for producing petroleum reservoirs by enabling extensive reservoir-borehole contact. Horizontal drilling in unconsolidated reservoirs requires a liner to control the wellbore's integrity. Slotted liners are prevalently used in horizontal well-based recovery processes to produce oil sand reservoirs. Slotted liners in horizontal wells producing from unconsolidated sandstone reservoirs are generally designed to prevent sand inflow, maximize inflow area, and resist modest collapse loads. They are relatively inexpensive and tolerant of installation loads, but historically they have not been able to provide the very small opening sizes achieved by using wire-wrap screens for controlling production of solid fines (Kaiser et al. 2003). Advancements in slot manufacturing tolerances and design provide for precise slotted liner slot aperture openings and keystone slot profiles which match or surpass wire wrap screen design of aperture opening and size (Kaiser et al. 2003).

1.2 Reservoir Characterization

The majority, about 80%, of Alberta's oil sands are too deep to mine. In the Athabasca deposit, SAGD is the preferred recovery method for oil production. The main reasons this is the case is because the solution gas content is too low and overburden cap rock integrity is generally not sufficient for the higher steam injection pressure CSS exploitation. The Athabasca deposit is mainly hosted in the McMurray Formation. In this formation, the oil sands contain mainly quartz sand, clays, water, and bitumen with a small amount of solution gas, water, and trace minerals. Bitumen in oil sands does not flow freely because its high viscosity is typically in the millions of centipoises (cP). One key property of bitumen is that its viscosity drops by several orders of magnitude when heated. For example, the viscosity of Athabasca bitumen drops to less than 20 cP when heated to 200°C. Therefore, thermal techniques, often using injected steam, are used to improve the mobility of bitumen to enable its movement to a production well.

1.3 Steam-Assisted Gravity Drainage

One of the most successful exploitation technologies for oil sands is the SAGD process (see Figure 5). The concept was originally developed by Dr. Roger Butler while working at Esso in 1978 and was patented (U.S. Patent # 4,344,485) in June 1980.

In SAGD, steam is injected into the formation from a horizontal injection wellbore and fluids are produced from a lower (typically 5 m vertically offset from the injection well)

horizontal wellbore which is largely parallel to the injection well. A steam chamber develops in the reservoir due to continuous injection of steam from the injection well. At the interface between the steam chamber and the cold bitumen, the steam condenses, giving up its latent heat. No temperature change is associated with latent heat of condensation; therefore the steam is now hot water at the same temperature as the injected steam. The released latent heat provides heat to the bitumen thereby reducing its viscosity and allowing it to flow downwards through the sands under the influence of gravity towards the production well at the base of the chamber. The bitumen is moved to the surface with wellbore pumps located typically in the heel of the production wellbore. Fresh bitumen becomes exposed as mobilized bitumen drains and is then subsequently contacted with steam. To reduce the potential for steam short circuiting from the injector wellbore (injection pressures above reservoir insitu pressure), a liquid head of subcooled condensate (condensed steam) and bitumen is maintained above the producer wellbore and below the injector wellbore. This method of controlling live steam production is called steam trap control or subcool and it ensures that steam chamber growth continues upwards and steam does not break-through or short circuit towards the lower producer wellbore. If the production rate is too high the liquid level between the wells drops and if it is too low, steam can short-circuit between the wells. The subcool refers to the temperature of the produced fluid below the thermodynamic condensation temperature at the chamber pressure (Edmunds 1986; Gates and Leskiw 2010). In current practice, SAGD wellpairs are on the order of 750-1000 meters long.

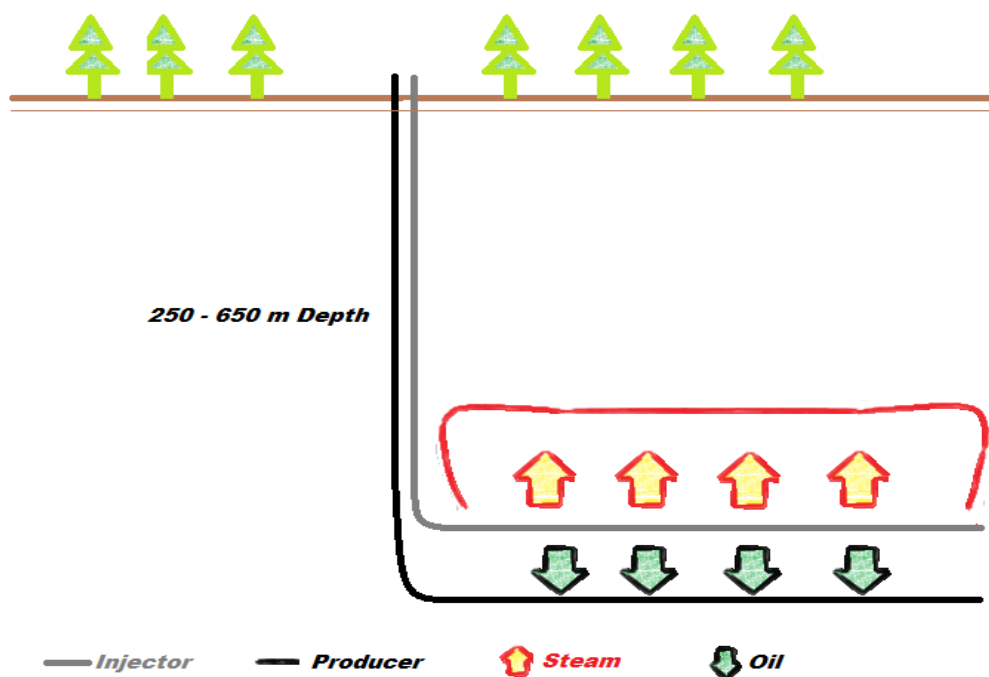


Figure 5 - SAGD well pair schematic showing continuous steam injection in the upper well and continuous production of heated bitumen from the lower producer well.

In clean reservoirs where vertical permeabilities are favourable (vertical to horizontal permeability ratio greater than 0.6) with horizontal permeabilities greater than 1,000 mD, SAGD can give potentially high recovery factor of greater than 50% (Farouq Ali 2010). Depending on the depth, a reasonably competent caprock is needed to seal the steam chamber from shallower water zones and aquifers. All SAGD exploitation designs in clastic unconsolidated reservoirs require some form of sand control and in current practice, the preference for sand control are low cost, robust slotted liner systems. The design of a slotted liner completion for SAGD requires detailed engineering and precise machining.

1.4 Problem Statement

In the research documented in this thesis the specific research questions tackled are as follows:

- 1). How can slotted liners be custom engineered and manufactured in accordance to oil sands reservoir properties for optimal SAGD exploitation given Particle Size Distribution (PSD), straight slot versus seamed slot, slot plugging, pore space plugging, fines and clays, and reservoir wettability?
- 2). Why does pipe chemistry and properties (carbon equivalent, hardness, sulphur content, and microstructure) improve or reduce machinability of slotted liner and slot tolerance and quality for sand control?
- 3). How can Taylor's Tool-life equation be used to improve slotted liner machinability and manufacturing so as to improved quality control of slot and reduce slot manufacturing costs?

1.5 Organization of Thesis

In Chapter 2, the literature is reviewed with respect of well completion design and sand control methods for SAGD wells. Chapter 3 describes the reservoir characteristics and parameters which influence sand control in SAGD operations. Chapter 4 describes sand control analysis and the development of the slot width model which is based on particle size distribution data. Chapter 5 describes the modes of manufacturing a slot into an oil country tubular goods (OTCG) pipe and slotted liner manufacturing principles and

laboratory testing. Chapter 6 describes tool-life, Taylor's tool-life equation, and machining. Chapter 7 lists the major conclusions and recommendations from the research documented in this thesis.

CHAPTER 2: LITERATURE REVIEW – SAND CONTROL TYPES

Many unconsolidated heavy oil and bitumen reservoirs require a sand control screen system to prevent sand particle influx into the wellbore to minimize surface casing erosion and environmental and remedial costs. Sand production can be a significant issue when producing from unconsolidated reservoirs. Tronvoll et al. (2004) recognized that hydrocarbon production from unconsolidated sandstone reservoirs can be plagued with potentially erosive but mostly problematic sand production or sanding, which can be induced by mobility of formation sand due to re-orientation of in-situ stresses causing disaggregation of formation sand or can be caused by fluid velocity to flow. Cohesive, tensile, compressive and shear stresses induce sand movement with unconsolidated sand reservoirs. Sand problems can reduce oil production and hence revenue due to plugging of the formation or the well perforations by formation sands and particularly fines and clays. Isehunwa and Farotade (2010) have shown that in addition to damaging pumps and down hole equipment, erosion of casing surface facilities may also occur. There are many different sand control systems each with pros and cons.

2.1 Barefoot Completion

A barefoot completion is one that has no casing or liner set across the reservoir formation, allowing the produced fluids to flow directly into the wellbore (Schlumberger 2012). Without casing, liner, screen or tools therein, there is a reliance on the formation sand being strong enough and shale beds stable enough, to resist fluctuating pressures as

the well depletes the reservoir. This works very well in strong sandstone, dolomite and limestone, but fails in weaker sandstone, such as unconsolidated sands or in reservoirs where tectonic activity is prevalent which will cause failure of the rock leading to rock accumulation in the open hole. Most unconsolidated sand requires some form of sand control.

2.2 Gravel Pack

Gravel packs are generally not used for heavy oil or bitumen reservoirs but are used extensively around the world for conventional/light oil clastic unconsolidated reservoirs requiring high inflow rates. Gravel packs are manufactured particles (gravel) of specified sizes to stop movement through the formation to the wellbore by providing a sand pack around the screen or liner. The gravel is sized according to what the in-situ sand particles are present and can be calculated according to the particle size distribution or sieves. An effective gravel pack is designed based on reservoir properties, sand control requirements, and well performance objectives. Gravel packing creates a permeable down hole filter that will allow the production of the formation fluids but restrict the entry and production of formation sand (Xiang 2003). The literature suggests mean gravel sizing criteria such as 4-10 times the D10 particle size of the sand, 5-6 times the D50 of the particle size of the sand or 4-6 times the D30 particle size (Coberly 1937). However, these are rules of thumb – there are no hard rules to follow to design the best sand control gravel pack since every reservoir is different. Fine migration and estimation of, into the gravel pack, is of significant importance. If the pore spaces of the gravel

become plugged with fines and clays then the effectiveness of the gravel pack, to control pressure drops and allowing for increased inflow performance, is compromised in accordance to production performance. Some of the advantages of gravel packing is that the gravel around the screen or open hole annulus, provides the filtering mechanism, which reduces solids invasion into the screen, can provide an increase in well productivity as the gravel pack fills the annular space thereby replacing the low-permeability sand with high-permeability gravel in this region and the screen damage is reduced (Sparlin 2005).

The most likely situation where gravel packing should be used is in a very weak formation where sand is likely to fill the annulus around the screen (Sparlin 2005). Gravel helps support the formation in stronger sandstones, reducing the effect of sand movement, screen plugging, and erosion. Horizontal gravel packs are relatively difficult since there are challenges associated with dispersing gravel around the annulus of the horizontal wellbore towards the toe of the well. Gravel packs can be expensive and if improperly deposited in the annular space of the wellbore can cause loss of a well. Table 1 lists gravel pack and proppant size designs (Carneuseis 2011). The designs reveal the wide variability in gravel packing for reservoir sands and also standardization of gravel packing designs with less customization to reservoir parameters than other sand control types.

Table 1 - Gravel Pack Sizing according to sieve sizes and the frequency distribution of each size of sand (Cameuseis 2011).

		8/16		12/20		16/30		20/40		30/50		40/70	
Sieve Analysis	U.S. Sieve Sizes /Percent Retained												
	Sieve	Percent	Sieve	Percent	Sieve	Percent	Sieve	Percent	Sieve	Percent	Sieve	Percent	
	6	0.0	8	0.0	12	0.0	16	0.0	20	0.0	30	0.0	
	8	3.0	12	3.2	16	1.1	20	2.0	30	7.6	40	1.6	
	12	61.9	16	55.0	20	64.5	30	51.0	40	22.3	50	55.0	
	14	26.0	18	26.0	25	25.0	35	33.0	45	45.1	60	27.3	
	16	6.3	20	12.5	30	8.0	40	11.4	50	21.9	70	11.3	
	20	2.3	30	3.1	40	1.3	50	2.5	70	2.6	100	4.4	
	Pan	0.5	Pan	0.2	Pan	0.1	Pan	0.1	Pan	0.5	Pan	0.4	

2.3 Stand Alone Screens – Wire Wrap

Wire wrapped well screens are manufactured by wrapping a triangular shaped wire on longitudinal rods situated on a perforated base pipe or by wrapping straight onto a perforated base pipe (Johnson Screens 2011). The wire is welded to the rods by resistance welding producing a cage-shaped cylindrical configuration or the wire is compression wrapped around a perforated base pipe. This type of screen is usually manufactured by using stainless steel, galvanized steel, or carbon steel.

The continuous wrap and slot opening design was developed in the early 1900's for sand control in water well applications and quickly transferred to oil and gas wells (Johnson Screens 2011). Wire-wrapped screens offer significant open areas; up to 15% surface

open area, to minimize frictional head losses through the screen. They can also provide very small aperture sized openings (as low as 0.005 inches), thereby controlling small sand grains and fines. The triangular or V-shaped slot aperture or opening configuration tends to reduce plugging of the screen.

Careful consideration must be made of the use of wire-wrap screen in situations or under conditions for which it was not originally designed. Wire-wrap screens are generally more expensive than other stand-alone screen types without necessarily providing higher production rates, greater sand control or greater overall durability. Wire-wrap screens generally have lower collapsing and tensile strength than slotted liners. Installation loads during installation and in-situ production service loads can tear or deform the wire-wrap opening design specification, thereby reducing its intended purpose – custom, reservoir specific sand control. Figure 6 shows an example of a direct wrap refers to the wire continuously wrapped around a perforated base pipe.

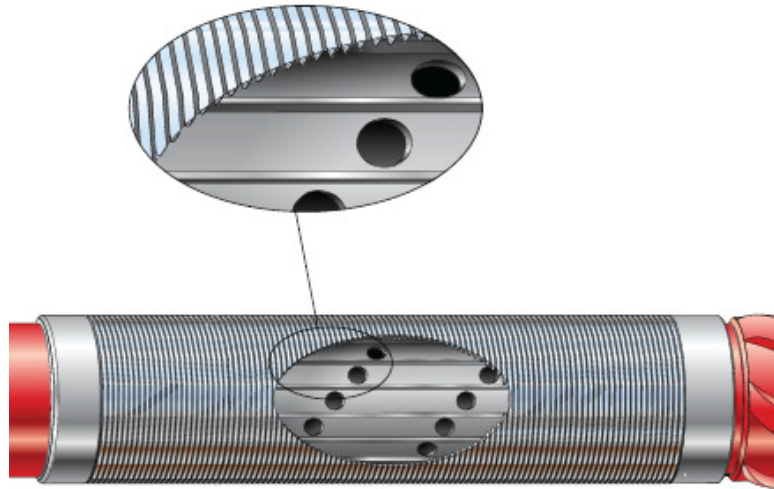


Figure 6 - Direct wrap - wire wrap screen showing the longitudinal ribs which provide the support for the wire which is wrapped around the perforated base pipe (Halliburton 2004, used with permission).

2.4 Slotted Liners

Slotted liners are designed to mimic a barefoot completion as best as possible. Slotted liners are effectively used to provide sand control in clastic unconsolidated reservoirs (Forsyth et. al. 2008). The primary factors requiring consideration in the design are: slot width, slot density or open area, slot lengths (O.D. and I.D.), pipe material or grade, and connection type (among others), which can all be thought of as being controlled and coupled with the reservoir conditions and the operating conditions. These liners can have a variety of configurations with varying slot density, slotting patterns, slot apertures and slot internal geometries.

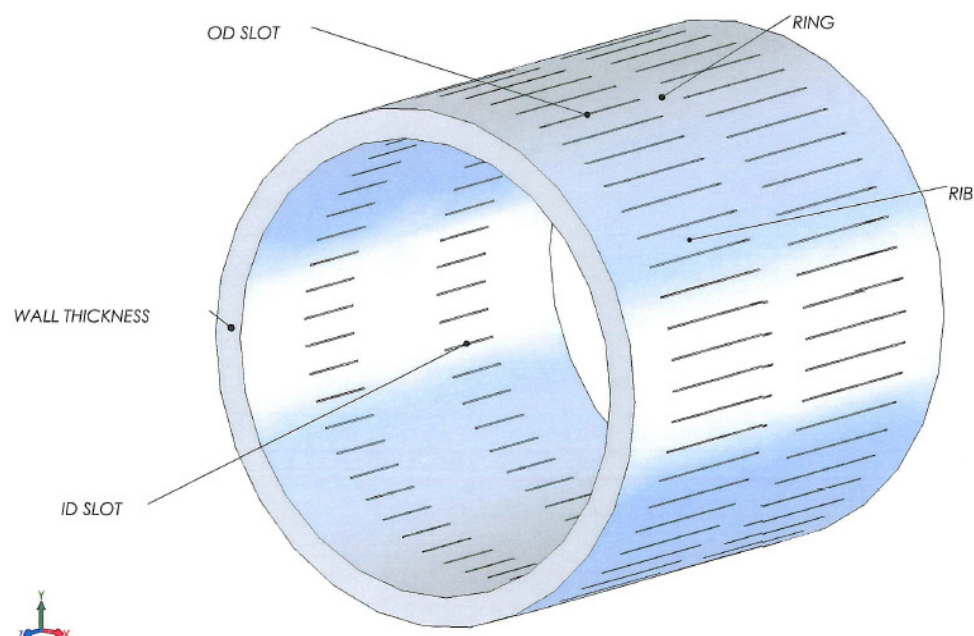


Figure 7 - Slotted liner configuration depicting the staggered offset pattern from column to column, the slot length differences from the outside to inside of the pipe due to the arc of the slotting blade and the small slot width required for sand control (Regent Energy Group Ltd. 2006).

Slotted liners are used extensively in the majority of SAGD operations conducted in Western Canada due to their superior mechanical strength and integrity in contrast to other mechanical sand-control devices (Bennion et al. 2008). Due to the majority of Alberta SAGD reservoirs being unconsolidated and with fairly low production rates, slotted liners are the low cost, robust and preferred sand control solution. The slotted liner's design objective is to mimic a barefoot completion as optimally as possible providing for minimal pressure drops, to provide optimal and reservoir specific sand control, to provide wellbore stability from formation sand preventing infill of the horizontal section, to allow for maximum production rates, and to provide mechanical integrity against installation loads and thermal loads. It has been found that in addition to

grain size of the sand under consideration and slot geometry, that clay content of the formation, flow velocity, wetting phase type and pH play crucial roles in the plugging mechanism of slotted liners (Bennion et al. 2008).

The literature reveals that there is little research on liner sizes, slot shape design, and slot spacing to optimize production in SAGD operations. It is not yet known what the optimal designs for SAGD injection and production wells are and how the sand size distribution in the reservoir impacts the design of the slots but efforts have been made in the past. It also remains unclear what the advantages of seamed versus straight slots for sand control and if sand plugging occurs, what are the key mechanisms that lead to plugging.

CHAPTER 3: CHARACTERISTICS OF RESERVOIRS UNDERGOING SAGD

Reservoir quality parameters almost always include porosity and permeability, but also include measures of clay content, cementation factors, and other factors that affect the storage and deliverability of fluids contained within the pores of the rock. Sand may be produced under transient, continuous or catastrophic conditions depending on rock strength properties, depth and pressure, depletion and drawdown, sand particle shape and size, shutdown and start-up frequency, water cut, reservoir fluid type, and reservoir rock wettability. In this chapter, reservoir characteristics in the context of sand control are discussed.

3.1 Wettability

Wettability is defined as the preferential surface attraction of one fluid (the wetting phase) on the surface of the solid/rock over that of another immiscible fluid (the non-wetting phase). Wettability is one of the largest factors controlling recovery of oil from a hydrocarbon reservoir for conventional oil (API, 1958). Although there are no direct calculations that use wettability, wettability affects relative permeability, residual saturations, recovery efficiency, capillary pressure, phase trapping, reservoir sensitivity to fluids and fines migration. The dominant wetting phase will always be attracted to the surface of the reservoir rock and therefore preferentially into the micro porosity. There are five types of wettability: water-wet, oil-wet, neutral-wet, spotted/Dalmatian-wet, and mixed-wet (Bennion 2010). A water-wet reservoir is one which the rock has a

preferential attraction to the water phase. Water saturation is a strong function of the absolute permeability of the reservoir rock as the micro pores will wick and preferentially attract the water phase into its space more than is the case with large pore space rock. An oil-wet reservoir is one which the rock has a preferential attraction to the oil phase. With an oil-wet reservoir, the oil saturation is not a function of the absolute permeability or pore size. A neutral-wet reservoir is one which the rock has no preferential attraction to the any fluid phases in the reservoir. A spotted/Dalmatian-wet reservoir is one which the rock has a spotted preferential attraction to the fluid phases present. A mixed-wet reservoir is one where the rock is water-wet in small pores and oil-wet in larger pores. The percentages of clastic sandstone reservoirs around the world that are water-wet, oil-wet and neutral-wet or mixed-wet are approximately equal to 30%, 15%, and 55%, respectively. The wettability of a surface is determined by the angle of contact between the fluid-vapor phase for water and the surface with wetting phase contact angles $<90^\circ$ giving rise to favorable wetting and $>90^\circ$ giving rise to unfavorable wetting. Factors that affect the wettability of a reservoir rock are mineralogy, interfacial tension, oil composition, biodegradation, thermal effects, temperature, oxidation and temperature.

Slot plugging and sand control are highly dependent on the mobility of the wetting phase, clay concentration, interstitial and superficial fluid flow velocity, the particle size distribution (uniformity coefficient), slot width and geometry and phases flowing (Bennion et. al. 2008). Strongly oil-wet formations generally create a significant potential for fines and clay migration from the onset of production; therefore proper sand

control slot widths require rigorous review, customization and specifics for sand control engineering (Bennion et al. 2008).

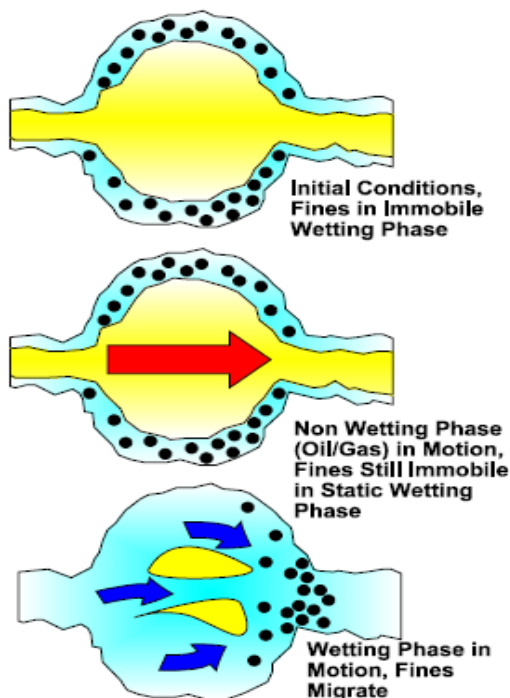


Figure 8 - Mobility of fines due to mobility of the wetting phase (Bennion 2002, used with permission).

Water-wet formations are most susceptible to plugging (Bennion 2002). Most water-wet formations are prone to a plugging potential due to the presence of fines, clays and quartz and the likelihood of increased mobility of the wetting phase, two-phase flow (as shown in Figure 8) and the increase in the apparent interstitial and superficial velocity. If the wetting phase is not mobile such as in a water-wet reservoir where the oil phase is only mobile and the water phase is not mobile, the fines and clays will be entrained in the static and immobile connate water phase encapsulating the surface of the reservoir rock. A remedial solution to a plugged slot is to backflow through the slot with dilute acid. Most unconsolidated heavy oil reservoirs are water-wet. Water-cut increases the

potential of sanding and plugging in water-wet reservoirs due to mobility of the wetting phase and due to the increase in apparent velocity of fluid flow.

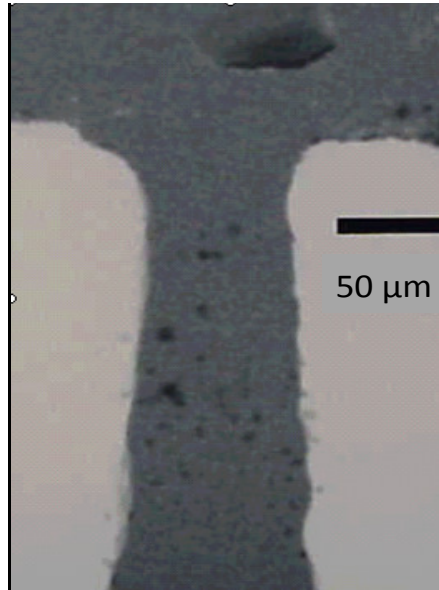


Figure 9 - Non-plugged seamed slot under simulated reservoir core flowing conditions in the laboratory setting (HYCAL/Weatherford Labs 2004, used with permission).

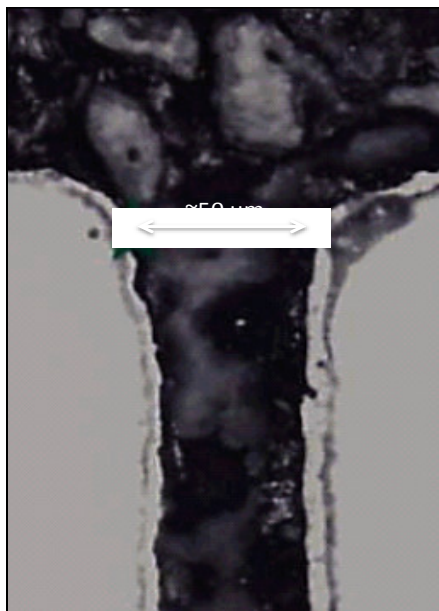


Figure 10 - Plugged straight slot under similar reservoir core with similar reservoir simulated flowing conditions in the laboratory setting (HYCAL/Weatherford Labs 2003, used with permission).

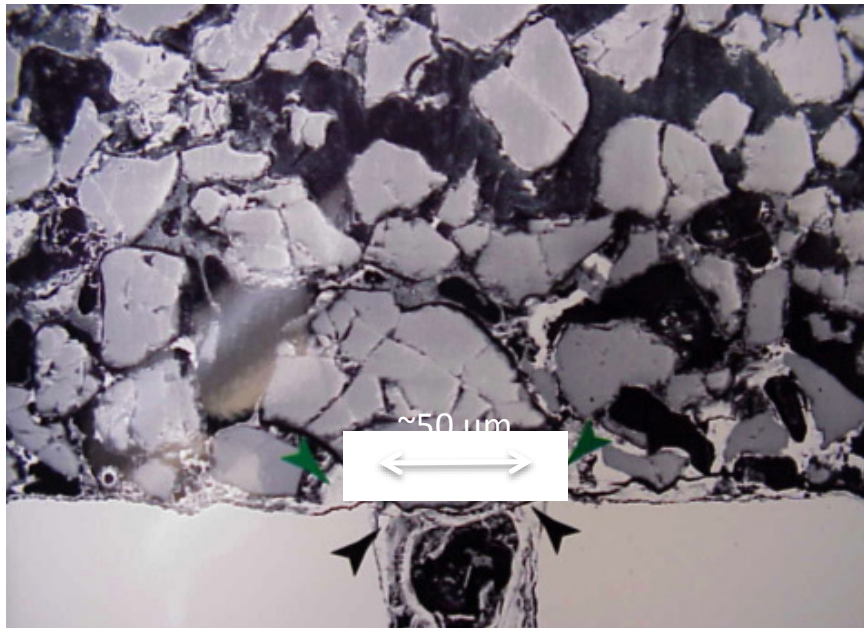


Figure 11 - Plugged slot due to clays present in the reservoir core becoming mobile (HYCAL/Weatherford Labs 2003, used with permission).

Figure 9, 10 and 11 depict the actual results from testing of flow from core through slots of various geometries (straight or seamed) under various flow rates and phases of flow. The highest plugging potential for a slot occurs with fines with clay content combined with large sand particles.

3.2 Permeability

Absolute permeability is the resistance to fluid flow in a porous media when it is the only fluid phase present. The permeability is a measure of the ability of the reservoir rock to transmit fluid; that is, it is the conductivity of the reservoir rock (Gates 2012). In 1856 Henry B. Darcy developed an experimental procedure for determining the flow behavior

of single-phase fluid flow in granular porous media, which can be thought of as the law of conservation of momentum (Dormieux et al. 2006). It forms the scientific basis of absolute permeability used in the earth sciences, which can be expressed as follows:

$$Q = -\frac{kA}{\mu} \frac{\Delta P}{L} \dots\dots\dots (1)$$

where Q is the volumetric flow rate, k is the absolute permeability, A is the cross-sectional area open to flow, μ is the fluid viscosity, and $\Delta P/L$ is the pressure gradient. Lower permeability reservoirs tend to have more severe plugging problems and fines migration than do higher permeability reservoirs, due to the smaller pore throats present in the lower permeability reservoirs.

3.3 Capillary Pressure

Capillary pressure is the pressure difference between two immiscible phases arising from the capillary forces (Gates 2012). With the presence of water in a porous media, capillary pressure and overburden pressure have an influence on the required pressure drop in the reservoir necessary to induce flow of fluids and therefore the influence sand control and the critical sanding failure or unconfined compressive strength that induces sand production. A high capillary pressure can hold the grains together reducing sand failure. As the wetting phase becomes mobile (generally water in oil sands) the capillary pressure decreases and the fines tend to migrate with the wetting phase and the sand failure potential, associated with a lower capillary pressure, rises. Also it is important to locate the sand control screen within a higher capillary pressure zone so as to reduce the

potential of installing the screen within a flushed zone (if water-wet reservoir rock) increasing heat losses in SAGD operations and causing phase trapping issues with injected fluids (condensed steam).

3.4 Plugging

An important feature of any sand control device is to maintain its primary objective of sand control while allowing the reservoir to “breathe” by not inducing a secondary change in the effective near-wellbore permeability. There are two types of plugging that impact production in-situ: pore space plugging and sand screen (or slot) plugging. Pore space plugging is the plugging of the reservoir pore space in the near wellbore region or far region due to too small of pore space, which restricts the free and unabated flow of fines and clay size particles through the pore space. If the pore space is too small, possibly due to too small of a slotted liner slot width which would create a small near wellbore pore space due to bridging of sand particle over the slot, then the fines ($<44\ \mu\text{m}$) and clays ($<5\ \mu\text{m}$) would plug in this region causing an increase in near wellbore pressure drops and reduction on fluid production. Fines migration refers to the motion of particulate material within a pore system caused when fluid(s) flowing within the interstitial spaces of the porous medium exert sufficiently high shear force that loosely attached naturally occurring particulates present in the porous medium are dislodged from their initial positions and transported to pore throat locations where they can bridge, block and cause reductions in permeability (Bennion 2002).

Slot plugging is the plugging of the slotted liner slot due to sand invading the slot and becoming lodged and impinged or clay building up within the slot, therefore becoming an extension of the reservoir porous media, with flow through the slot then becoming Darcy flow instead of open channel flow, which increases flow losses. This can cause significant pressure drops and reduced fluid flow rate and production due to the plugged slot and the convergence to flow that the slot would initially create, relative to barefoot, to fluid flow. It is therefore important to manufacture a slot width that provides optimal sand control while allowing for low pressure drops, unabated flow of fines and clay sized particles. The seamed slotted liner helps to prevent slot plugging. The near-wellbore permeability can be affected through reservoir pore-throat plugging or slotted liner slot plugging.

By controlling the pressure drop over the slotted liner (largest amount of slots possible for a production profile and the least amount of slots possible for an injection profile) we can effectively control/reduce the drag forces (interstitial and superficial velocity) on sand particles near the slotted liner due to convergence and required fluid production.

3.5 Superficial and Interstitial Velocity

Superficial velocity is the total flow rate divided by the cross sectional area to flow whereas the interstitial velocity is equal to the superficial velocity divided by the void fraction or bed porosity of the porous media. The interstitial velocity is the average velocity in the pores. The superficial velocity, u_s , is given by:

$$u_s = \frac{Q}{A} \dots\dots\dots (2)$$

Where Q is the volumetric flow rate and A is the cross-sectional area open to flow. By using the concept of porosity, the dependence between the advection velocity of fluid through the pores and the superficial velocity can be expressed as (McCabe et al. 2001):

$$u_s = \phi v \dots\dots\dots (3)$$

Where ϕ is the porosity and v is the velocity vector. The Reynolds' number, Re , measures the ratio of inertial to viscous forces and can be applied to flow within pores:

$$Re = \frac{\rho v d_p}{\mu} \dots\dots\dots (4)$$

Where ρ is the density, v is the velocity vector, d_p diameter of the pores and μ is the viscosity of the flowing fluid. The Reynolds' number is an effective measure of the tendency of sand particles to be mobilized by the drag forces of the fluid. It depends on the velocity of the fluid permeating through the reservoir, which in turn is a function of the drawdown and the unconfined compressive strength (UCS) of the reservoir. Since the highest flow velocities occur in the vicinity of the wellbore, the majority of the plugging occurs in this area (Bennion, 2002). High flow velocities or turbulent flow can clean up the near wellbore pore space as opposed to low velocities or laminar flow. A critical velocity test is generally conducted in the laboratory to identify the potential flow rate of which will induce fines migration (Crowell et al. 1991).

3.6 Unconfined Compressive Strength (UCS)

The unconfined compressive strength or uniaxial compressive strength of a soil sample is generally used in drilling operations as a key input of failure criteria for wellbore stability analysis, but it can also be used to estimate the drawdown which could cause sand failure. Sand production is normally caused when the shear stresses acting on the rock surrounding the perforation cavities or wellbore exceed the rock strength, and lead to rock failure (Weatherford, 2011). The sand sample must have some cohesiveness and be saturated with fluids during the test. To help determine the strength of the soil sample or rock, the test is conducted with a compressive uniaxial force applied to a soil sample, which is without lateral constraint, until failure. The peak strength of interlocked structure occurs before the peak strength of oil sand, but drops significantly thereafter [and] the strength derived from the interlocked structure increases with increasing confining pressure (Wong 2001). The unconfined compressive strength of oil sand is probably attributed to the interlocked structure (Wong 2001). Figure 12 provides a typical representation of the stress-strain relationship obtained from a UCS test.

The linear region of the stress-strain graph would be representative of an elastic material responding according to Hooke's Law:

$$\sigma = E\varepsilon \dots\dots\dots (5)$$

where σ is the stress, E is the Young's modulus, and ε is the strain. The major principle stress is calculated as follows:

$$\sigma = \frac{F}{A} \dots\dots\dots (6)$$

where F is the force applied over a cross-sectional area A . Research performed at Exxon showed that the compressive strength and the incidence of rock failure can be attributable to the UCS multiplied by 1.7 to provide a general estimation of the critical drawdown limit that would induce sand failure of the reservoir rock (Ott and Woods 2005). The unconfined compressive strength is the maximum value of the principle stress (σ). It is also equal to the diameter of the Mohr Coulomb's circle described next.

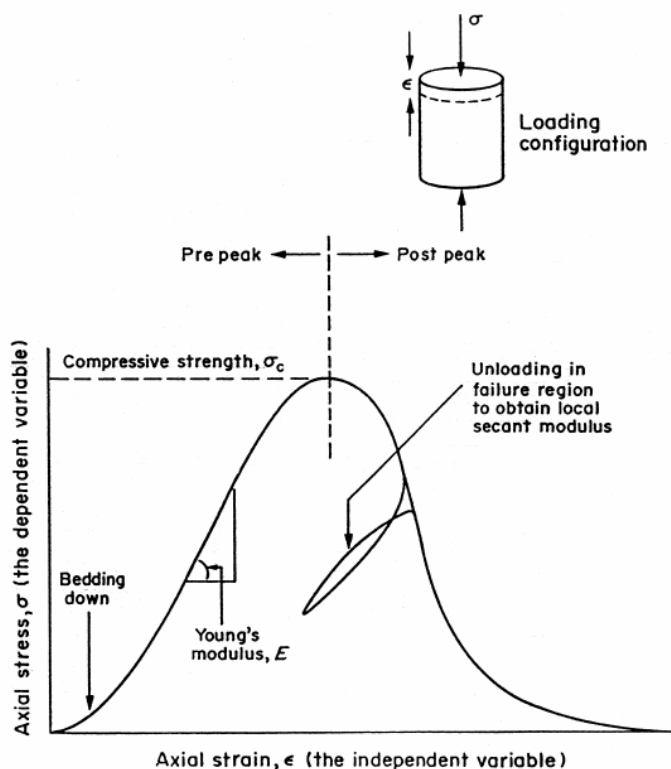


Figure 12 - Uniaxial compressive stress-strain curve (Fairhurst et. al 1999).

Typical “c” values for oil sand materials from direct shear tests under different test conditions are less than 20 kPa; whereas typical “f” values range mostly between 30 and 60° (Round 1960, Dusseault & Morgenstern 1978b). From laboratory testing of oil sands under passive triaxial compression exhibit a strain-softening response and therefore a strain-softening Mohr-Coulomb model can be applied to a coupled geomechanic simulation for identification of the failure criteria.

3.7 Mohr-Coulomb Circle

Mohr Coulomb analysis (Figure 13) provides formation cohesion (initial shear strength) and angle of internal friction. These are necessary parameters for reliable wellbore stability issues and sand production/failure analysis, which is not easily measured from well logs.

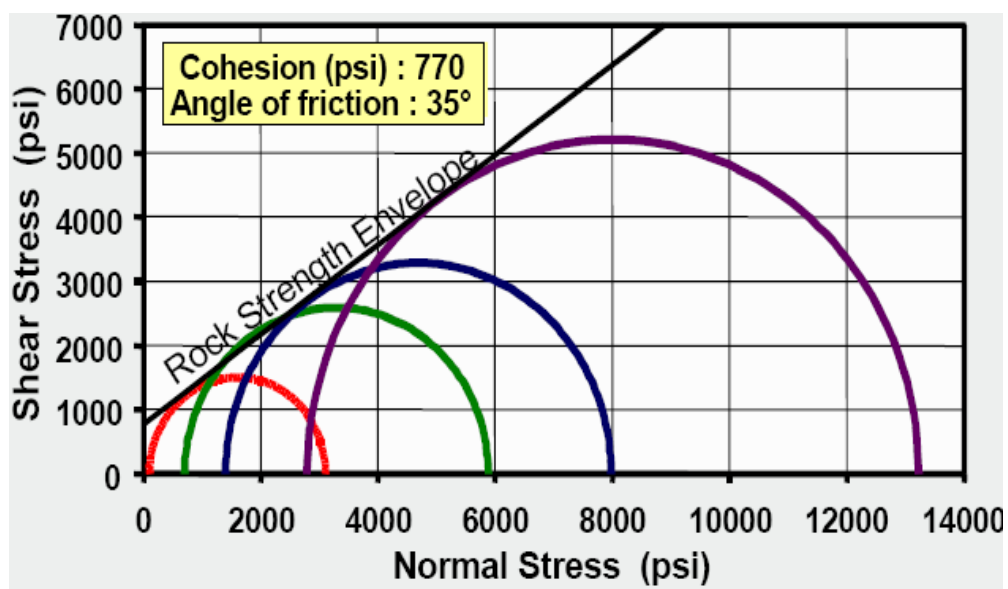


Figure 13 - Rock strength envelope - Mohr-Coulomb failure (Core Labs 2000, used with permission).

Chalaturnyk recorded through laboratory confined tri-axial testing under 20°C and also at an elevated temperature of 225°C, the effective cohesive strength (peak) and friction angle of shear failure of the oil sands to be 0 MPa for both 20°C and 220°C and from 48 – 52° for the 20°C testing and 46° for the 225°C testing. Clearly, heat consolidation leads to a denser pre-shear structure resulting in higher Young's modulus at 220°C than 20°C at a given confining stress (Chalaturnyk 1996).

It was found that gas nucleation in heavy oil is the major factor in causing the initiation of sand production in oil sand (Wong 2003). Solution gas evolved at the pressure state just below the bubble point could induce negative effective stresses in oil sand at unsupported cavities or unscreened perforations (Wong 2003). This unravels the oil sand interlocked structure by tensile failure or parting, resulting in massive sand production (Wong 2003). Wong (2003) identified that the interlocked structure of the oil sands can provide high resistance to shear loads created during fluid flow through the oil sand, however if the sand undergoes gas exsolution, then it is fairly poor in resisting the tensile failure loading mechanism.

Wong et al., had developed a analytical solution for identification of the destabilization of a sand arch around a perforation or cavity relating to shear failure and the critical pressure gradient and found that if the friction angle was 45° the cohesive strength could be as high as 0.9 MPa. Oil sand material has little or no cohesion strength between grains.

3.8 Flow Rate

There is a critical fluid-flow rate beyond which the hydrodynamic force exceeds the binding forces holding fines particles together and fines ($<44 \mu\text{m}$) begin to become fluidized. Not surprisingly, the flow rate through a sand pack can affect sand retention. In general, the lower the flow rate, the better the retention (Ballard and Beare 2006). Production can be affected by non-optimized inflow distribution. Drawdown and plugging can be affected by asphaltene and/or wax precipitation due to temperature reduction (thermal applications or cold water injection), high viscosity of produced oil, resins present, near-wellbore pressure drop and/or flow convergence resistance created by the slotted liner (Trent 2005). Multiphase flow increases plugging potential and sand control issues. Depending on formation characteristics and multiphase flow, the interstitial flow velocity can either enhance or reduce near wellbore permeability (Bennion et. al. 2008). When only one phase flows in a reservoir, then there can be an allowable increase in the flow velocity to the slot more than if there is multiphase flow. Plugging and significant solids production generally occurs with two phase flow where water and oil flow since fines migration and transport only occurs when the wetting phase is in motion in the porous media (Bennion et al. 2008). There is a critical fluid-flow rate beyond which the hydrodynamic force exceeds the binding forces holding fines particles together beyond which the fines begin to move. A sudden increase in flow rate also could induce fines migration.

3.9 Sand Screen Open Area

All sand control screens induce a convergence skin factor as compared to a barefoot completion which causes an increase in the flow velocity to the slot, thereby increasing pressure drops and creating a potential increase in the drag force coefficient that could cause failure of the sand in this convergence zone. This affects inflow performance and sand control. Inflow performance is usually considered to be controlled by the open area exposed to the reservoir, and the sand control governed by slot opening size (Kasier et al. 2000). In reservoirs containing fines sands and clays, the open area and slot opening become competing considerations because to maintain open area the slot density must be increased if the slot size is reduced. With the large open areas targeted for some reservoirs and with the slot width opening requirement being small to control fines and clays, their size would demand very high slot densities. The basis for this open area design requirement most likely stems from applying open channel flow theory to flow loss through the slots. Therefore this basis would lead one to believe that fewer larger slots width would induce a lower flow resistance than smaller slot widths, all with respect to the exact same open area for each scenario. However, this design basis and conclusion ignores that the largest pressure drop associated with fluid flow near a wellbore is that arising from the reservoir sand medium and its associated flow convergence to the slot. In fact, the flow loss through an open slot (non-plugged) is negligible compared with that induced by the flow disturbance associated with the slot and the near wellbore porous medium.

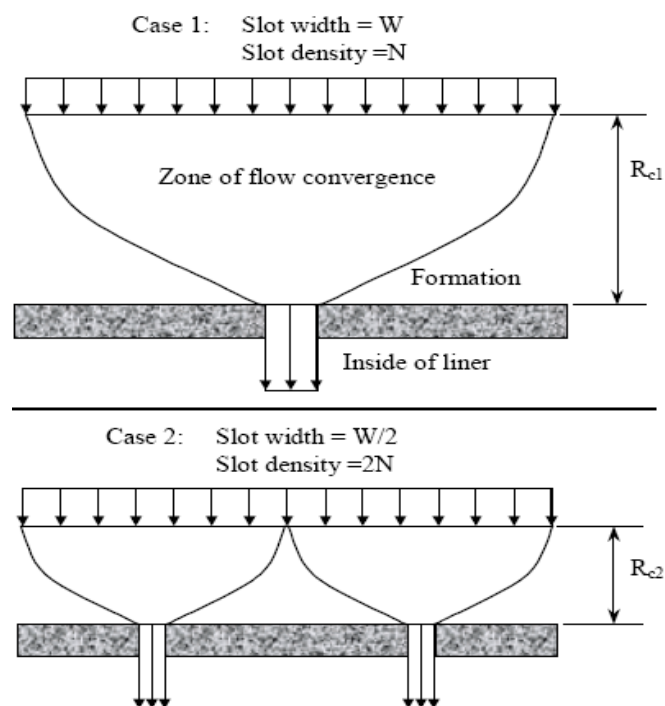


Figure 14 - Flow convergence effects due to slot density (Kaiser et al. 2000).

From Figure 14, as the slot density is increased by a factor of two, the flow convergence skin factor is decreased by nearly a factor of two (Kaiser et al. 2000). Therefore, slot density is the largest factor controlling flow convergence.

3.10 Clay Content

Most oil and gas reservoirs contain clays. Clay plugging at the top portion of the slots has been found to be the dominant damage mechanism causing plugging of slotted liner slots (Bennion et al. 2008). It is predicted that generally severe pore space plugging at low flow rates occurs when both coarse-grained sand particles and clay sized particles are both present with small slot width sizes $<0.012''$ ($\sim 305 \mu\text{m}$) (Bennion 2010). Clays are

generally 5 μm or less in size and are anionic and therefore have a strong attraction to positively charged materials. Clays tend to form microfilms on the surface of the slot, which eventually lead to slot plugging and productivity impairment.

Generally if slot width size is properly designed, in accordance with the particle size distribution for a target portion of the reservoir, then quartz sand grains will not be entrained within and which if entrained would lead to slot plugging as would be the case with clay particles. Total solids control, one which does not allow the passage of at least clay sized particle fractions, will inevitably plug a slot. Generally at typical SAGD well production rates and flow rates within the wells, settling of these colloidal sized fines in the wellbore are not an issue, but some allowance may need to be made for their presence in surface handling and processing facilities (Bennion et al. 2008).

Injected water and steam tend to be at higher pH than that of the formation water and as a consequence, kaolinite clays tend to disperse (Bennion et al. 2008). At low pH they tend to aggregate (flocculate) (Bennion et al. 2008). With respect to slot plugging, dispersed (deflocculated) kaolinite clays tend to become more problematic clays than aggregated clays. Dispersed kaolinite clays are freer to travel within the reservoir thereby becoming mobile clays which can cause plugging of pore spaces or slots due to migration. Deflocculation can occur due to low salinity-high pH, 'salinity shock', and natural repulsion forces due to not enough cations available. Once deflocculated, kaolinite clays tend to migrate when the wetting phase becomes mobile.

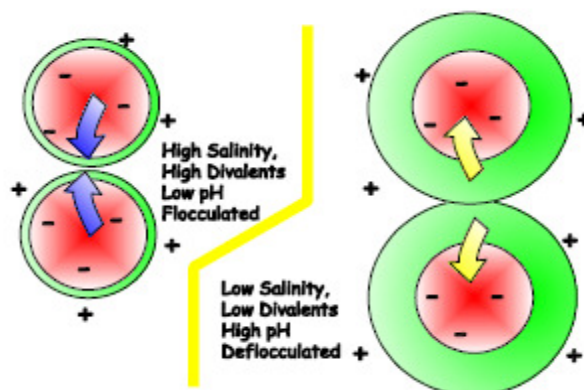


Figure 15 - Clay deflocculation due to anionic charge of clay particles and the unstable valent bonding of clays which are easily affected by salinity and pH (Bennion 2002, used with permission).

Kaolinite clays tend to migrate as “booklets” rather than individual particles. A significant pore space plugging potential exists with the combination of kaolinite clays and dendritic illite clays. Non-equilibrium water-based drilling fluid can cause deflocculation of kaolinite clays in a water-wet formation. This is because the clay particles are in equilibrium with the in-situ formation brine and when low saline brine (low cation concentration) is in contact with the clay surfaces they attract the clay’s equilibrium cations thereby reducing the clays counter ion layer’s equilibrium with the in-situ formation brine – salinity shock. A gradual decrease in salinity of the mixing of the in-situ formation brine with introduced water can reduce the deflocculation of kaolinite clays. Deflocculation tends to be much more rapid (almost instantaneous) in comparison to clay swelling – which is also rapid but is slower in effect due to mass transfer limitations associated with the water substituting into the clay matrix. (Bennion 2009).

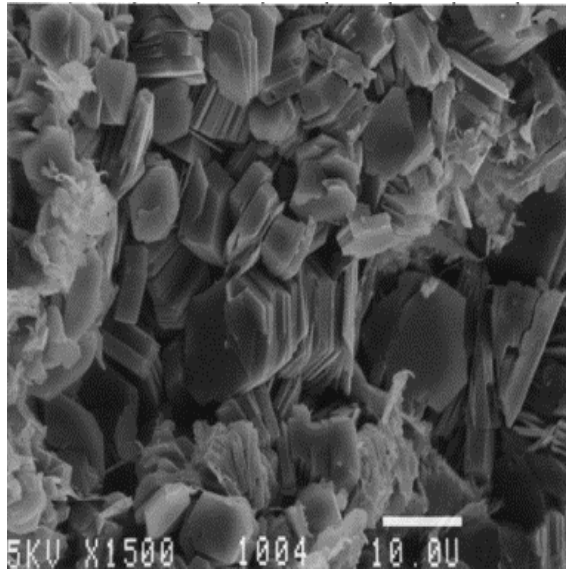


Figure 16 - Kaolinite clay (vermicular) under 1500x magnification showing the booklet stacked configuration, white bar is 10 μm long (Bennion 2009, used with permission).

Clay swelling occurs when water or steam is injected into the formation and is problematic for sand control and plugging of the pore space of the reservoir. The swelling of smectite clays can cause severe permeability reduction and completely plug pore throats. Smectite clay layers are generally $<3 \mu\text{m}$ thick and can swell to 10 times in size after water absorption occurs, but is dependent on the type of interlayer cation present – a sodium-rich clay expands more than a calcium type, the nature of the cations introduced, and the clay's ionic strength. Clay swelling can be caused by a 'salinity shock', where high salinity to fresh water ratio is introduced quickly in a reservoir rock causing a 'shock' to the system. Smectite or montmorillonite clays can become mobile and then migrate causing issues with plugging of the pore space of a reservoir rock or due to it being anionic charged can form thin microfilms on the surface of the slot or sand control

screen. Non-equilibrium water-based drilling fluid can cause swelling of smectite clays in a water-wet formation.

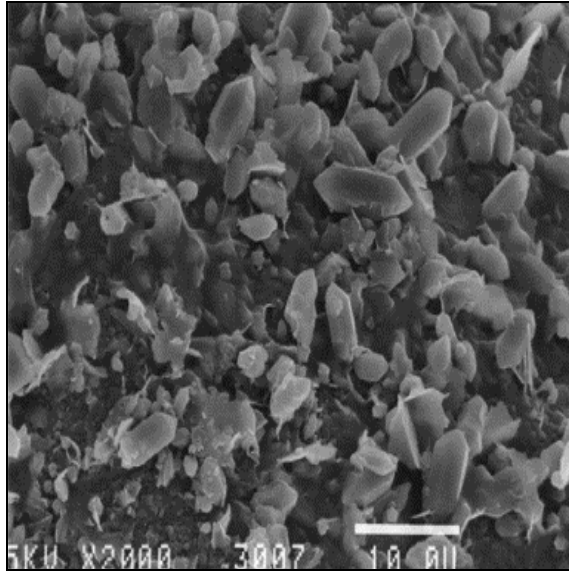


Figure 17 - Smectite Clays (swelling) under 2000x magnification, white bar is 10 μ m long (Bennion 2009, used with permission).

Dendritic illite clays are problematic clays as they form finger-like particles that act like “fishnets” inducing a plugging potential when they become mobile as they can physically block pore throat aperture openings causing fines and clay entrapment. Although similar to smectite clays in chemistry, illite clays do not swell.

3.11 Problematic Clay Content

The maximum range of clay content which would cause a potential for slot or pore space plugging is dependent on the amount of coarse sand grains present but can be estimated to be within <0.5% for clay content, <5% for fines content and a total of <5.5% for both

finer and clays. Clay content near or above this value would be cause for concern for inducing the slots and/or the pore space plugging potential and therefore a seamed slot will help in remediating the plugging potential.

CHAPTER 4: SAND CONTROL ANALYSIS

4.1 Introduction

In the research documented here, the relationship between the slot widths in a liner for a SAGD well is linked to the Particle Size Distributions (PSD's). In practice, when slot sizes are decided for a liner, the most important factor examined is the Sieve Analysis or particle size distribution of core samples obtained from the reservoir. The next issue is then to ensure that the core samples taken from the reservoir provide a good representation of the particle size distribution of the fines and sand within the reservoir.

C.J. Coberly, who published his work on "Selection of screen openings for unconsolidated sands" in 1937, provided a starting point for technical means of designing sand control screens. However, design of screen openings has not received much attention in the literature. The main finding of the laboratory testing results for unconsolidated sands suggest a sand control screen width that is 1 to 2 times the D10 of the particle size distribution. The D10 equates to a value within the particle size distribution which 10% of the particles are greater and 90% of the particles are less than this value. This generalization does not take into consideration the uniformity of the reservoir sand and the differing production conditions which can take place during the life of the well. Therefore, development has been made within this thesis paper by the author, which the optimal sand control slot width for slotted liner's, using the reservoir

particle size distribution, which takes into consideration the uniformity coefficient and other influential parameters.

In the research documented here, a semi-empirical slot width modeling program has been developed out of necessity due to insufficient industry slot width-to-sand control analysis programs. This slot width model analyzes the particle size distribution (PSD) of a sample of reservoir sand and couples theoretical sand control estimations with empirical data.

4.2 Procedure

In the research documented here, core samples were obtained from cored wells in the McMurray Formation, a target for SAGD operations. For analysis of particle size distribution, the following procedure was used:

1. The formation core sample of specific weight is subjected to bulk solvent (the solvent used is Toluene and/or Methanol) extraction to remove all hydrocarbons, water and salt, resulting in clean solids representative of the formation matrix. The amounts of hydrocarbon, water, and solids are measured to ensure that the mass balance is closed.
2. The solids are then dried within an oven.
3. After the solids are dried, the sample is shaken physically through a series of stacked sieves/screens each of finer mesh size as shown in Figure 18. For dry sieving, the required sample size is between 10 and 2000 g. To prevent anionic clays from adhering to larger sand particles, the solids sample can be washed first

and then dried – this method is referred to as a combined wet/dry sieve analysis. The combined wet/dry sieve analysis is the preferred analysis of choice as this gives a better representation of the reservoir particles required for sand control (Bennion 2004). This is because the smaller particles may become electrostatically charged and therefore may be attracted to the surface of larger sand grains, which results in skewed weight measurements for the larger grain sizes and also lower count of smaller sized particles. An example of the data obtained from wet/dry sieve analysis is listed in Table 2.

4. As an alternative to the dry or wet/dry sieve methods, the solids sample can be passed through a laser diffraction meter. However, the required sample size for this analysis is constrained to a maximum of 1 g and thus this technique does not give a good representation of the particles of the reservoir.

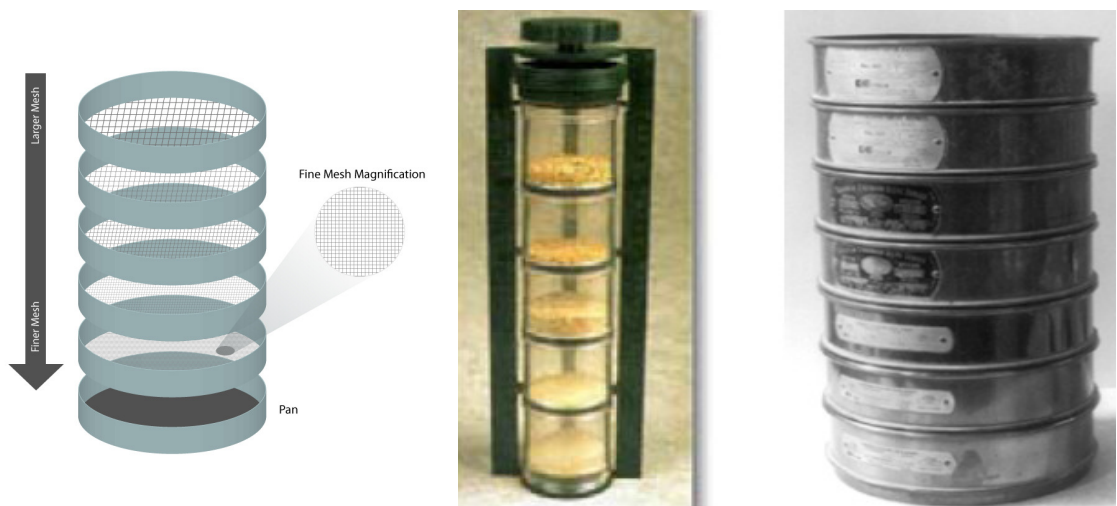


Figure 18 - Series of stacked sieves with progressively smaller sieve sizes below each stacked sieve allowing for the smaller particles to fall through to their respective sieve screen size-to-particle size while the system is being agitated (Introduction to Sieve Analysis University of Memphis 2008).

Table 2 - Experimental results - sieve/screen size and category for retained fraction and cumulative fraction with accordance to the particle size.

<i>Depth (ft)</i>						
<i>Partricle Size (in)</i>	<i>Partricle Size (microns)</i>	<i>Cum. % Sample 1</i>	<i>Cum. % Sample 2</i>	<i>Cum. % Sample 3</i>	<i>Cum. % Sample 4</i>	<i>Cum. % Sample 5</i>
0.0787	2000.00	0.0	0.0	0.0	0.0	0.1
0.0662	1909.00	0.0	0.0	0.0	0.0	0.1
0.0557	1739.00	0.0	0.0	0.0	0.0	0.3
0.0468	1584.00	0.0	0.0	0.0	0.0	0.5
0.0394	1443.00	0.0	0.0	0.0	0.1	1.0
0.0331	1314.00	0.6	0.0	0.0	0.9	1.6
0.0278	1197.00	3.7	0.1	0.8	2.7	2.6
0.0234	1091.00	10.4	1.3	3.7	5.8	3.9
0.0197	993.60	21.3	4.6	9.6	10.6	6.2
0.0166	905.10	35.7	10.7	18.6	17.4	9.9
0.0139	824.50	52.0	20.0	30.7	26.3	15.5
0.0117	751.10	67.7	32.0	44.6	36.8	23.5
0.0098	684.20	80.5	45.7	58.8	48.4	33.9
0.0083	623.30	89.4	59.7	71.7	60.1	45.9
0.0070	567.80	94.4	72.4	81.9	70.8	58.6
0.0059	517.20	96.6	82.6	89.0	79.8	70.6
0.0049	471.10	97.2	89.9	93.2	86.8	80.8
0.0041	429.20	97.2	94.5	95.4	91.6	88.6
0.0035	391.00	97.2	96.9	96.3	94.7	93.8
0.0029	353.10	97.5	98.1	96.9	96.6	96.9
0.0025	324.40	98.2	98.7	97.6	97.9	98.6
0.0021	295.50	99.1	99.2	98.7	98.9	99.4
0.0017	269.20	100.0	100.0	100.0	100.0	100.1

4.3 Particle Size Distributions

Five particle size distributions (PSD's) were measured for an oil sands reservoir that is the target for a SAGD operation. The reservoir location, depth, and thickness are proprietary and will not be disclosed in this thesis. However, the formation is known to be water-wet. The data is listed in Table 2 above. The data was obtained from a wet (laser) sieve data and therefore the percent fines and clay content in the table were not as completely resolved as would be the case for a combined wet/dry sieve analysis. But the data can be manipulated to reduce the fines and clay content measured by excluding the particles less than 44 μm and recalculating the retained weight and thusly the retained

percentage and cumulative percentage per sieve size. This most closely simulates a dry sieve analysis without re-preparing the core and re-testing. This allows the engineer the ability to review and compare the data and results from both the Laser Particle Size Analysis (LPSA) and the modified Laser Particle Size Analysis (modified LPSA) for variability in slot specifications. An LPSA is another mode for measuring particle sizes of sand. LPSA is where a laser light is beamed across falling particles of sand and measures the diffraction and diffusion rate of the light relating to the size of the particle. LPSA takes into account both diffraction and diffusion of the light around the particle. The LPSA measures all sizes of particles passing through the beam of light. This gives rise to very small particles (micron and clay sized particles) being measured. These small micron and clay sized particles are not necessary to be measured as they must be produced through the pore space of the reservoir sand and through the sand control slot. A modified or dry sieve normalized LPSA is more representative of the sand control objective of the slotted liner and of a properly designed sand control slot width as the fines and the clays should be allowed to flow freely and unabated through the pore space and then through the slot. These small and generally suspended within the flowing fluid particles must be handled at and within the facilities.

Figures 19 and 20 display the particle size distributions for Depth 1 and cumulative particle size distributions for all five depths, respectively. The cumulative particle size distributions are listed in Table 3 for completeness.

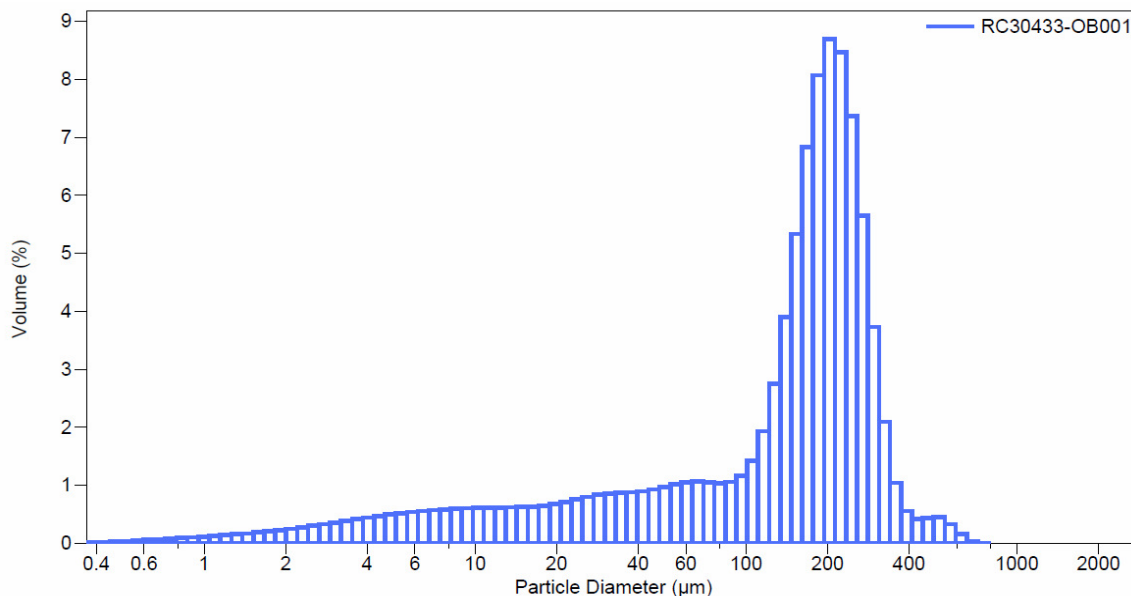


Figure 19 - Experimental results - particle size distribution graph for Depth 1 for the oil sands reservoir.

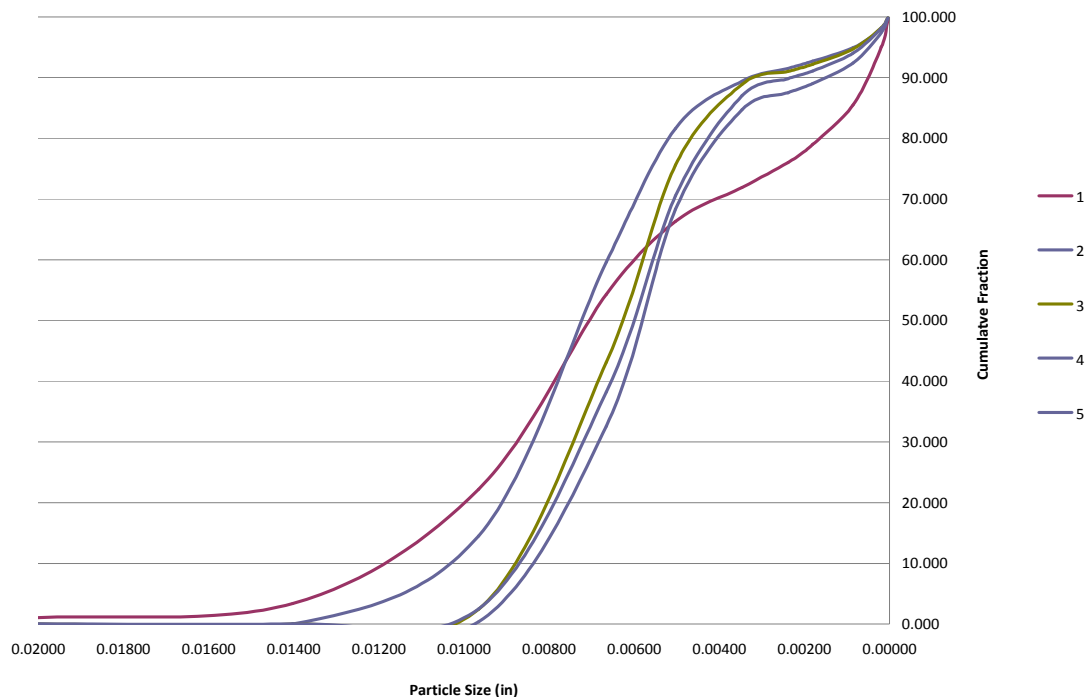


Figure 20 - Experimental results - cumulative particle size distributions of samples obtained at five depths for the oil sands reservoir.

The results of the PSD analysis reveal that the mean size of the sand is equal to 0.0065 inches (165.1 μm). The results indicate that the first depth interval contains a higher percentage of fines and clays as compared to the rest of the data. Each of the intervals and depths analyzed indicate reasonably uniform sand as well as no bimodal distribution of the sand particles. The PSD's analyzed were based on sieves/laser measurements of 517.2 μm , 356.1 μm , 245.2 μm , 168.9 μm , 127.6 μm , 87.9 μm , 60.5 μm , 45.8 μm , 21.7 μm , 4.9 μm and 1.0 μm sizes.

Table 3 - Experimental results - particle size analysis table of results of the five samples or depths for the oil sands reservoir.

Location	Cumulative %				
<i>Size (in)</i>	<i>1</i>	<i>2</i>	<i>3</i>	<i>4</i>	<i>5</i>
0.02036	0.950	0.000	0.000	0.000	0.000
0.01402	3.400	0.000	0.000	0.000	0.000
0.00965	22.200	14.500	2.440	0.380	2.490
0.00665	54.300	59.600	43.100	32.600	38.200
0.00502	66.300	81.600	75.600	68.300	70.500
0.00346	71.900	89.400	88.900	84.700	87.000
0.00238	76.000	91.500	91.000	87.500	89.800
0.00180	79.000	92.700	92.200	89.000	91.100
0.00085	85.500	94.900	94.700	92.400	94.000
0.00019	95.000	98.000	98.200	97.400	98.100
0.00004	99.500	99.800	99.800	99.700	99.800

4.4 Model Development

A simple heuristic model, based on observations from design of slotted liners at Regent Energy, has been developed to estimate limits of the slot size. The necessary input information is obtained from a standard LPSA and consists of the D10, D40, D50, D70, D90 and D95 data. As an example the D10 is the cumulative weight of particles on a

sieve that represents the particles which are larger than 90% of the rest of the particles within the sand sample. This is similar for D40, D50 and so on.

The maximum slot width, $MaxSW$, is estimated as follows:

$$MaxSW = 3.50 D50 \dots\dots\dots (7)$$

The minimum slot width is estimated from:

$$MinSW = 2.00 D70 \dots\dots\dots (8)$$

The Average Slot Width (ASW) is defined as the estimate of the slot width required to prevent sand production from the reservoir. Here, four values of the ASW are calculated.

$ASW1$ is calculated from:

$$ASW1 = 2.00 D10 \dots\dots\dots (9)$$

whereas $ASW2$ is similar to $ASW1$:

$$ASW2 = 1.50 D10 \dots\dots\dots (10)$$

$ASW3$ and $ASW4$ are used as consistency checks on the required slot width size and variability:

$$ASW3 = 1.36 D10 \dots\dots\dots (11)$$

$$ASW4 = 2.29 D50 \dots\dots\dots (12)$$

According to the Wentworth size classification system for grain sizes, listed in Table 4, at 44 microns the typical in-situ particle of this size is classified as mid-ranged coarse silt.

Table 4 - The grade scale that has traditionally been used to classify sediments, called the Wentworth scale (Wentworth 1922).

Millimeters	μm	Phi (ϕ)	Wentworth size class	
		-20		
4096		-12	Boulder (-8 to -12 ϕ)	
1024		-10		
256		-8	Pebble (-6 to -8 ϕ)	
64		-6		
16		-4	Pebble (-2 to -6 ϕ)	Gravel
4		-2		
3.36		-1.75		
2.83		-1.50	Gravel	
2.38		-1.25		
2.00		-1.00		
1.68		-0.75		
1.41		-0.50	Very coarse sand	
1.19		-0.25		
1.00		-0.00		
0.84		0.25		
0.71		0.50	Coarse sand	
0.59		0.75		
1/2	500	1.00		
0.42	420	1.25		
0.35	350	1.50	Medium sand	Sand
0.30	300	1.75		
1/4	250	2.00		
0.210	210	2.25		
0.177	177	2.50	Fine sand	
0.149	149	2.75		
1/8	125	3.00		
0.105	105	3.25		
0.088	88	3.50	Very fine sand	
0.074	74	3.75		
1/16	63	4.00		
0.0530	53	4.25		
0.0440	44	4.50	Coarse silt	
0.0370	37	4.75		
1/32	31	5	Medium silt	
1/64	15.6	6	Fine silt	
1/128	7.8	7	Very fine silt	
1/256	3.9	8		Mud
0.0020	2.0	9		
0.00098	0.98	10		
0.00049	0.49	11		
0.00024	0.24	12	Clay	
0.00012	0.12	13		
0.00006	0.06	14		

The fines and the clays are calculated as follows:

$$\text{Fines \%} = 100 - [\% \text{ Cumulative Value @ } 44 \mu\text{m}] \dots\dots\dots (13)$$

$$\text{Clay \%} = 100 - [\% \text{ Cumulative Value @ } 4\text{-}5 \mu\text{m}] \dots\dots\dots (14)$$

The clay size of 4 to 5 μm as used in Equation (18) has been generally defined and classified by sedimentologists (Wentworth 1922).

4.5 Pore Space Calculation

If the pore space can be calculated to allow for unabated flow of fines and clays, then the plugging potential of the slot is drastically reduced. The pore space and respective slot width size and geometry must be large enough to allow for clay-sized fractions to be freely produced through the pore space and the slot. Also the slot must not be too large that influx of sand into the slot and wellbore takes place with a loss of sand control; therefore a fine line of slot width sizing to particle sizes is required. Based on geometry, the volume of the pore space (*PS*) directly adjacent to the slot is given by:

$$PS = ASW \sqrt{\frac{3}{2} - 1} \cong 0.7071 ASW \dots\dots\dots (19)$$

where *ASW* is chosen from *ASW1*, *ASW2*, or *ASW3* based on the uniformity coefficient, *UC*. The uniformity coefficient is the measure of the relative size variation of the measured sand size and is representative of the slope of the graph of the particle size

distribution. It can also be thought of as the degree to which particles in a sample are the same. It is defined by:

$$UC = d_{40}/d_{90}..... (20)$$

where d_{40} is the effective grain diameter by weight of which 60% will be smaller than this value and d_{90} is the effective grain diameter by weight of which 10% will be smaller than this value. A large value of UC denotes a large range in particle sizes; a gradual slope to the PSD curve denotes a well-graded sand whereas a small value implies uniformly graded sand. Not always, but a uniform sand usually provides an easier means of sand control. If the uniformity coefficient is greater than 10 then the pore space is calculated based on $ASW3$. If the uniformity coefficient is less than 5 then the pore space is calculated based on $ASW1$ and if the uniformity coefficient is between 5 and 10 then the pore space is calculated based on $ASW2$.

4.6 In-situ Particle Arching

The particle arching mechanism of in-situ sand around the slot is calculated based on the slot width, which is critical to sand control and to a reduction in pore space plugging potential. The slot width should be designed to allow fines and clays to be produced through the slot and the pore space in the near wellbore region so as to provide optimal sand control. Factors controlling this optimal design and the formation of in-situ particles arching is slot density, slot width and a seamed slot profile. Equation 19 is developed

from theoretical information on gravel packing and the formation sand and the relationship to infiltration or grains and particles into the gravel. If the median particle size of the formation sand is greater than one third the median pore size of the gravel sand, the formation will form bridging just outside of the gravel, little-to-no sands would come out of the gravel pack. The smaller the formation sand, especially when the formation sand is less than one-seventh of the median pore size of the gravel, the more formation sand would come out. If the median pore size of the gravel sands match well with most of the median particle size of the formation sands, effective bridging would form quickly and easily to prevent smaller particles to flow out. Following Xiang et al. (2003), if the median particle size of the formation sand, D_{50} , is greater than one-third of the slot width, the formation sand will arch over the slot. On the other hand, if the median formation particle size is less than one-seventh of the slot width, the particles will flow through the slot. This rule of thumb is commonly referred to as the one-seventh and one-third rule and provides a simple means to estimate the minimum slot width requirement to invoke arching of in-situ particles at the slot. Based on this one-seventh rule, if a 44 μm fine is required to be produced through the slot then the minimum slot width to achieve this would be 0.012" ($\sim 305 \mu\text{m}$).

The natural bridging tendency (NBT) calculation using the one-seventh and one-third rule is an estimation of the potential for the reservoir sand to arch around the slot during the production phase of the well life. It is understood that the operation of a well can fluctuate which can impact the stability of the arches over a slot. The natural bridging tendency, *NBT*, is defined as:

$$NBT = ASW / D50 \dots\dots\dots (20)$$

From observations of slotted liners, an *NBT* between 3 and 5 typically yields stable sand arches at the slot.

The calculation of whether a seamed slot is required or not is based on the amount of fines and clays within the sand sample. If the amount of fines and clays is larger than 5.5% then it results in a requirement for a seamed slot. This is because more fines and particularly more clays give rise to a higher potential for a slot to become plugged due to these migrating fines and clays with the wetting phase. The seamed slot helps mitigate the risk of plugging due to fines and clays.



Figure 21 - Arched in-situ particles from actual core flow tested under simulated reservoir conditions, 50 μm scale (HYCAL/Weatherford Labs 2003, used with permission).

4.7 Near Wellbore Flow Velocity and Slot Density Calculation

In three phase flow (oil, water and gas) interesting results were observed with the severe turbulence effects associated with concurrent high rate oil, water and gas phase flow resulting in some cases in drastic increases in liner pressure drop and plugging, and in other cases the apparent disruption of the plugging bridges and increases in permeability (Bennion et al. 2008).

A high near-wellbore flow velocity and skin factor can cause plugging issues due to drawdown and drag forces on sand particles. There is an optimal ratio of slot density-to-produced fluids rate which is established by the balance between inflow capability and inflow-induced plugging.

The optimal slot density depends on the length of the wellbore, production rate variability, plugging effects, and phases produced. From observations of slotted liners, the optimal slot density, SD_{opt} , at a given liquid production rate for a minimum flow velocity and volume of fluid to the slot:

$$SD_{opt} = 0.505 \frac{qJ_L}{VLS_L} \dots\dots\dots (21)$$

where q is the fluid production rate (bbl/d), J_L is the joint length (m), V is the volumetric flow rate per slot (L/hr/slot), L is the horizontal length (m), and S_L is the slotted portion

per joint (m). Equation 21 was formulated through identification of flow rate commonality with respect to minimum pressure drops recorded from tests conducted in the laboratory experiments utilizing many different cores and core-slot flow tests. The assumption with Equation 21 is that the flow rate is the same for every slot and by decreasing the volumetric flux linearly can accommodate for slot plugging potential. Alternately, for completions that include blank joints with slotted liner joints, then the optimal slot density is given by:

$$SD_{opt} = 0.505 \frac{q(J_L + B_L R)}{VLS_L} \dots\dots\dots (22)$$

where B_L is the blank joint length (length of liner which has no slots) and R is the ratio of the total length of the blank joints to the total length of the slotted liner joints.

4.8 Results and Discussion

The results of the analysis by using the new model are listed in Tables 2 and 3. The model calculates the uniformity coefficient (UC) and the sorting coefficient (SC). The sorting coefficient is also a measure of the uniformity but over most of the range of particles; this will always give a larger number than the uniformity coefficient and a full spectrum range of variation in sand grain sizes. It is given by:

$$SC = d_{10}/d_{95} \dots\dots\dots (23)$$

where d_{10} is the effective grain diameter by weight of which 90% will be smaller than this value and d_{95} is the effective grain diameter by weight of which 5% will be smaller than this value. Again a large value of SC denotes a well-graded sand whereas a small number denotes uniformly graded sand. Typical ranges for optimum sand control requirements are $UC < 5$ and $SC < 10$ coupled with $< 5\%$ fines and clays. Media aperture selection is often considered difficult for sands with high fines content (Ballard and Beare, 2006). This does not mean that sand control cannot be obtained if one or more of these values rest outside of these ranges, but that it is easier to identify and control if the values are within these ranges. These values are generally specific to a dry sieve analysis or a dry/wet combination sieve analysis but not for laser sieve analysis. Generally, a sand will have a higher uniformity coefficient from a laser particle size analysis (LPSA) than from a sieve measurement, i.e. it will appear to be more poorly sorted with LPSA than with dry sieve (Ballard and Beare, 2006).

Dry or dry/wet sieve will provide a better means of optimum sand control slot width engineering/estimation. The $MaxSW$, $MinSW$, $ASW1$, $ASW2$, $ASW3$, and $ASW4$ are used collectively for selection of a slotted liner slot width for sand control. Slotted liner slot width calculations and corresponding sand control predictions are typically best selected from a dry or dry/wet sieve analysis rather than a laser sieve analysis. But, laser particle size analysis still can be effectively used for selection of a slotted liner slot width by modifying or normalizing the LPSA results to simulate a dry or dry/wet sieve analysis. This can be done by re-calculating the retained weight or measured percentage for any

particles greater than 44 μm and the corresponding cumulative weight retained. This provides a quick and easy modification to the laser sieve so as to simulate a dry sieve analysis. The modified results of the LPSA can now be input into the slot width model to better predict the sand control slot width for the slotted liner. This allows for any particles below 44 μm to be eliminated from the analysis as these particles will need to flow through the slotted liner slot width as well as the pore space within the reservoir sand unabated and freely. The slot widths are based on the *UC* and *SC* and the natural bridging tendency (*NBT*). The pore space, *PS*, is used to estimate the particle size that will be produced and the particle size that will form a stable bridge around each slot. This can vary with drawdown and amount of produced water. This is a rough estimate of the producing particle size and the bridging particle size and naturally these will change with varied well geophysical properties and production dynamics. The *NBT* is the estimated ratio for optimal bridging to occur around the slot and it should have value between 3 and 5. Bridging of the sand over a slot will be disrupted by pressure disturbances/fluctuations and flow reversals. The Seamed Slot requirement is based on the fines and clay content being within a specific range along with the *NBT*. The slot width model results indicate a significant need for a seamed slot width (100% of the samples) and are a result of each of the intervals analyzed showing greater than 5.5% content of fines and clays.

For the example data set used here, the results in Table 5 reveals a maximum slot width equal to 0.0228" and the minimum slot width equal to 0.0101". From the PSDs, the ASW1, ASW2, ASW3, and ASW4 are equal to 0.0201", 0.0151", 0.0138", and 0.0149",

Being that this reservoir has been identified as being an intermediate water-wet, a slot width decrease must be taken into careful consideration since this may increase the plugging potential of the slot or the pore space in the near wellbore vicinity. The maximum slot width specification is the upper limit of a slot width, which would pertain to a potential issue with sand control due to too large a slot width, too large interstitial or superficial velocities, and/or too large drawdown. The base slot of the seamed slot width is designed to also provide sand control if the seamed slot becomes eroded; this is a secondary sand control slot width. It is important for the slotted liner to control the potentially erosive sand while allowing smooth production of the clays and fines.

The maximum slot width is calculated to provide a basis for evaluating the PSDs for the largest slot allowable before sand control becomes no longer applicable. In other words, a large slot would provide little to no sand control and increase the slot plugging potential and wellbore filling with sand. Logically, the minimum slot width is the exact opposite evaluation as the maximum slot width. A slot which is equal or smaller than the minimum slot width provides too much sand control which reduces the pore space created in the arching of sand particles above each slot and therefore would increase the pore space plugging potential of fines and clays being mobile and the respective drawdown requirements. The slot width recommendation from the results of analyzing the 5 PSDs is between 0.023" and 0.010", but it is understood that selecting a slotted liner slot width less than 0.012" could give rise to an increase in pore space plugging of fines and clays. Therefore, from Table 5 the slot range will be from 0.0228" (effectively

0.023”) to 0.0138” (effectively 0.014”). From generally accepted slot manufacturing capabilities and blade widths, the slotted liner slot base width will be from a selection of the circular saw blade sizes of either 0.012”, 0.014”, 0.016”, 0.018”, 0.020”, 0.024”, 0.028” or 0.034”. The seamed slot width (the seaming machine forms a keystone profile of the slot on the outside diameter of the pipe’s slot(s) through plastically deforming the slot(s) locally and the inside diameter of the pipe’s slot(s) will be the same width as the circular saw blade selected to initially cut the slot(s) into the pipe) does not have a limit on the size it can seam down to except that it is generally acceptable not to seam more than a 0.010” differential. When reviewing the results in Table 5, ASWs 2, 3 & 4 converge, as an average, on a slot width of between 0.014” and 0.015”. Therefore, when using the results as a basis of selecting a slot width the requirement for seaming is reviewed first, which in Table 5 suggests that 100% of the sieves should be seamed, and the fact that ASWs 2, 3 & 4 converge on a slot width between 0.014” and 0.015”, this should develop the basis of a recommended O.D. slot width. The base slot and the seamed slot should be selected for separate sand control means against the sieve analysis results. It could be viewed that if the seamed slot width were to erode for any reason then the base slot width should provide the backup sand control. This provides for a primary selected sand control slot width defined as the seamed slot width on the O.D. of the pipe and the secondary sand control slot width defined as the base slot width. Therefore, from the results in Table 5, the base slot width must be smaller than the maximum slot width of 0.023” and equal-to or greater than 0.004” bigger than the selected seamed slot width. From Table 5 results all slots should be between the minimum and maximum slot widths identified by the model. A slot larger than the identified maximum slot width will give

rise to higher potential for sand infiltrating into the slotted liner and a slot width less than the identified minimum slot width will give rise to a higher potential for pore space plugging in the reservoir. Therefore, from Table 5 the recommended slot widths, and in no particular order, could be as follows:

- 1) 0.018" I.D. Slot Width and 0.014" O.D. Seamed Slot Width
- 2) 0.020" I.D. Slot Width and 0.015" O.D. Seamed Slot Width
- 3) 0.024" I.D. Slot Width and 0.014" O.D. Seamed Slot Width
- 4) 0.024" I.D. Slot Width and 0.015" O.D. Seamed Slot Width
- 5) 0.024" I.D. Slot Width and 0.018" O.D. Seamed Slot Width

Although due to manufacturing tolerances on the slot widths, the 0.014" and 0.015" seamed slot width would be close to being one and the same. Therefore, the actual slot recommendations reduce to the following options:

- 1) 0.018" I.D. Slot Width and 0.014" (0.015") O.D. Seamed Slot Width
- 2) 0.020" I.D. Slot Width and 0.014" (0.015") O.D. Seamed Slot Width
- 3) 0.024" I.D. Slot Width and 0.014" (0.015") O.D. Seamed Slot Width

It must be taken into consideration the fact that the pipe's yield point must be exceeded to plastically deform the slots during the seaming process and the selection of seamed slot width with a slot differential of 0.010" (0.024" subtract 0.014") may see excessive forces and may cause the pipe to locally deform greater than the wall thickness. Therefore, a slotted liner specification of 0.020" seamed to 0.014" (0.015") should provide good sand control.

100% of the sieve intervals require a seamed slot and due to the relatively good UC and the higher percentage of fines and clays particles present; the O.D. slot width is recommended to be near 0.014”-0.015” for these reasons.

The pore space size of the in-situ reservoir sand that would form an arch around the slot is estimated from the slot size selected for that sieve depth analyzed and is calculated based on Equation 19 and the respective slot width selected and is averaging 0.013”, which is very close to the recommended slot width. This pore space geometry provides for a particle size of ~47 μm , which is of fine particle size range and is estimated to be produced through the pore space. The particle size that is estimated to provide the arching over the slot, the corresponding pore space geometry and the fines and clay migration is equal to about 110 μm .

The results listed in Table 5 of the analysis reveal that the optimal sand control will be conducted with a slot width between 0.023” and 0.014”, which would provide sand control with reduced potential for near wellbore plugging represented by the five (5) sieves intervals provided.

More complex slot width specifications can be derived by delving deeper into each subgroup of sands with additional PSDs from more samples and developing a detailed target depth-to-sand interval and specific slot width, as shown in Figure 22. It is important for the slotted liner to control potentially erosive sand while allowing

production of clays and fines. Figure 22 is an example of the results of many PSD's analyzed for a reservoir sand and the samples at interval 1990.00 and at 1993.00 provides clear indications of shale baffles as the program identified an extremely small slot size requirement. These values have all of the slot specifications being well below the minimum slot width requirement, which is generally an indication of a non-sand sample or interval of shales. The model also can provide an indication of the variability from depth-to-depth.

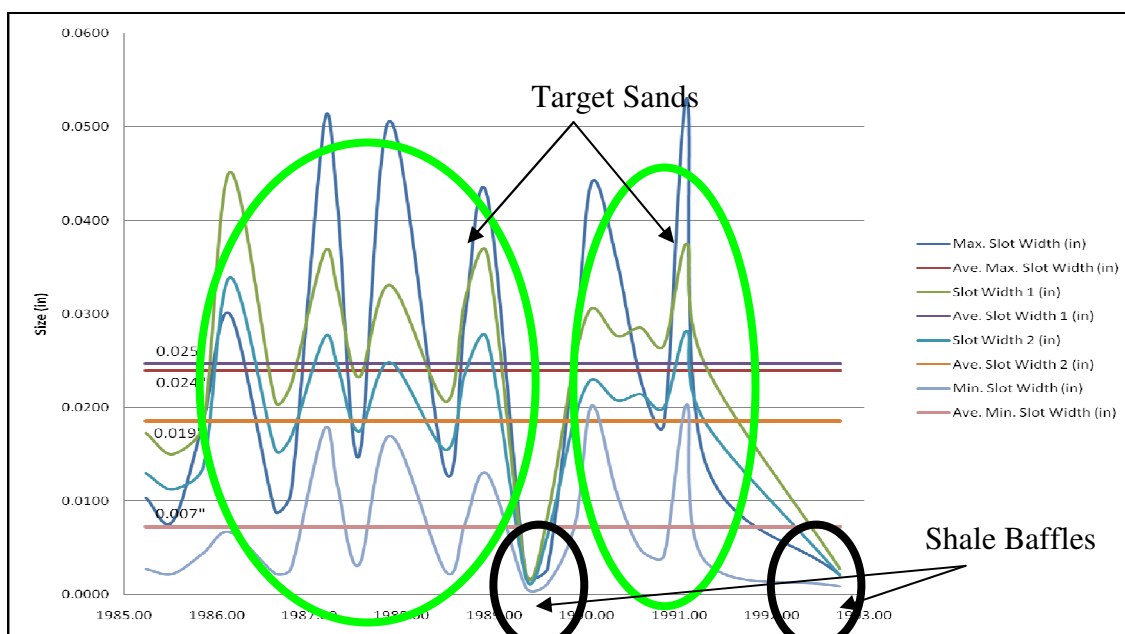


Figure 22 - Example of slot width modeling program displaying the analyzed sieve results with optimal slot width specifications and zones of shales.

4.9 Conclusions

A new simple heuristic model was developed that provides estimates of the perceived slotted liner slot width requirement for sand control. The model analyzes standard PSD's in a comprehensive manner and provides for a good estimate of the slotted liner sand

control slot width required. The uniformity coefficient, the pore space geometry and empirical data are utilized in the model for estimating the required slot width. The model predicts the natural bridging tendency of the in-situ sand and also estimates the pore space geometry and corresponding particle size that will most likely be produced through this pore space and the particle size that will most likely form stable arches over the slot. The model also provides an estimate of the maximum slot width and minimum slot width.

Analysis of PSD's alone can provide a good starting point for sand control slot width requirements on a small scale and a reservoir sand specific interval. It is necessary to continue to develop and to calibrate the model specifically to other reservoir sands through flow testing in the laboratory as well as field data.

CHAPTER 5: SLOTTED LINER MANUFACTURING

5.1 Introduction

Slot size and open area play major roles in throttling inflow. Therefore, the slot geometry should be chosen to prevent sand entry and bridging or plugging within the slot. To do this, a slot width calculated from the particle size distribution which allows production of fines and clays is essential. It is important to control the velocity of flow near the wellbore to an acceptable value as this will help to reduce pore space plugging potential and slot plugging potential. Here, results on mechanical manufacturing of slots for slotted liners are described. Besides metal-to-metal slotting, there are several other methods briefly discussed which include laser slotting, electric discharge milling, and water-jet slotting, although less common, these modes can also be used to cut slots into well liners. They are briefly reviewed in the following sections.

5.1.1 Laser Slotting

Laser cutting is considered more difficult and more expensive than water jetting and mechanical blade slotting for maintaining the precision tolerances of the slot profile and finish as is required for optimal sand control. Furthermore, the capital costs for a laser-cutting machine is considerably higher than a full metal blade slotting machine. Laser slotting technology is better suited for end cutting and not for piercing through the pipe. Previous research has shown that the quality of laser slots tend not to meet slotting

industry standard slot width tolerances of $\pm 0.002''$ and sometimes as low as $\pm 0.001''$. Furthermore, heat generation causes welding of material within the slot which leads to an unfinished slot as shown in Figure 23, as well as a heat affected zone; thereby altering the pipe's composition and the pipe's microstructure. The time required to initiate the hole in the pipe, before traversing takes place to create the slot, is long which further creates a tapered pierced hole larger than the slot width created by the traversing laser.

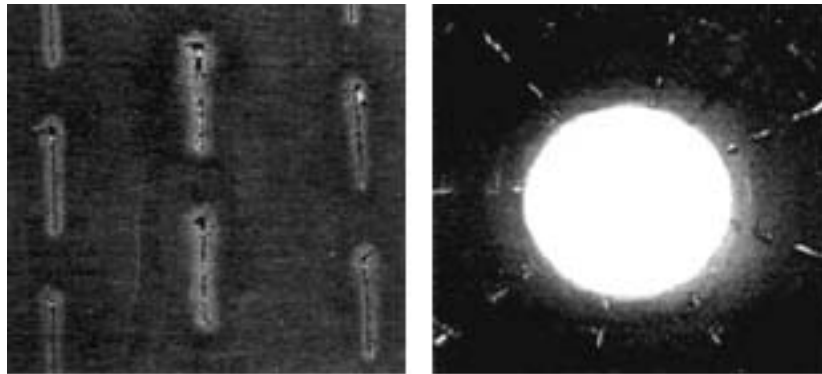


Figure 23 - Laser cut slots with intermittent slots created, heat affected zones and low quality slots (Roscoe moss Company 2006).

5.1.2 Electric Discharge Machining

Electric discharge machining (EDM) cutting technology produces excellent surface finish making its perceived performance for sand control excellent. However, similar problems exist as is the case with laser slotting technology in that EDM works best if the start of the cutting process is from an end instead of from a created pierced hole from which the slot is extended. With current equipment, EDM slots are not commercially available because of process and mechanical deficiencies (Moulton, 2000). Manufacturing an

EDM cut slot may work for testing of one slot at a time but is not economic on a commercial scale (Moulton, 2000) where up to 10,000 slots may exist in a single liner.

5.1.3 Water-jet Slotting

The quality of the cut obtained from abrasive water jet (AWJ) slotting, in comparison to the cut quality created by mechanical slotting (described below), is observed to be of equal to slightly higher quality (Kern, 2009). The slight improvement is more recognizable at reduced cut rates in comparison to cut rates which are achievable with the mechanical cutting technology (Kern, 2009). A problem arises with water jet cutting technology with respect to cut start and cut lag. The water jet abrasive water stream must penetrate through the wall thickness of the casing and so requires the cutting head to be moved back and forth rapidly over a length scale equal to approximately 0.030". After the cutting head has penetrated through the wall thickness, there is a cut lag time created which at the end of the slot cut requires the cutting head to be held at the localized area to finish the cut (Kern, 2009). Otherwise the slot is of a 'funnel' or 'taper' creating a larger outside slot width than the inside slot width. As a result, AWJ slotting requires more time to start the cut and to finish the cut, which reduces production time, than a mechanical slotting process. One benefit of AWJ slotting is that the water jet slot generally does not have metal wickers created on the inside diameter of the casing as is often found with mechanical cutting, and therefore reduces the need to rigorously clean the slots on the inside of the pipe to remove these metal wickers. An issue with AWJ slotting is that the AWJ requires significant energy to perform the cut, which needs to be

dissipated upon exit from the inside of the slot as the water jet could “sandblast” or “cut” the opposite side of the casing on the inside diameter wall creating thinning of the pipe wall. This could create structural casing damage which could affect the performance of the liner under combined installation loads or thermal in-situ loads.

5.1.4 Metal-metal Slotting / Slot Milling

Custom reservoir specific engineered slotted and seamed liner provides the highest of quality representative sand control. Metal-to-metal blade created slotted liners have been utilized in a wide range of oil and gas applications such as Steam Assisted Gravity Drainage (SAGD), Cyclic Steam Stimulation (CSS), Coal bed Methane (CBM), Cold Primary, Cold Heavy Oil Production with(out) Sand (CHOP(S)), and water wells/dewatering wells.

Slot milling presents one of the most severe machining environments of any of the macro or micromachining processes (Knight, 2005). The correct cutting speed is an integral part of the cutting process. Exceeding the optimum cutting speed, with high speed steels, has detrimental effects on the blade’s wear rate and can present instantaneous wear (Trent, 1977). The diameter of a slitting saw is much larger than that of a mill cutter and it has more teeth. This corresponds to a surface cutting speed that is larger than the mill cutter, even at a low cutting speed. Therefore, a reduction in the surface cutting speed is very important due to the fact that the correlation of heat due to friction and wear rate is high. The major cause of tool failure at high cutting speeds is thermal cracking and burn-up

(Knight, 2005). Thermal cracking occurs because the edges are exposed to a high level of thermal shock due to the high temperatures caused by high speeds and high degree of temperature changes typical of the process. At low cutting speeds, cracks of a mechanical nature are mainly responsible for tool failure, as cutting forces are higher and temperatures are lower. Therefore, there is a trade-off between cutting speed and feed rate. Cracks of a mechanical origin may occur due to shocks either at the entrance of the blade tooth into the pipe or during the exit of the blade tooth from the pipe. Coolant is applied liberally to control the temperature originating from friction-generated heat. The cutting blade enters and exits the liner several times per second leading to blade breakage. In addition, the chip thickness, which is a small strip of metal created during the cutting process from a blade's tooth removing the pipe's material, varies as the cutting edge penetrates the work piece (related to the rake angle and the shear cutting angle). Regular (acceptable) tool wear will be predominant only if the tool is tough enough to resist the mechanical and thermal shocks of the process (referred to as blade fracture toughness).

Problems due to shocks at the entrance of the blade tooth into the pipe can be worsened by the tendency of the chip to adhere to the tool rake face. When the blade tooth is ready to exit the pipe, it causes a rotation of the primary shear plane or angle, making its angle negative and instantaneously increasing the force on the blades edge. This phenomenon can be seen with curled edges of the slot on pipe material and can be associated with wear rate of the blade tooth and/or high tooth loads/hard pipe surface. The entrance of the blade tooth into the pipe is more critical for the chipping of the cutting edge than its exit

(blade fracture toughness). The frequency of entrance of cutting edges into the work piece is very important factor influencing the tools wear and tool-life (number of teeth). What is very important is the number of times each cutting edge enters into the work piece (impact frequency) and the heat generated by the friction between work piece and tool and between chip and tool, which are caused by the increase in cutting speed.

In micromachining, the cutting edge, and not the overall tool geometry, determines the effective rake angle which is normally largely negative. It's important that the cutting edge radius be less than the feed-per-tooth. More care must be taken when constraining the work piece against the cutting forces. If the pipe clamp contact force is too small, the pipe may move or vibrate during machining, so the idea is to apply a larger clamping force but too large a force (i.e. large stress) also induces strain (surface and internal displacement and stored strain energy) in the work piece, which upon unclamping the work piece the stored strain energy will be released and the pipe will change shape causing machining error.

5.1.5 Slotted Liner Geometry and Simple Slot Mathematics

The slotted liner configuration and mode of manufacture is important. The slots are staggered and offset from column to column. This provides for maximum torque capacity for a slotted liner configuration. The column of slots or slots per column is the number of slots in a radial column of slots in a specified length of pipe. The columns are radially spaced three, six or twelve inches apart. The strength of the slotted liner is

important for resisting deformation loads during installation and/or under thermal production loads typical of SAGD operations. The ring is the uncut axial area in between the column of slots and because the column is separated by 3, 6 or 12 inches, the uncut length is 3, 6 or 12 inches minus the slot length on the outer diameter. As a general rule of thumb, the radial spacing of the slots in a column (sometimes called the rib) should not be smaller than the wall thickness of the pipe, so as to maintain geometric similarities and strength.

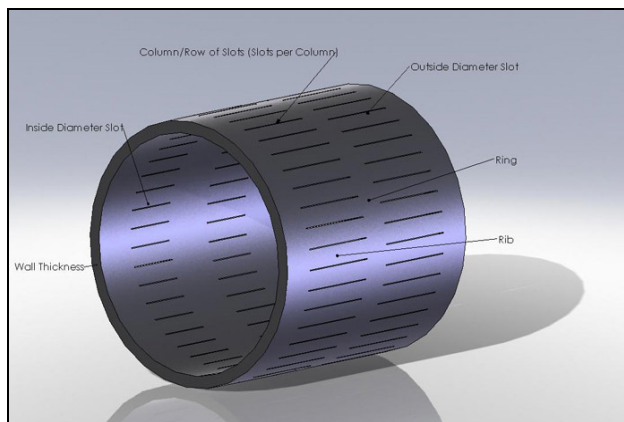


Figure 24 - Blade slotting configuration and depicting the staggered offset per column and an uncut column between slots so as to provide axial pipe strength (Regent Energy Group Ltd. 2010).

An analytical solution for calculating the pipe wall thickness, D_{WALL} is given by:

$$D_{WALL} = \frac{D_{OD}}{2} - \sqrt{\frac{D_{OD}}{2} - \frac{P_w}{12\pi C_f}} \dots \dots \dots (24)$$

where D_{OD} is the pipe outside diameter (inches), P_w is the pipe weight (lb/ft), and C_f is a constant between 0.280 and 0.290. The value of the constant was developed in-house and is based on taking a weight function and converting it into a linear function mathematically and is referenced to the pipe wall thickness in API 5CT. The blade plunge depth, B_{PD} , required to obtain a specific outside diameter slot length is equal to:

$$B_{PD} = \frac{B_{OD}}{2} - \sqrt{\left(\frac{B_{OD}}{2}\right)^2 - \left(\frac{SL_{OD}}{2}\right)^2} \dots\dots\dots (25)$$

where B_{OD} is the blade outside diameter in inches and SL_{OD} is the outside diameter slot length in inches. The calculation for the inside diameter slot length, SL_{ID} , is given by:

$$SL_{ID} = 2\left(\sqrt{(B_{PD} - P_w)(B_{OD} - (B_{PD} - P_w))}\right) \dots\dots\dots (26)$$

5.1.6 Straight and Seamed Slot

Historically, slotted liners have not been able to offer the very small opening sizes of wire-wrap screens to prevent fine sands from being produced, until now (Kasier et al. 2000). Advancements in slot manufacturing methods can now provide openings that can surpass the size and tolerance of wire-wrapped screens while still providing the robust nature of slotted liner for installation. Most slotting of pipe is done mechanically by using slitting cutters on a gang-type milling machine (Milovric 1983). Due to mechanical

limitations on slitting cutter dimensions, a post slitting process must be applied to obtain thin slot widths. Regent Energy Group Ltd. has developed such a process referred to as seaming which produce slot geometries having a “keystone” slot geometry. Figures 25 and 26 compare the geometry of regular slots and seamed slots.

In seaming, the slot is formed with a low invasive strain-induced technology called circumferential seaming or transverse rolled slot. No material is added to or removed from the pipe during the seaming process. The pipe itself provides the material necessary to create a seamed slot profile, which is created through local plastic deformation. Stress and strain applied on the outside diameter of the pipe, above the yield point of the pipe material, provides the necessary stresses to create the tapered seamed profile of the slot. This manufacturing technique provides an extremely precise slot width quality control, with accuracy of $\pm 0.002''$ on target slot widths of $< 0.030''$. Precision seamed slotted liner reduces slot plugging potential by providing anti-plugging, self-cleaning characteristics superimposed on a straight slot thereby creating a “true” keystone slot.

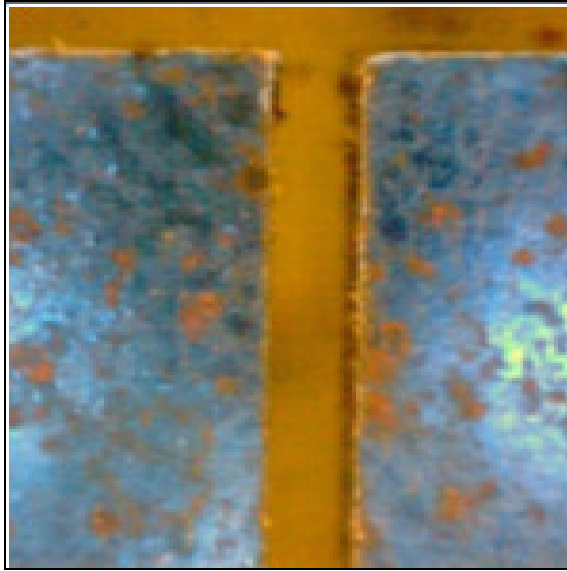


Figure 25 - A typical straight slot profile of a blade created slot (Regent Energy Group Ltd. 2003).

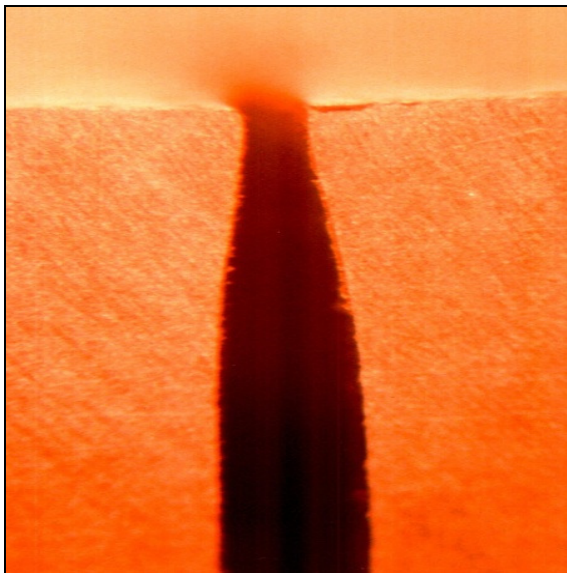


Figure 26 - A typical seamed slot profile showing the differential slot widths from O.D. to I.D. with the larger aperture opening on the I.D. of the pipe (base slot) (Regent Energy Group Ltd. 2003).

It is imperative that sand control devices not plug or produce sand and the seamed slot provides an added assurance that the slot will not plug. Seamed slots offer anti-plugging

characteristics to a straight slot and are extensively used in unconsolidated heavy oil and bitumen reservoirs. This can also be attributed to the fact that the steam's thermal effects on the chemical and inter-granular bonding can dramatically increase or decrease the sanding potential not necessarily typical when little to no thermal recovery is introduced. Also the amount of fines and clays present in the reservoir, above an identified threshold value, can significantly increase the plugging potential of a slot. A plugged slot dramatically increases the skin factor due to the slot becoming an extension of the reservoir (instead of an open channel), resulting in an added slot convergence skin factor. A plugged slot's flow behaves as a porous medium and thus its flow is governed by Darcy's law and not open-channel flow expressed by an analog to Poiseuille's equation for flow in a rectangular slot.

5.1.7 Slot Surface Finish

Slot surface finish quality is a key control on plugging with sand in the liner production setting. Small particles and clays can adhere to the rougher surface finished slots and, due to the particles' polarity, can attract more particles and eventually plug the slot. Surface roughness is proportional to the cutting speed. The harder the pipe material, the lower the cutting speed i.e. L-80 is harder than K-55 which is harder than J-55. A pipe's microstructure is the single most important factor in identifying the machinability of the pipe. Two entirely different microstructures of a similar pipe grade can have the same hardness but give different machinability ratings. A pipe's hardness is not the best method of qualifying machinability of a pipe but when coupled with microstructure can

be very helpful. As a general rule the harder the pipe material (greater the carbon content) the harder the cutting forces and increased tool wear and reduced tool-life. Any given pipe is more difficult to cut when it is harder than when it is softer (warm pipe versus cold pipe). Hot rolled pipe can create a hard surface finish ($<0.030''$) making cutting difficult. Cold working the pipe increases its hardness. It is necessary to reduce cutting speed when cutting harder material (L-80 versus J-55). Normalizing the pipe can help reduce inclusions and hardness variation among the pipe.

5.1.8 Slotting Blade Nomenclature

Figure 27 and 28 depict the nomenclature and common design and parts of a slotting blade, which are common to all slotting cutters. The pitch refers to the angular distance between like or adjacent teeth. The pitch is determined by the number of teeth. The cutting edge is the angle on each tooth that performs the cutting. The land is the narrow surface behind the cutting edge on each tooth. The rake angle is the angle formed between the face of the tooth and the centerline of the cutter. The rake angle defines the cutting edge and provides a path for chips that are cut from the work piece.

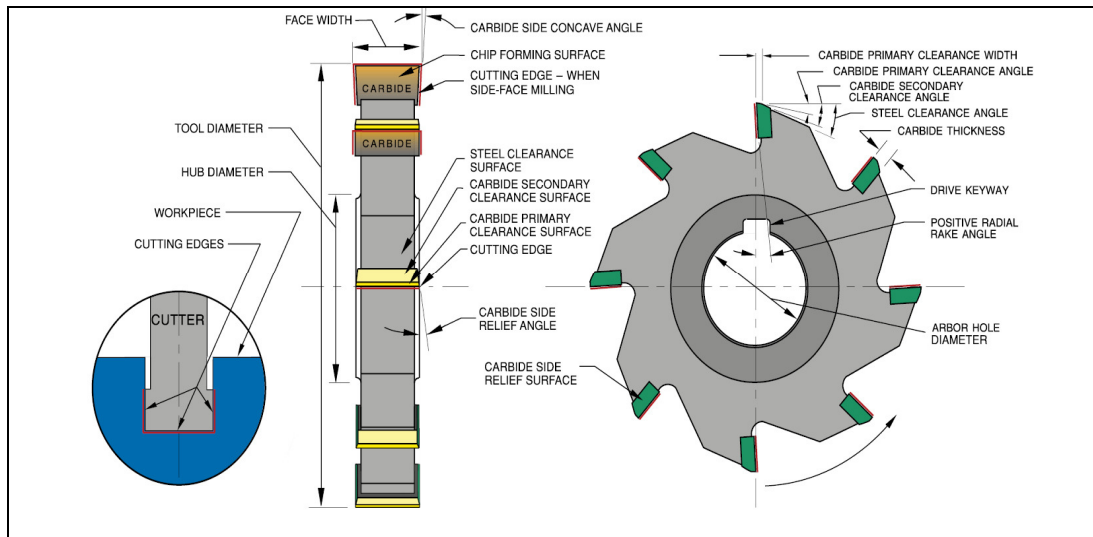


Figure 27 - Slotting blade nomenclature, geometry and cutter surface (www.steelcuttingtoolspeedsandfeeds.com 2010).

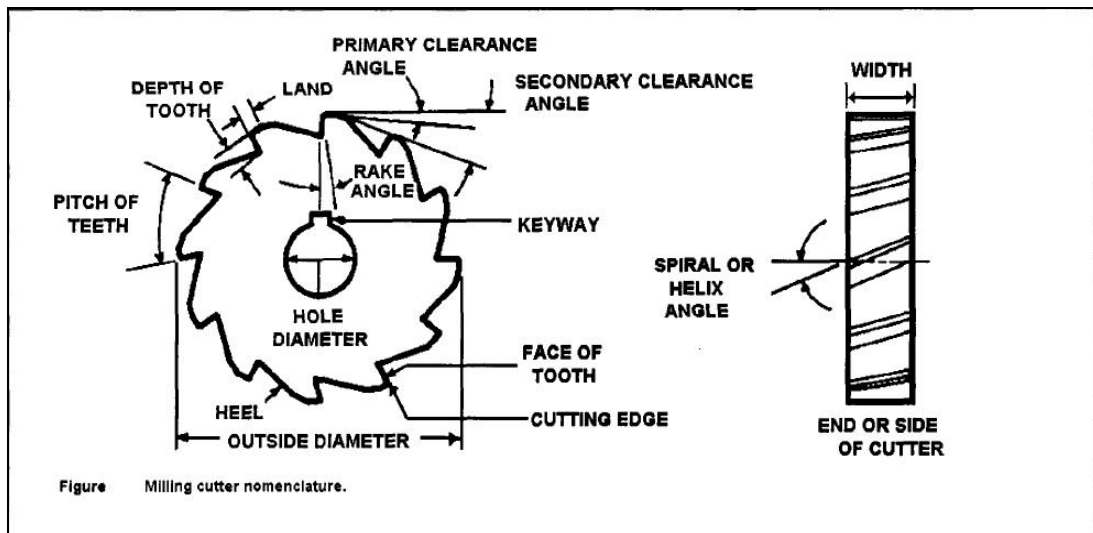


Figure 28 - Slitting saw blade nomenclature, geometry and helix angle for chip formation relief (Mechlook 2010).

The primary clearance angle is the angle of the land of each tooth measured from a line tangent to the centerline of the cutter at the cutting edge. This angle prevents each tooth from rubbing against the work piece after it makes its cut. This angle defines the land of

each tooth and provides additional clearance for passage of cutting oil and chips. The hole diameter determines the size of the arbour necessary to mount the milling cutter.

The effectiveness of a cutting blade by its rake and relief angle, and subsequently the blades tooth form, are important blade characteristics to understand for maximizing blade use and tool-life. Generally, changing the blade's rake angle changes the effective primary shear cutting angle, tooth load-to-chip ratio, and therefore power requirement. The changes in the blade's rake angle will ultimately affect the tool-life of the blade. It is important to note that the pipe material plays an important role in the effectiveness of the blade's rake angle and tool-life. Changing the pipe material can change the primary shear cutting angle, tooth load-to-chip ratio and power requirement.

5.2 Experimental Apparatus

Laboratory testing was conducted on a single milling machine head with a single arbour as well as being classified as a surface grinding machine to reduce the influence of outside parameters and the degrees of freedom that a typical slotting operation would be faced with so as to provide for unbiased or low variability in results. The milling machine was equipped with an NC controller along with an electronic data acquisition software program as well as contained a simple fluid delivery system and reservoir for application towards the blade for cooling and lubricating the blade during the slotting process. This machine provided the means to maintain good control on the system for gaining tool-life and spindle torque feedback as well as insight into the slotting process on a general scale. But due to the demands of the industry and the multispindle slotting

operations as well as the fact that there is significant interference of one spindle and blade to another spindle and blade, the transferability of the single milling machine and labour laboratory results did not transfer very well to the industrial setting.

Therefore, testing was removed from the laboratory and into the industrial setting. Effort was made to generate general trends and understandings in the laboratory slotting process, which were to be used on the industrial slotting machines to minimize the degrees of freedom of the industrial testing of the tool-life of the blades. This not only provided a very good means to identify the largest contributing factors to the slotting process and tool-life, but it allowed a means to conduct economies of scale with respect to differing parameters and machines. The industrial machines have multiple arbours or spindle heads equally spaced apart with single circular slitting blades mounted to each, which are then plunged simultaneously into the pipe and in parallel to the longitudinal axis of the pipe during the slotting process. Each machine is equipped with a data acquisition system and are computer numerically controlled (CNC). Quantitative analysis of tool-life per spindle was recorded and results analyzed as well as the data captured machine dynamic results.

5.3 Results

5.3.1 Slotting Blades Up Milling and Down Milling

In the up milling cutting mode, as shown in Figure 29, the blade rotates against the direction of feed of the work piece and in the down milling cutting mode, the blade

rotates with the direction of feed of the work piece. The chip formation is completely different with respect to the two different cutting modes. In up milling, the chip is very thin at the start of the cut and progressively thicker to the finish of the cut. The opposite is true in down milling; here the chip is maximized at the start of the cut subjecting the tool to high forces due to impact loading. Slotting is an interrupted cutting process wherein entering and leaving the slot subjects the tool to impact loading, cyclic heating and cycle cutting forces and due to plunging into the work material causes the impact loading, cyclic heating and cyclical cutting forces to rapidly change for each increment of plunge depth. This form of cutting is susceptible to highly random tool-life results and unpredictable tool-life estimations, especially with smaller width blades. The highest cutting force, indicative to the slotting process, is at 90° to the surface of the pipe material in the tool's plunge direction and the highest spindle cutting torque recorded is precisely prior to the blade penetrating through the pipes' wall thickness. The cutting torque was recorded between up milling and down milling tests to differentiate between process torque requirements. Figure 29 represents the maximum relative cutting torque requirements between up milling and down milling with a single slotting blade.

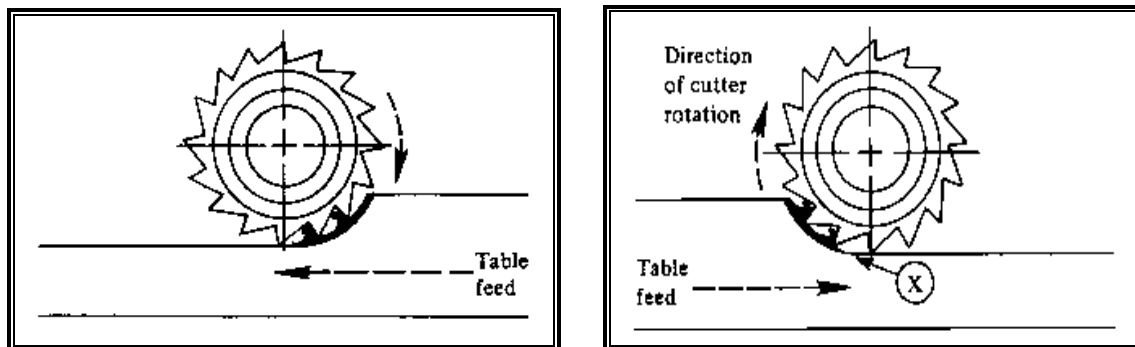


Figure 29 - Schematics of down milling and up milling, respectively, depicting the milling orientation and table feed direction, which depict that down milling starts the cut with a high tooth load (Fundamentals of Machining and Machine Tools 2005).

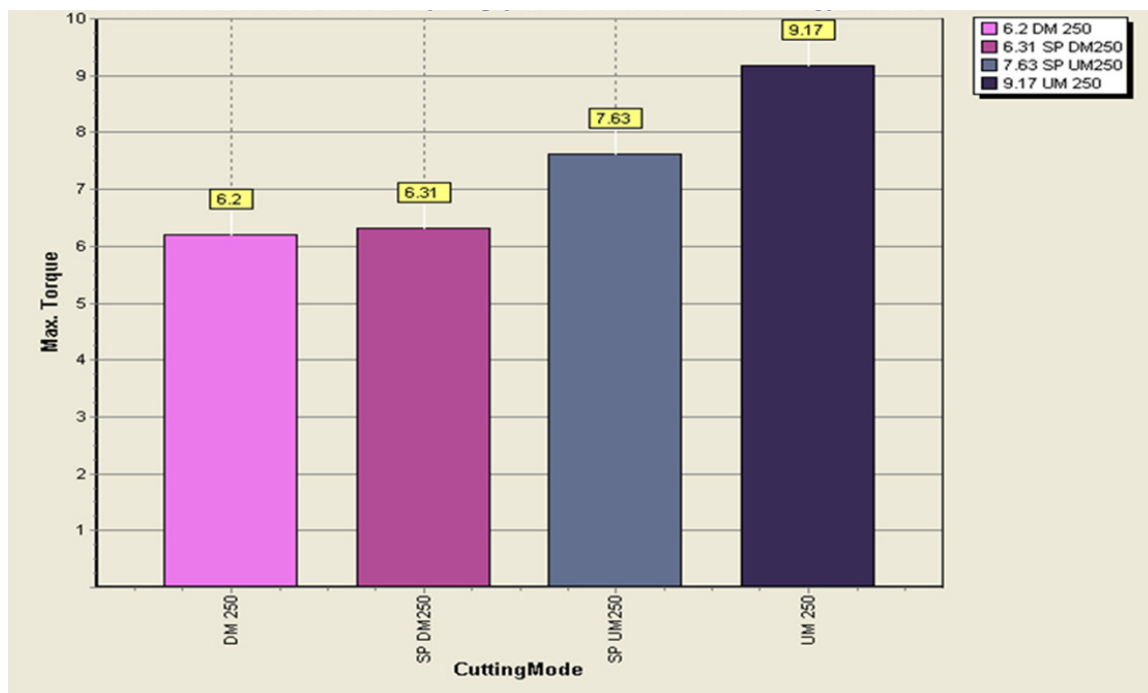


Figure 30 - Experimental results - up milling and down milling laboratory test torque results on a single material and under similar machining conditions.

The results in Figure 30 reveal that there is a 20 to 40% increase in relative cutting torque required for up milling when compared to down milling under identical cutting

conditions. This may be due to up milling requiring high compressive forces to start the cuts and down milling requiring impact strength to start the cuts. In slotting “up milling” and “down milling” are occurring simultaneously, dynamically and interruptedly. When the blade has penetrated through the wall thickness of the material major interrupted cutting occurs to the magnitude of twice that of cutting the pipe’s wall thickness. During the slot’s formulation, the blade penetrates the pipe’s wall thickness and performs two modified down milling processes and therefore doubles the interrupted cutting. Incorporating the lowest spindle cutting torque required milling process (down milling according to the test results) whilst simultaneously plunging, as the blade penetrates through the wall thickness of the pipe, may be an area for valid testing for the subsequent effects on blade torque and tool-life.

5.3.2 Cutting Geometry and Shear Cutting Angle

For effective cutting, the cutting tool matrix must be harder than the work material. This indicates that the process of cutting is of plastic deformation of material work piece with the degree of plastic deformation dictating the chip formation; Figure 31 provides a depiction of chip formation. Figure 32 displays chip formation observed in the experiments conducted here. Figures 33 and 34 display cutting terminology and illustrate the location of heat generation during cutting.

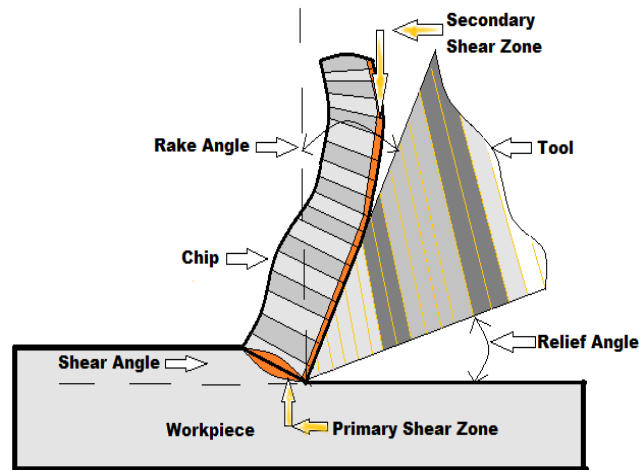


Figure 31 - The primary shear cutting angle gives rise to the chips thickness and the secondary shear cutting zone generates heat into the chip and the tool's tooth during the cutting process.

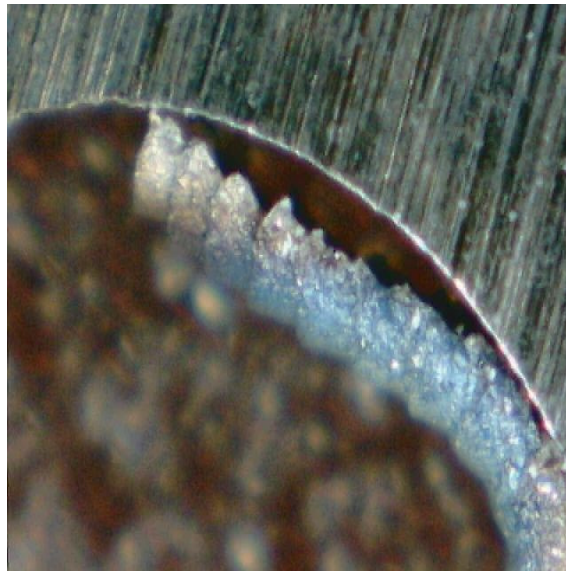


Figure 32 - Shear cutting angles and chip form from an actual cut slot.

The shearing zone shears the metal atoms immediately ahead of the cutting edge by severely compressing the metal atoms within the shear zone, which result in temperatures great enough to permit plastic deformation (cutting). Work hardening (the increase of

dislocation density) is a principle of resisting stresses of a work material exceeding the work material's elastic limit, therefore generating a new elastic limit and deformation resistance. This is demonstrated most dramatically in stainless steels.

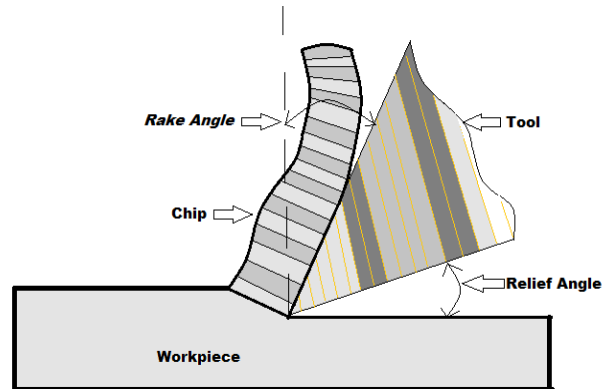


Figure 33 - Cutting nomenclature showing the relief angle, blade tooth, rake angle and chip formation.

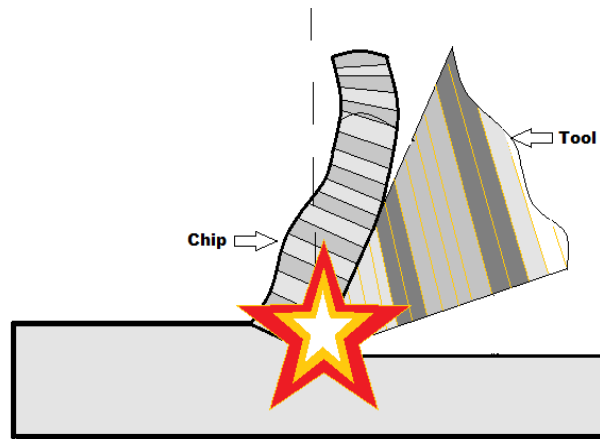


Figure 34 - Cutting force and impact zone causing tooth breakage due to impact forces.

The dynamic cutting process of a dull tool is one which is “plowing” through the pipe instead of “cutting” the pipe. This generates unnecessary heat dulling and wearing out the tool and possibly premature breakage.

The friction involved within the primary shear zone is the deformation of the material by the tool and is responsible for approximately sixty (60%) percent or more of the total heat generated. The ductility and hardness of the pipe play an important factor with machinability and tool-material interface friction of this primary shear zone. The secondary shear zone is the tool-chip interface along the rake face, which generates approximately thirty (30%) percent of the total heat through friction, assuming the tool is sharp with correct rake, clearance and relief angles. The tertiary shear zone is friction between material surface and flank faces and accounts for approximately ten (10%) percent of the total heat generated.

The tooth forms associated are triangular and curvilinear and are depicted in Figure 35. The triangular tooth form has one relief angle and the curvilinear has two relief angles – primary and secondary. This gives the curvilinear blade strength but also provides for more heat generation as the blade wears out as there is more blade material to rub and generate heat on the tooth. There are two standard tooth forms – they are:

- 1). Ratchet – has a primary relief angle but no secondary relief angle, sometimes called triangular tooth form.
- 2). Parrot – has a primary relief angle and also a secondary relief angle, sometimes called curvilinear tooth form.

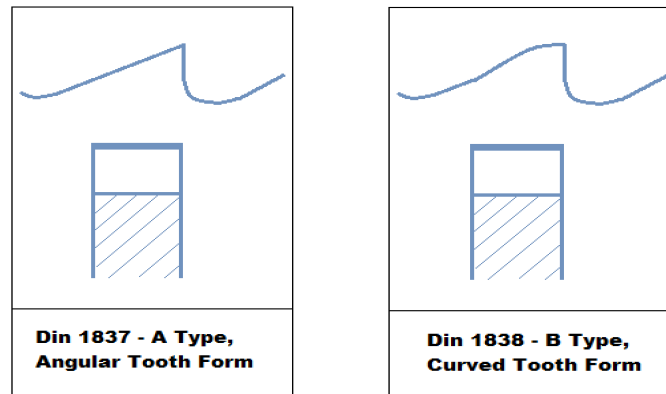


Figure 35 - Triangular and curvilinear tooth formed blades with DIN standardization quality configuration. DIN stands for Deutsches Institut fur Normung, meaning German Institute for Standardization.

The triangular tooth form will last longer from a tool-life stand point than the curvilinear tooth, but is dependent on the machine's dynamics and the blade-to-blade interference. This is not as pronounced with thin blades ($<0.020''$) as the fracture toughness of the blade is weakened by the thinness and the curvilinear is not stronger than the triangular tooth form and therefore the triangular tooth form is preferred over the curvilinear tooth form as blade thickness is reduced.

5.3.3 Cutting Process - Chips and Form

As the rake angle is decreased the friction at the tool-chip interface increases, the shear angle decreases resulting in the chip being thicker. The rake angle can thus be used to control the chip thickness and ultimately cutting energy required. Thicker chips mean a higher cutting energy is required; more input power is converted and used as heat due to an increase in shear strain. Different types of chips are formed with different chip

thicknesses and this can significantly influence the surface finish. Lack of tool rigidity will permit greater deflections, as a result of higher forces, and greatly affect the surface finish quality. The shear angle is directly controlled by the coefficient of friction between the tool and the chip. The lower the friction the less drag the tool exerts on the chip and the larger the shear angle (path of least resistance). The reduction in friction causes the shear angle to become larger; allowing the chips to slide easier and consequently reduces the heat impending from the primary shear zone, the largest source of heat generation.

It is important to capture record and measure the chip form and thickness along with the associated cutting parameters to calculate the cutting forces, angle of shears and geometric gullet capacity. From the measure of the chip thickness we can calculate the shear cutting angle and the cutting energy required to perform the cut. Chips from a curvilinear tooth form are depicted in Figure 36.

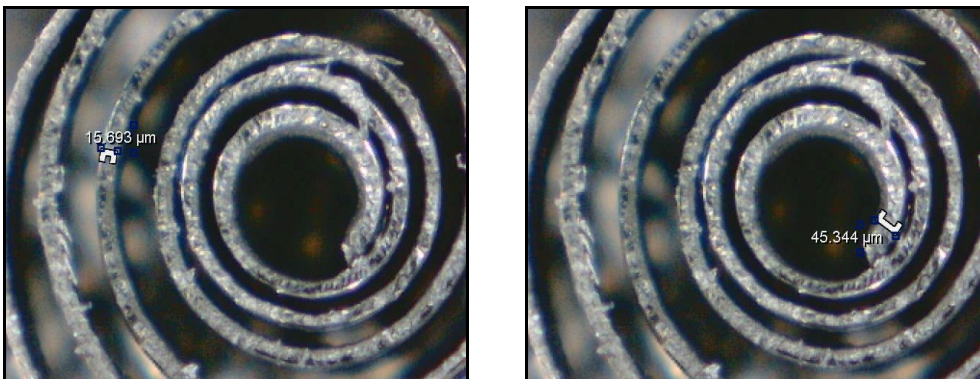


Figure 36 - Experimental results - chip form and thickness of an actual slot created with a blade.

From the measured chip thickness, the primary shear-cutting angle for the rake angle blade is calculated as follows:

$$F_{Tooth} = \left(\frac{Feed}{RPM \times T_{No.}} \right) 25400 \dots\dots\dots (27)$$

where F_{Tooth} is the feed per tooth in microns, $Feed$ is the feed rate, RPM is the revolutions per minute and $T_{No.}$ is the number of teeth on the blade.

$$S_A(\theta) = \tan^{-1} \left(\frac{F_{Tooth}}{T_{Chip.}} \right) \dots\dots\dots (28)$$

where $S_A(\theta)$ is the shear angle in degrees and T_{Chip} is the chip thickness.

Due to the cutting process being an interrupted down milling process, the calculated shear angle will be within a range. It has been found that the range of the chip's thickness is dependent on the following:

- 1) Beginning of the cut O.D. feed rate,
- 2) I.D. feed rate,
- 3) Final feed rate, and
- 4) RPM variation.

By measuring the chip thickness in Figure 36, the primary shear cutting angle range can be calculated and is as follows:

- 1) Start of the chip (45.344 μm) = 5.6° (O.D. Feed rate), 4.1° (I.D. Feed rate), 5.9° (Final Feed rate), (Range = 4.1° – 5.9°)

- 2) Midpoint of the chip ($15.693 \mu\text{m}$) = 15.8° (O.D. Feed rate), 11.8° (I.D. Feed rate), 16.6° (Final Feed rate), (Range = $11.8^\circ - 16.6^\circ$)

It is unknown why the chip thickness at the start of the cut is larger than the chip thickness in the midpoint of the cut. These chips are curled and continuous, possibly to the degree that is undesirable for excess tooth load (force) during the curling of the chip. It is not known which chip form is most desirable at this point as the chips are limited by the gullet area. Chip breakers may need to be incorporated in the design of the cutting tool rake face to allow for discontinuous chips to form. Another possible way to form discontinuous chips is to cut with a feed per tooth which is below the amplitude of the natural frequency of the pipe. This cutting process would utilize vibration as a cutting method but would be highly specific, as the natural frequency, based on an induced load, would be measured and recorded for each pipe prior to cutting.

5.3.4 Built-up Edge

As the cutting tool continues to cut, chemical reactions are occurring at the contact surfaces of the tool and work material, which form the so-called built-up-edge (BUE). These reactions are temperature dependent and once the critical temperature for these chemical reactions are reached; the wear rate is relatively rapid. These constant chemical reactions induce two types of buildup characteristics: temperature weld buildup and pressure weld buildup. Temperature weld buildup is the welding or buildup of metal atoms on the tool and the work material due to high temperatures obtained during the

cutting process. The pressure weld buildup is welding or buildup of metal atoms on the tool and the work material due to chemical reactions and pressure between the work piece and the tool.

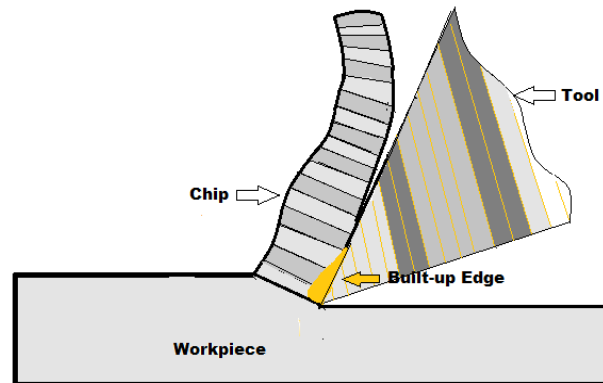


Figure 37 - Illustration of built-up edge of a portion of the primary shear cutting zone with overheated work piece material, which becomes "welded" onto the rake face of the tooth during the slotting process.

A BUE consists of layers of material from the work piece that are gradually deposited on the tool. The BUE eventually builds up to an unstable amount and eventually breaks up. BUE is most likely to form if the work piece is highly plastic. BUE can result in the formation of a poor surface finish and can change the rake's angle and effectiveness. The tendency of BUE to form can be reduced by increasing the rake angle and therefore decreasing the depth of cut. Figure 38 and 39 below show the effect of BUE on the tool and material work piece. Pictures of flank wear and buildup are shown in Figure 40.

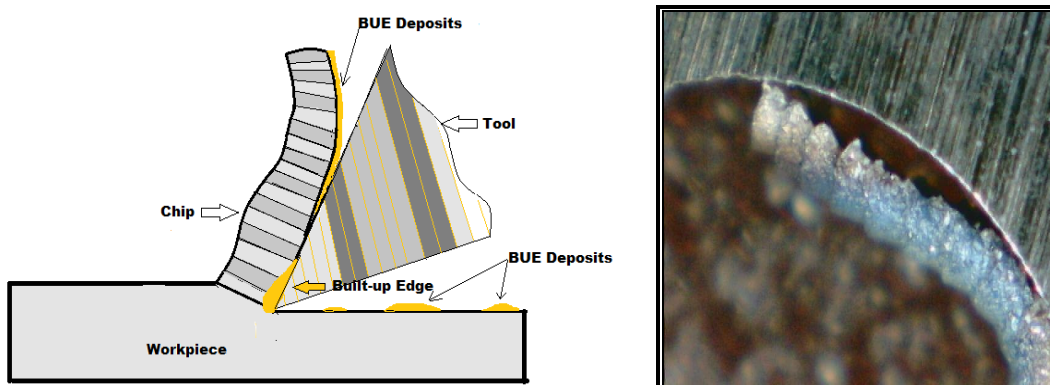


Figure 38 - Experimental results - BUE depiction theoretical drawing and actual picture of a chip welded to the rake face of a tooth during the cutting process.

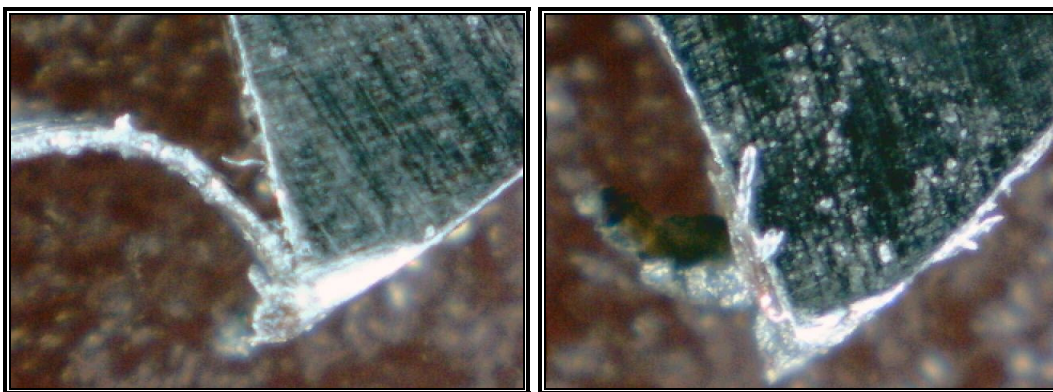


Figure 39 - Experimental results - BUE on the rake face of a blade during the slotting process.

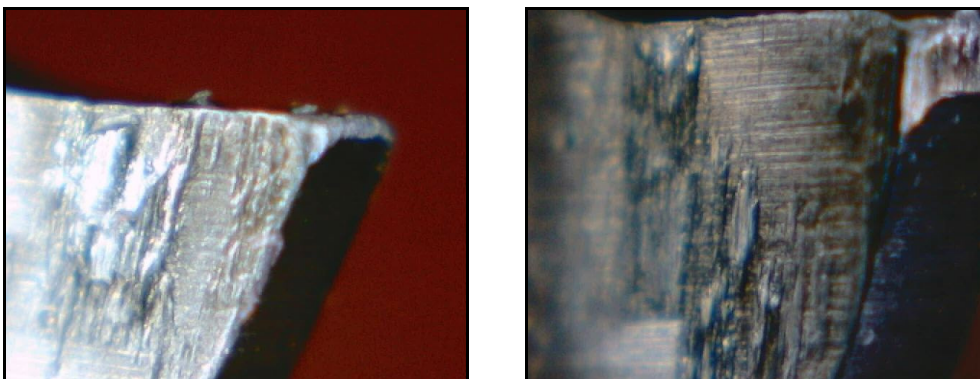


Figure 40 - Experimental results - BUE and flank welding of work piece material to the flanks of the blade from overheating in the cutting zone and flank zones of the blade slotting process.

Material welding and buildup is present on the flank of non-coated blades only. The welding of material to the flank of the non-coated blades is proof of high temperature during the cutting process. This is an important factor to consider from a re-sharpening perspective – de-burring of the flank as an initial process for re-sharpening. BUE affects the cutting dynamics of the slotting process, tool-life and blade wear.

5.3.5 Blade Wear

The experimental observations indicate that tool wear is a complex phenomenon and is influenced by many factors. There are two modes of tool failure during the cutting process. The first being premature failure, which occurs due to fracture failure, thermal failure, or ductile (flexibility) failure. Fracture failure is the point when the cutting forces become too large, excessive and dynamic resulting in premature failure. Thermal failure is when the cutting temperature becomes excessive for the tool material resulting in premature failure. Ductile (flexibility) failure is tool flex failure prior to actual cutting. The second mode of tool failure during the cutting process is gradual failure. This is also identified as gradual wear; wear due to flank wear, crater wear, notch wear, and nose radius wear. Flank wear is wear located about the sides of the blades tooth. Crater wear is wear located along the rake face of the blades tooth. Notch wear is exaggerated wear nodules about the flanks of the blades tooth and nose radius wear is rounding off of the blades tooth. Figure 41 displays different profiles of the flank wear of an actual blade tested in this study.

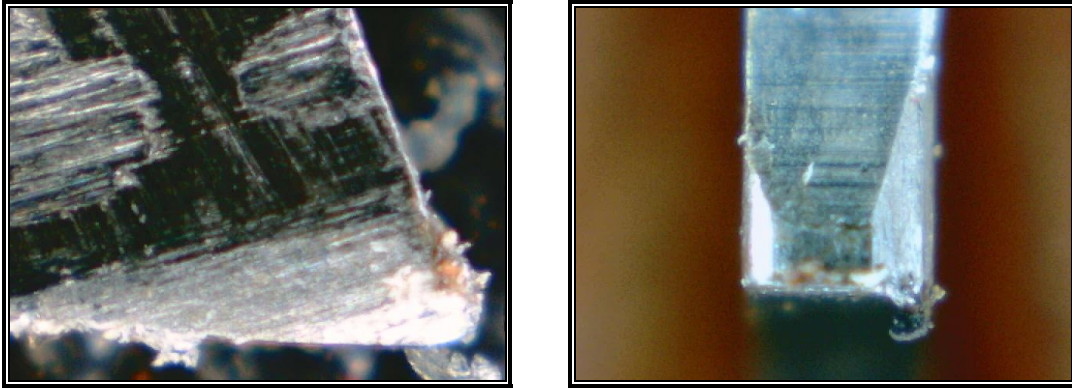


Figure 41 - Experimental results - slotting blade flank wear.

Crater wear is wear located along the rake face of the blades tooth. Notch wear is exaggerated wear nodules about the flanks of the blades tooth and nose radius wear is rounding off of the blades tooth. Figure 38 to 44 depicts different wears for actual blades tested.

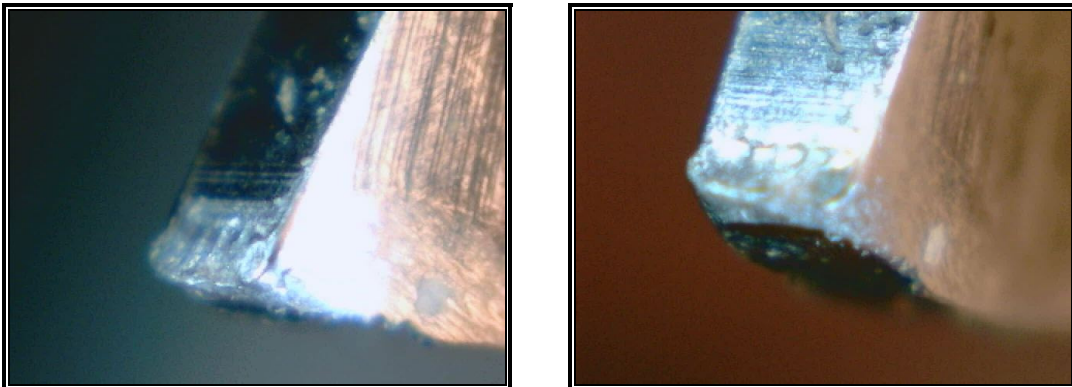


Figure 42 - Experimental results - slotting blade crater wear caused by heat and vibration during the slotting process.

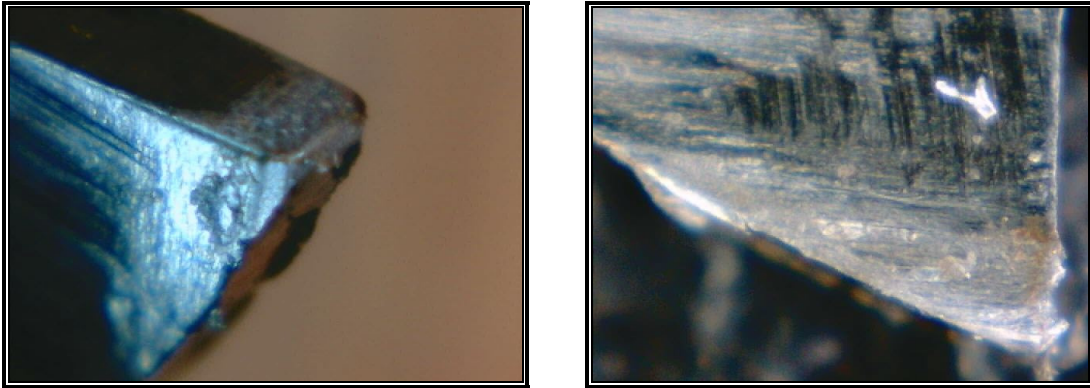


Figure 43 - Experimental results - slotting blade notch wear shown on the flank of the blade due to excess heat generated during the slotting process and due to impact forces.

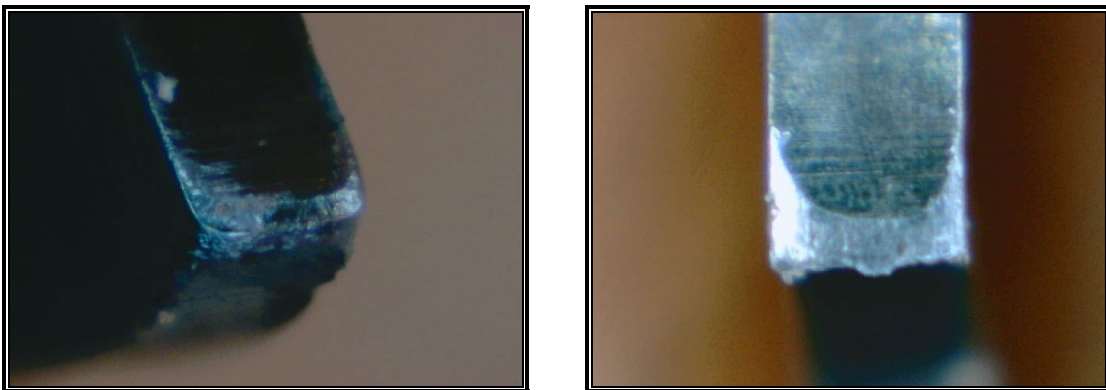


Figure 44 - Experimental results - slotting blade tooth showing rounded wear on the tip of the blades tooth also called nose radius wear.

The cutting speed has a great influence on the tool-life compared to the feed or depth of cut and it is a key control on the overall economics of the machining process. For a given combination of work material and tool material, a 50% increase in speed results in a 90% decrease in tool-life, while a 50% increase in feed results in a 60% decrease in tool-life. A 50% increase in depth of cut produces only a 15% decrease in tool-life. (Knight 2005).

Each cutting speed and cutting parameters, such as blade rake angle etc. comprise of their own specific model for total tool wear rate. Cutting speed affects temperature of the tool and work material, which in turn affects tool-life. The rapid fall-off in hardness of high-speed steels above about 600°C limits their use to temperatures below 600°C (Milovic 1983). Chip form and shape at high cutting speeds can cause difficulties when dealing with ductile work material. This can be dealt with by controlling the tooth gullets and geometries. It is reported that wear rate of the tool is constant below a certain cutting temperature where the tool wear is simple mechanical wear without thermal wear (Mills 1983). A graph is shown as an example of how cutting speed affects wear rate of the tool (see Figure 45).

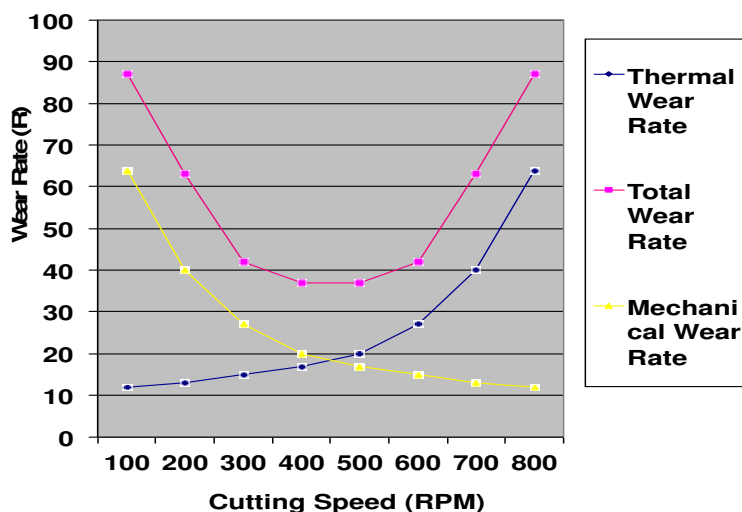


Figure 45 - Experimental results - cutting speed vs. tool wear rate and the relationship of the summation of both types of wear with the point of optimum speed-to-wear rate combination.

For effective cutting, the cutting tool matrix must be harder than the work material. This indicates that the process of cutting is of plastic deformation of material work piece with

the degree of plastic deformation dictating the chip formation. The shearing zone shears the metal atoms immediately ahead of the cutting edge by severely compressing the metal atoms within the shear zone, which result in temperatures great enough to permit plastic deformation (cutting). Work hardening (increase of dislocation density) is a principle of resisting stresses of a work material exceeding the work material's elastic limit, therefore generating a new elastic limit and deformation resistance. This is demonstrated most dramatically in stainless steels.

The friction involved within the primary shear zone is the deformation of the material by the tool and is responsible for approximately sixty percent or more of the total heat generated. The ductility of the pipe plays an important factor with machinability and tool-material interface friction of this primary shear zone. The secondary shear zone is the tool-chip interface along the rake face, which generates approximately thirty (30%) percent of the total heat through friction, assuming the tool is sharp with correct clearance, rake and relief angles. The tertiary shear zone is friction between material surface and flank faces and accounts for approximately ten (10%) percent of the total heat generated.

Cutting speed (expressed in rpm) was found to be the most influential cutting parameter on tool-life, followed by feed rate and then by depth-of-cut (plunge depth). An increase in cutting speed in all machining operations increases cutting temperature, which decreases the hardness of the tool material and facilitates the occurrence of phenomena like abrasion (flank welding). An increase in cutting speed increases the impact

frequency of tool edge entrance into the work piece (increasing the number of shocks per minute) and also the energy of the shock between the cutting edge and the work piece. This makes cutting speed even more important to the end of tool-life. As cutting speed increases, tool wear increases strongly, even with a decrease in feed-per-tooth (energy of a system). The larger the blade diameter the lower the cutting speed.

A low cutting speed will cause an increase in tool-life and a high feed rate will make the cutting time per pipe less (economic based and blade fracture toughness based). A limitation of this procedure is the high cutting force and power consumed by cutting (energy in = energy out), caused by the high rate and volume of material removed per minute (due to the high feed velocity). Changes in cutting speed have a predominant influence on tool life, regardless of whether there are changes in either feed rate, depth of cut or feed-per-tooth.

Changes in tool geometry that result in higher shear angles, less chip distortion, lower frictional resistance, and thinner chips allow for lower cutting forces and a decrease in cutting temperatures, thusly contributing to a reduction in the rate of tool wear. Heat transfer characteristics may also be adversely affected if the cutting point (edge) of the tool is too thin as a result of high rake, clearance and relief angles. This is due to the heat at the cutting point (edge) not being dissipated as rapidly as needed resulting in higher temperatures and greater tool wear. Work piece materials that have a relatively high hardness, shear strength, coefficient of friction, work-hardening capacities, and contain hard constituents promote a more rapid tool wear rate. Materials such as titanium,

stainless steels, and low-carbon steels, which have poor thermal conductivity, do not dissipate heat from the cutting zone as rapidly as required and result in temperature failure of the tool (rapid tool wear). This is due primarily to frictional issues with the tool-material interface. Frictional changes, due to changes in cutting speed, feed rate and cutting fluid can greatly affect tool-life.

As the rake angle is decreased the friction at the tool-chip interface increases, the shear angle decreases resulting in the chip being thicker. The rake angle can thus be used to control the chip thickness and ultimately cutting energy required. Thicker chips mean a higher cutting energy is required; more input power is converted and used as heat due to an increase in shear strain. Different types of chips are formed with different chip thicknesses and this can significantly influence the surface finish. Lack of tool rigidity will permit greater deflections, as a result of higher forces, and greatly affect the surface finish quality. The shear angle is directly controlled by the coefficient of friction between the tool and the chip. The lower the friction the less drag the tool exerts on the chip and the larger the shear angle (path of least resistance). The reduction in friction causes the shear angle to become larger; allowing the chips to slide easier and consequently reducing the heat impending from the primary shear zone, the largest source of heat generation.

5.3.6 Blade Material and Coatings

Standard blade matrix material is M2 High Speed Steel. Special blades are manufactured from M35 Cobalt Steel for cutting high alloy steels. Generally speaking the curvilinear tooth form does not perform as well as the triangular tooth form, regarding tool-life due to continuous chips forming resulting in higher heat generation. 5 to 12% cobalt content in HSS blades helps to increase the wear resistance of the blade by increasing the blades hardness at the temperatures encountered in the blade slotting process. Cobalt slightly increases the brittleness of HSS tools, making them susceptible to chipping at the cutting edge.

The tool blade material properties are very important in determining tool life and economics of the cutting process. Some important tool material properties are high toughness, high hot hardness, high wear resistance, high stiffness (high Young's modulus, E), high thermal shock resistance, chemical inertness (stability), low coefficient of friction, high coefficient of thermal conductivity, and low coefficient of thermal expansion. The most important property of any cutting tool is that it retains its hot hardness. Hot hardness is central to resisting tool abrasions and wear resistance in respect to chemical solubility between tool-material interfaces. Toughness is an important tool material property required to help avoid fracture of the tool. Coating or plating of the tool helps improve the material properties of the tool with single coating applied tools and multiple coating applied tools. The important properties of coatings are to have chemical stability, to resist oxidation, to improve hot hardness, and to reduce

friction (surface topography). Table 7 below describes commonly used coating materials and quality characteristics.

Table 6 - Blade coatings and representative properties enhancement and their indication of best-to-worst tool-life response (How Metals Are Cut 1976).

<i>Best</i>	Al ₂ O ₃	Al ₂ O ₃	Al ₂ O ₃	TiC
	TiAlN	TiAlN	TiAlN	TiCN
	TiN	TiN	TiN	Al ₂ O ₃
	TiCN	TiCN	TiCN	TiAlN
<i>Worst</i>	TiC	TiC	TiC	TiN

Here, the blade coatings studied were:

- 1) No coating (control),
- 2) Titanium Nitride (TiN) coating,
- 3) Titanium Aluminum Nitride (TiAlN) coating, and
- 4) Steam Oxide (O_x) coating.

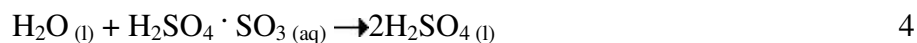
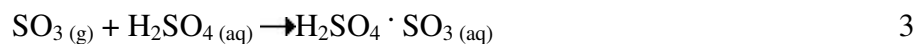
The Titanium Nitride (TiN) coatings are gold in color and helps increase wear resistance by producing higher surface hardness and by preventing pressure and temperature welding due to its high lubricity. The properties of Titanium Aluminum Nitride (TiAlN) coatings, dark purple in color, are theoretically stated as ideal for high temperature cutting operations due to it forming a hard aluminum oxide layer with low thermal conductivity and high chemical stability. As cutting temperatures increase, TiAlN insulates the tool and rejects heat into the chips, and allows for increased production levels with higher cutting speeds, reduced down time, stabilized cutting forces and longer tool-life. Steam oxide coatings, black in color, prevent the tool from temperature and pressure welding. The black surface finish is produced on the tool by means of a steam furnace and creates a porous coating, which helps retain cutting fluid in the work area of

the tool. Steam oxide coating is best for low carbon steels and ductile pipe material due to prevention of a built-up edge (BUE) forming.

After conducting testing it was observed that the steam oxide blades were “burning-up” causing premature failure. It is theorized that the sulphur content in the cutting fluid is the reason the steam oxide blades “burnt-up” upon rapid return of the tool out of the pipe slot. A breakdown of the theoretical chemical reaction is depicted below. Vanadium is an element in the pipe, which acts as a catalyst to cause a chemical reaction with sulphur dioxide gas and oxygen gas to form sulphur trioxide gas which at a gaseous temperature of 450°C causes an exothermic reaction. The reaction is depicted below.



Vanadium (V) oxide is used as a catalyst in step two. The reactants are absorbed on the surface of the V_2O_5 - hence the name "contact process".



This process produces sulphuric acid that is about 98% pure. From a machining point of view vanadium (V) is an undesirable chemical element. All other chemical elements in the pipe are under good ranges except for the Vanadium (V) content being slightly on the higher side and the sulphur content being slightly low. The steam oxide (Fe_3O_4) coated blades could be reacting chemically with the chemicals in the pipe or the cutting fluid.

Sulphur and chlorine are sometimes added as a top treatment in the cutting fluid to help improve machinability. It is possible that the steam oxide (Fe_3O_4) is oxidizing with the sulphur in the cutting fluid (see reactions (1), (2), (3), & (4)). The heat generated by the friction between the blade and the pipe is high enough to cause a chemical reaction between the steam oxide coating and the sulphur content in the cutting fluid. This is an exothermic reaction (i.e. the reaction gives off heat as a by-product) which is temperature dependant (approximately at 450°C), thus increasing the temperature of the blade, which causes a greater propensity for the reaction to occur more vigorously continuing the reaction cycle. This is quite feasible due to the cutting temperature of the blade, before failure, reaching approximately 600°C to 650°C during the cut. The results show that the steam oxide blades did not “burn-up” upon rapid return of the blade out of the slot for the series of tests conducted on another slotting machine with zero sulphur cutting fluid.

As long as the structural strength or fracture strength of the blade is maintained so as premature failure of the tool does not occur (i.e. <0.020 ” blade) then coatings are important in improving tool-life. The best improvement in tool life is obtained with the steam oxide coated blades, which ironically were the cheapest of the coatings. This holds most true in correspondence to the larger width blades. The smaller width blades fracture strength is reduced due to its flexibility range (stabilized vs. non-stabilized blade test) and therefore has a greater influence on the tool-life than the coating type and typically will not show the coating relationship. There seems to be a complex relationship between the blade width, the hardness of the work material, cutting speed, feed, and coolant type and machine integrity when relating the cost effectiveness of the coated blades.

Another coating which may likely be tested is the diamond-like coating. Diamond is the hardest known material, has the lowest coefficient of thermal expansion at room temperature, is chemically inert and wear resistant, offers low friction, and has the highest known thermal conductivity at room temperature. Progress in implementing diamond-coated tools has been hampered by the comparative scarcity of natural diamond and price. Hence, routes to synthesize diamond in the laboratory have formed and the so-called 'industrial diamond' has been synthesized (Milovic 1983). This is the chemical vapor deposited diamond coating applied to tools, which strives to achieve the diamond's qualities, but at a reasonable price and availability. Re-coating of the tool must also be considered after re-sharpening.

Two different blade matrices were tested for tool-life: 1. the M2 blade material and 2. the M5 blade material. The M2 Molybdenum tool steel is theoretically stated as being slightly inferior to the M5 Molybdenum tool steel. Testing for the different matrices generally appears that the M2 material, which is less expensive, performs slightly better than the M5 material. Figure 46 shows the results from tests on the tool-life percentage differences for the comparison of the M2 and M5 blade material.

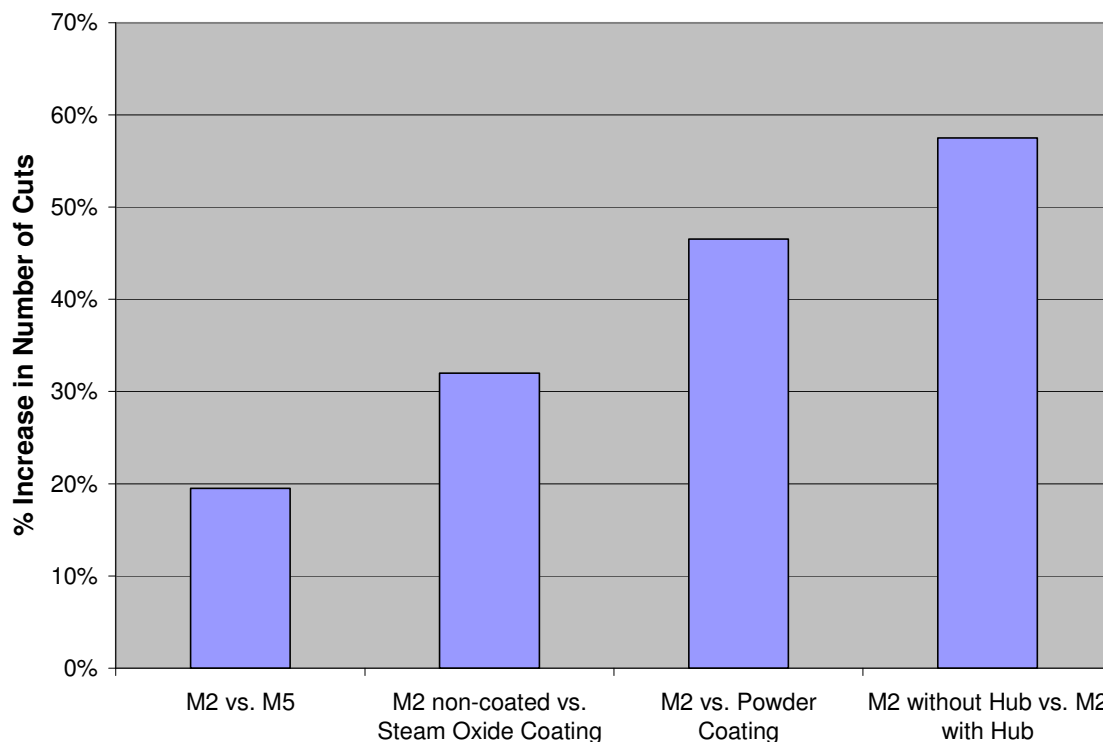


Figure 46 - Experimental results - tool-life and blade matrix material and/or coating material and their respective blade material response recorded as tool-life increase.

Generally, blades tested of which had a boss or hub were found to be less productive in tool-life or number of cuts than a blade without a boss or hub. This was consistent between almost any parameter changes. Our hypothesis for the blades with and without the hub was that if the blades were similar in composition, hardness and tensile strength, then the extra structural strength the hub creates, would support higher cutting torques and thus improve tool-life. Figure 46 display the tool-life differences between the blades with the hub against the blades without the hub, for the different size of blades tested.

The tool-life results contradicted the hypothesis, and to confirm the findings, four (4) samples, two (2) blades with a hub and two (2) blades without a hub, were sent to a third party test facility for metallurgical assessment. The metallurgical assessment found that the hub blades and the non-hub blades were of similar microstructure and chemical composition, but that the hardness of the blades with the hubs was lower than the hardness of the blades without the hub; this may be the correlating factor for their differences in tool-life. Structural strength (fracture toughness) of the blade is of considerable importance in relating the tool-life of the blade

A blade's coating cost must be more than offset by the improved tool-life. It is understood that the purpose of coating is to reduce friction between the tool and pipe. This allows for less heat generation, thusly less tool wear and consequently an increase in the tool-life. A re-sharpened blade strips the coating of the tool from the rake and relief faces but not from the flank face of the tool. For this reason alone, we may not see an improvement in tool-life between coated and no coated blades.

Two (2) re-sharpened blades of similar geometry were chosen:

- 1) M2 blade with steam oxide coating and triangular tooth form, and
- 2) M2 blade with no coating and triangular tooth form.

The testing objective was to identify which blade coating would produce the best tool-life when cutting low carbon steel pipe on a slotter, and how will the coefficient of variation

changed for the re-sharpened blades. A ranking of the performance results is displayed in Figure 46.

Both the steam oxide coated and non-coated blades show there is no benefit to surface treating with a steam oxide coating while cutting with mineral oil. This is due to the fact that the beneficial coating has been stripped off as the blades were re-sharpened. The increased cost for steam oxide blades does not justify the tool-life of the blades. The steam oxide blades did not cut more on average than the non-coated blades. Due to the pipe materials low yield properties and the blades high/competent strength and fracture toughness, the coating differentiation could not be easily identified. Nevertheless, the steam oxide coated blades did not perform as well as the non-coated, regular M2, HSS blades. Therefore, the higher cost of coating the blades is not warranted, even with re-sharpened blades.

Testing was conducted to disprove or prove the theory that powder metallurgy blades would perform better than regular M2 blades or no powder metallurgy blades. Also steam oxide coating was again tested to verify that steam oxide coating in an oil application does not improve the blades tool-life through the reduction of friction. The results are also depicted in Figure 46.

The results in Figure 46 prove that the powder metallurgy does not improve the tool-life of the blades; but is inconclusive with regards to the steam oxide coating effects (rigorous testing of this coating in the years prior proved that steam oxide coating was ineffective

in improving the blades' tool-life; must more than offset the higher incurred blade costs for the coating). Slot testing has clarified that the best value and best tool-life blades are the regular M2 blades.

5.4 Conclusions

There are different modes of slotting a pipe with the goal of creating a sand filter mechanism for the pipe for down hole applications, but the most economical, successful and most accepted slotting process is the mechanical blade slotting. Slotted liner manufacturing and slot cutting dynamics is complex and blade slot tests are sometimes difficult to translate into meaningful information which is transferable to machine design and operation. The process of slotting is one of an interrupted cut and is of one of the most difficult machine dynamics of all machining. The up milling process of machining showed a 20-40% increase in the relative cutting torque requirement than down milling.

HSS blades of high hardness are used to effectively cut each slot. With any metal-to-metal cutting process, considerable heat is generated and the cutting tool must be harder and more resistant to deformation than the work piece. Also the work piece must not significantly work harden during the cutting process or difficulty in slotting will arise. Typically, stainless steel work hardens more than regular OTCG pipe of J-55, K-55 and L-80.

Heat created in the cutting zone effects tool-life more than any other parameter and cutting speed directly influences the heat generation. For a given combination of work material and tool material, a 50% increase in speed results in a 90% decrease in tool-life, while a 50% increase in feed results in a 60% decrease in tool-life. A 50% increase in depth of cut produces only a 15% decrease in tool-life (Knight 2005). The primary shear zone of slotting generates 60% of the total heat, the secondary shear zone (along the chip-rake face) generates 30% and the tertiary shear zone (flank area of the blade) generates 10% of the total heat. There is an optimum relationship between the mechanical wear rate of a blade and the thermal wear rate of a blade during the slotting process. By decreasing the cutting speed the heat generated is reduced but the blades tooth load is increased which increases the mechanical wear rate of the blade.

A triangular blade tooth form (DIN 1837-A) provides better tool-life than a curvilinear tooth form (DIN 1838-B), which is attributed to the land wear area as the blade wears out during slotting – curvilinear has more area to generate heat due to friction than the triangular tooth blade. A seamed slot will generally perform better for sand control than an equally manufactured O.D. slot width or opening of a straight slot. The quality of the manufactured blades is extremely important with the concentricity or run-out of the blade being one of the most important as this related directly to amplified tooth loads and resultant increase in fracturing or chipping of a tooth which has sustained too much tooth load.

By measuring the chip thickness the primary shear cutting angle can be back calculated to identify the shear cutting forces generated, which is referenced to the blades rake angle. By changing the rake angle, recording the chip thickness and the shear cutting angle the optimal rake angle can be identified for the material being slotted. The gullet area of the blade is important as this is the area that the chip will need to form within without filling this space too quickly thereby increasing the heat generated on the tooth by rubbing.

Heat generated during the slotting process can greatly increase the formation of a built-up edge (BUE). The BUE is detrimental to the blades tool-life and affects the cutting dynamics, shear cutting angles, heat generation and forces. Generally, from a tool-life standpoint and from economics of slotting, the low cost M2, HSS slotting blade out performed all other types of blades or coatings on the blades. This suggests that the machine operating parameters that were tested did not generate too much heat, as the coatings are generally applied to the blades to reduce the coefficient of friction which in turn reduces the thermal wear rate, but that the tooth loads were high enough to influence tool-life more. Steam oxide coated blades seemed to “smoke” or “burn-up” during the slotting process and it is thought to be associated with the vanadium content in the pipe reacting with the steam oxide coating under contact pressure and heat. Blades with hubs did not perform as well as blades with out hubs.

The optimal slotting operational approach would be to lower the cutting speed or RPM of the blades and increasing the feed rate of the blades into the work piece. Work piece or pipe grade is of importance here as with harder and higher tensile pipe, such as L-80 vs.

J-55, their becomes a limit to the lowering of the RPM and increasing of the feed rate, as the fracture toughness corresponding tooth load of the blade, which is dependent on the blade material and width, may become too high for stable slotting/cutting.

CHAPTER 6: TOOL-LIFE AND MACHINABILITY

6.1 Introduction

Tool-life Testing is the testing of a different set of parameters to establish the tool-life (blade life). Here, for each set of parameters manipulated, the number of cuts was recorded along with torque, spindle speed, distance, and elapsed time. Cutting speed is considered the single largest controlling factor with respect to tool-life (Boboulos 2010). This is due to high friction created when machining two pieces of metal at great cutting speeds. The friction between tool and chip, and tool and material interfaces can be quite large due to the relatively small cutting surface area. Therefore, with all other parameters constant, the upper cutting speed limit or upper limit linear cutting speed generates a greater coefficient of friction value and thermal wear which results in a decrease of tool-life. Furthermore, the lower limit cutting speed also creates more friction and mechanical wear which causes a decrease of tool-life. The graphical relationships between tool wear (friction) and cutting speed have opposing effects which results in an optimum linear cutting speed which minimizes the friction coefficient. The problem is that tool-life is not only influenced by cutting speed since feed rate also influences tool-life. To find the optimum cutting speed we need to correlate the feed rate, depth of cut, and machine natural frequency with cutting speed setting.

There are three stages of tool-life:

- 1) Break-in region - the time the tool takes to reach gradual wear region or steady-state region. This region will change with changes in rake angle and cutting parameters. The tool requires this time to form equilibrium status with the cutting parameters and the shear-localization area and rake angles. Therefore by reducing this break-in region time we will have optimized the parameters of the blade and the machine
- 2) Steady-state region - the gradual wear equilibrium time of the tool
- 3) Failure region - the region of time where the tool has worn past the point of wear equilibrium and is wearing exponentially, depicting unpredictable and eventual failure.

The “Tool-life Criteria” is the identifiable length of time that the tool performs until failure. There are three stages of tool-life: break-in region, steady-state region, and failure region. The break-in region is the time the tool takes to reach gradual wear region or steady-state region. This region will change with changes in rake angle and cutting parameters. The tool requires this time to form equilibrium status with the cutting parameters and the shear-localization area and rake angles (tool wants to form an angle of least resistance with the cutting parameters). Therefore, by reducing the break-in region time, we will have optimized the parameters of the blade and the machine. Figure 51 displays an example of the stages of tool-life from a laboratory tool-life test.

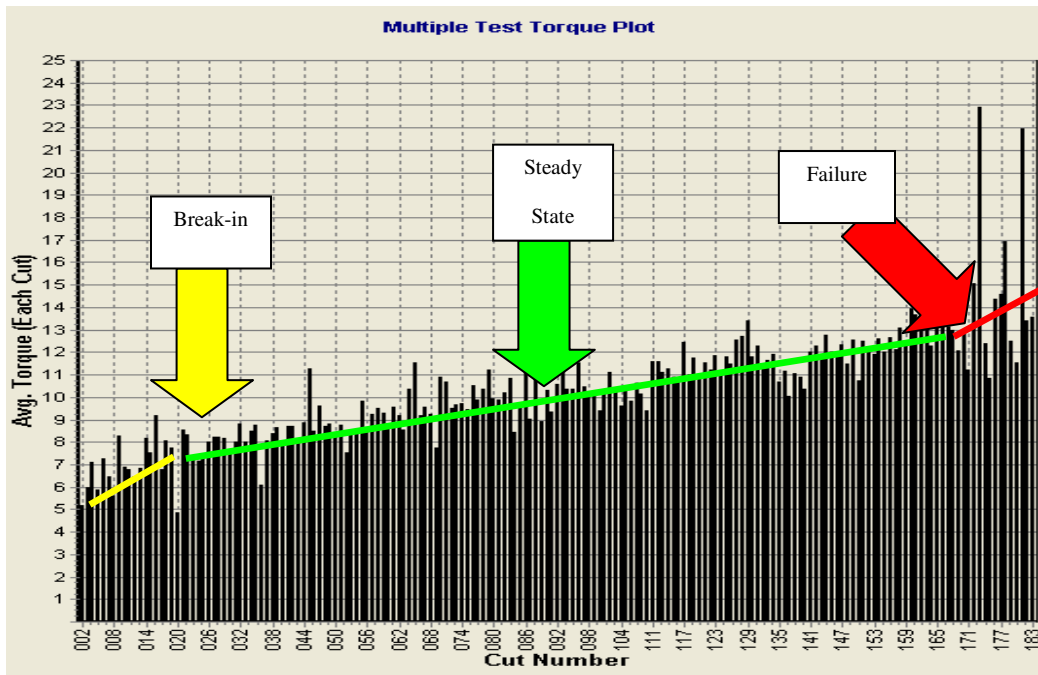


Figure 47– Experimental results - actual tool-life graph showing the break-in region, the steady-state region and the inflection point for the unstable region or failure region of the slotting process.

The steady-state region is the gradual wear equilibrium time of the tool. The failure region is the region of time where the tool has worn past the point of wear equilibrium and is wearing exponentially, depicting unpredictable and eventual failure.

6.2 Experimental Apparatus

The experimental apparatus is the same as that described in Chapter 5. Please refer to Section 5.2.

6.3 Results

6.3.1 Taylor's Tool-life Equation

The criteria used to establish tool-life was time to cut to complete catastrophic blade failure, to use auditory evaluation on the cut, visual inspection on chip and tool, degradation of surface finish, increase in power required or torque required, exact cut count the tool is expected to perform, and/or cumulative cutting time. These are the characteristics of the tool and operation, which can be used to help identify tool-life. Taylor's (1937) tool-life equation is important in identifying the different characteristics of the cutting process and material with respect to tool life. The equation is given by:

$$C = vT^n \dots\dots\dots (29)$$

where C and n are parameters which depend on feed rate, depth of cut, work material, tool material, and the tool life criterion used v is cutting speed and T is tool-life. According to Taylor's Equation, tool life is inversely and exponentially proportional to cutting speed. Tool life has a direct effect on economics. The equation y-intercept is the value of C , the x-intercept is the maximum tool life and the slope of the log-log graph/equation is the value of n . Taylor's theory states that the range values of n can be from 0.1 to 1.0 and can even cover negative values for n . The value of n is highly dependent on the type of tool wear with a low value of n corresponding to thermal tool wear and a high value of n corresponding to mechanical wear. Simple mechanical wear

modes are characterized by n values close to 1. When thermal damage occurs, because temperature increases with cutting speed and thermal damage increases with temperature, n values reduce, the more so the more temperature sensitive is the wear (Mills 1983). It is noted that changes in feeds as well as cutting speeds will affect the values of n and C and that the machining ‘process’ is assumed to not have an influence on these values. Tool-life is viewed as a random variable with a log normal distribution and a large coefficient of variation between 0.3 and 0.4. Taylor’s tool-life equation is depicted in Figure 48.

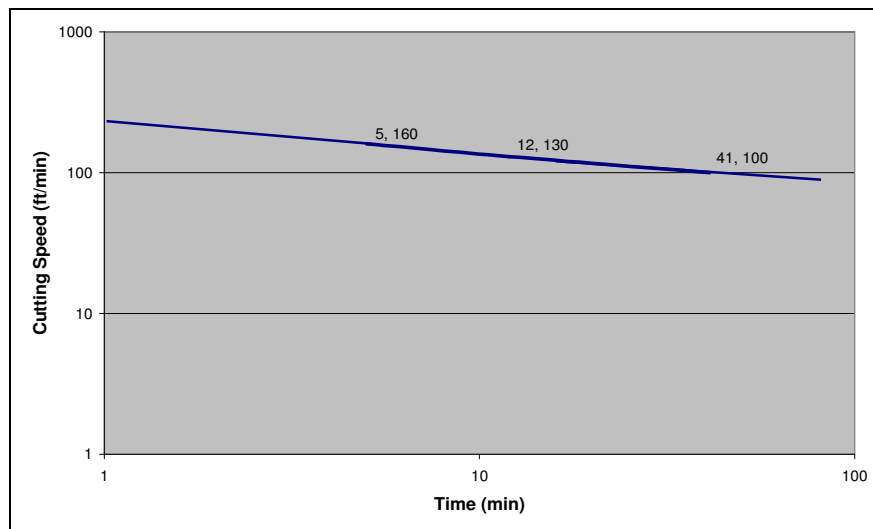


Figure 48 – Taylor’s (1937) tool-life equation presented on a log-log scale of tool-life.

Here, all tool-life tests were conducted until tool failure (break) with a minimum of three sets to get repeatability and statistics. The research questions for this study were: what is the tool-life definition? what effect does cutting parameters have on tool-life? what parameter/variable change is the largest factor controlling tool-life? what is a realistic tool life expectancy for a blade of a specific size and width to ensure that the tool is

replaced prior to ultimate (catastrophic) failure? and what is the mathematical relationship between tool-life and major process variables and how it can be used to theorize on tool-life?

All blades need to have an established tool-life criterion based on a set of parameters for proper prediction of blade performance, realistic production expectancy and tool life economics and production predictions. Because the wear mechanisms can vary greatly depending on many factors, it is necessary to determine how the tool material, work piece material, tool geometry, and cutting conditions affect the tool wear rates and tool-life. For improved tool-life slower cutting speeds should generally be selected in combination with increased feed rates. This is because material removal rate is linearly related to both feed rate and cutting speed, halving the cutting speed while doubling the feed rate maintains an equal removal rate. There are, however, limitations on acceptable feed rates – determined by the ability of the tool to withstand increased cutting loads without fracture. Different blade sizes (widths) have different tool-life expectancy - because of the increased cutting loads/tooth loads, and the ductility (flexibility or stability) failure of the tool. Increased cutting speed (commonly expressed as revolutions per minute, RPM) diminishes tool-life more than increased feed or depth of cut.

The tool-life identifying criterion is to cut to complete failure, to use auditory evaluation on the cut (changes in sound emitting from the cutting operation (highly subjective and generally not recorded)), visual inspection on chip and tool, degradation of surface finish, increase in power required or torque required, exact cut count the tool is expected to

perform, and/or cumulative cutting time. These are the characteristics of the tool and operation, which can be used to help identify tool-life.

Because the wear mechanisms can vary greatly depending on many factors, and the complex relationship between the tool and the work piece (cutting dynamics), further work is required to determine and model how the tool material, work piece material, tool geometry, and cutting conditions affect tool wear rates and tool-life. For improved tool-life, slower cutting speeds should generally be selected in combination with increased feed rates. This is because material removal rate is linearly related to both feed rate and cutting speed, halving the cutting speed while doubling the feed rate maintains an equal removal rate. There are, however, limitations on acceptable feed rates – determined by the ability of the tool to withstand increased cutting loads without fracture. Different blade sizes (widths) have different tool-life expectancy - because of the increased cutting loads/tooth loads, and the ductility (flexibility or stability) failure of the tool. Increasing cutting speed diminishes tool-life more than increasing feed or depth of cut.

To calculate tool-life, test parameters were held constant except for cutting speed. By maintaining all parameters constant, only changing the cutting speed allows us to generate tool-life graphs similar to the theoretical tool-life graph as above. Therefore, only the results with changes of cutting speed while all other parameters are held constant will be used for the tool-life calculation (i.e. Taylor's Tool-life equation). The equation used to calculate n is:

$$n = \frac{\log v_1 - \log v_2}{\log T_2 - \log T_1} \dots\dots\dots (30)$$

and C is given by:

$$C = v_1 T_1^n \dots\dots\dots (29)$$

where

$$T_1 = \left(\frac{Pd}{Feed} \right) \times Nc \dots\dots\dots (30)$$

where v_1 is the cutting speed in revolutions per minute, T_1 is the tool-life, Pd is the plunge depth in inches, $Feed$ is the feed rate in inch per minute, and Nc is the average number of cuts or slots created.

Figure 49 displays the best fit of the tool-life versus cutting speed for K-55 pipe material experimental results. The tool-life of the blade is calculated as $437 = VT^{0.055}$. The equation and the results to produce this equation need further investigation, analysis and testing, to prove or disprove the accuracy of the results and equation above.

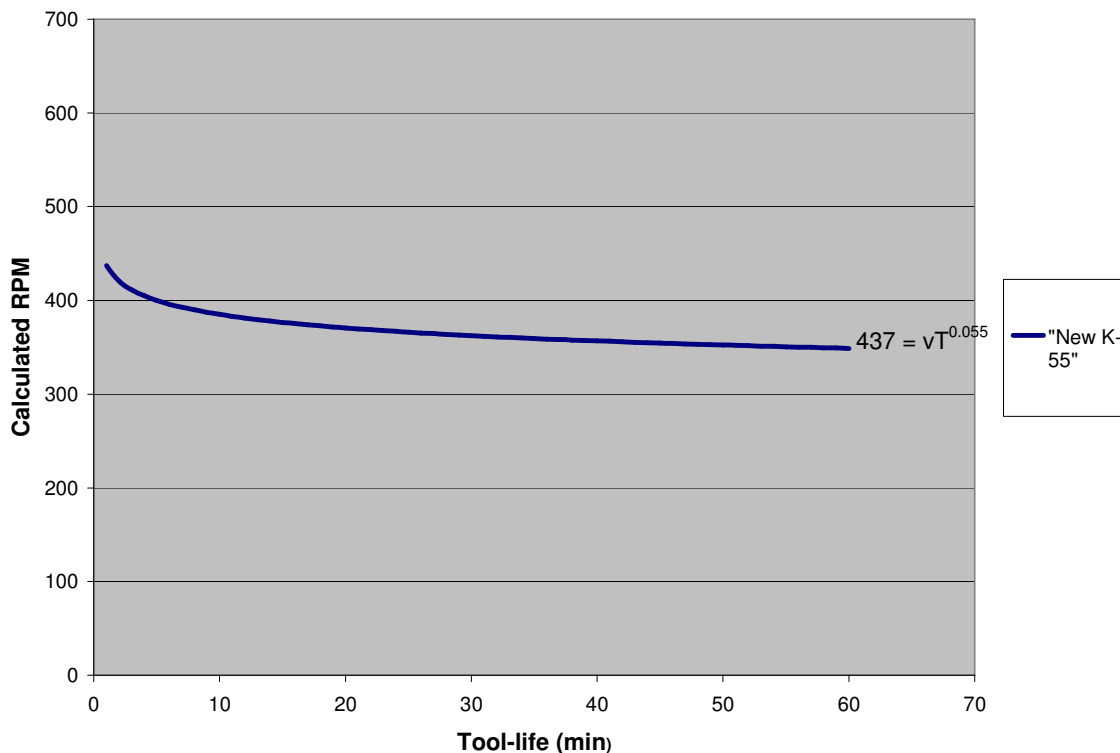


Figure 49 - Experimental results - calculated Taylor's tool-life equation with revolutions per minute and tool-life response slotting a specific pipe material.

Figure 50 displays the best fits of laboratory determined tool-life versus cutting speed for various K-55 pipe samples: $367 = VT^{0.038}$ for "New" pipe material cut with a low tooth blade, $426 = VT^{0.086}$ for K-55 "New" pipe material cut with a high tooth blade, $618 = VT^{0.320}$ for "Old" pipe material cut with a low tooth blade, $801 = VT^{0.342}$ for "New" pipe material cut with a low tooth blade, and $2160 = VT^{1.000}$ for "Old" pipe material cut with a low tooth blade. The results reveal that the tool-life depends on number of teeth and pipe material.

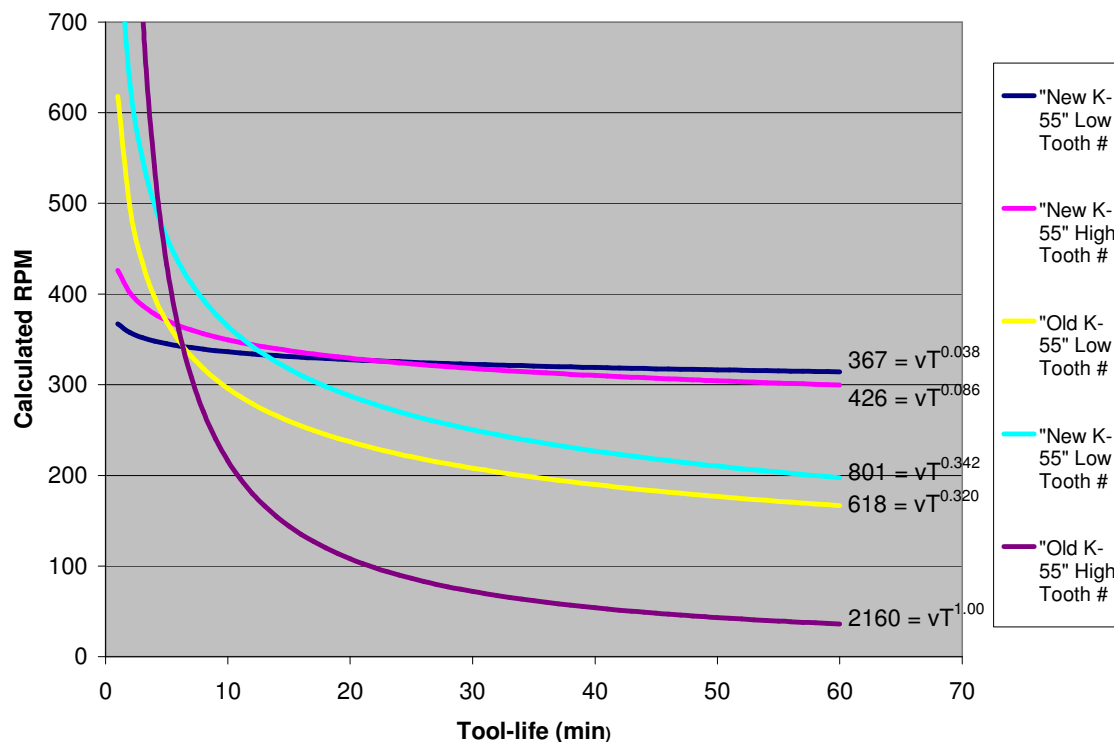


Figure 50 – Experimental results - revolutions per minute versus tool-life response for various pipe grade materials, slotting under the same parameters and conditions.

The largest factor controlling tool life is the cutting speed rather than depth of cut or feed rate. This is due primarily to frictional issues with the tool-material interface. Frictional changes, due to changes in cutting speed, can greatly affect tool life. Taylor's Tool Life Equation is a power-law equation. By taking the log of Taylor's Tool Life equation, it becomes a straight line with cutting speed against tool life y-axis versus x-axis, respectively. The y-intercept is C and the slope of the graph is the value of n . High speed steel has an n value equal to approximately 0.125.

The tool life identifying criterion is to cut to complete failure, to use auditory evaluation on the cut (changes in sound emitting from the cutting operation (highly subjective and generally not recorded), visual inspection on chip and tool, degradation of surface finish, increase in power required or torque required, exact cut count the tool is expected to perform, and/or cumulative cutting time. These are the characteristics of the tool and operation, which can be used to help identify tool life:

- 1) Flood the cutting fluid (increase fluid flow to reduce friction and cooling effects)
- 2) Use water based coolant instead of an oil
- 3) Reduce the cutting speed (energy of a system)
- 4) Reduce the cutting speed and increase the feed rate (crossing of energy/wear mechanics)
- 5) Reduce the feed rate (energy of a system)
- 6) Change the rake angle (increase to reduce cutting forces) or remove burrs created during the re-sharpening process
- 7) Change the relief angle (increase to reduce heat generation and friction due to rubbing)
- 8) Use an Extreme Pressure (EP) additive cutting fluid
- 9) Lightly hone the cutting edge and the flank of the blade to reduce the burrs and sharpness and chipping potential.
- 10) Chipping of the blade tooth can be caused by excessive vibration
 - Work piece vibration – check clamping pressure
 - Tool vibration – check tool run out
 - Re-sharpen – do not overheat the blades when re-sharpening

The energy approach is based on the specific cutting energy which is defined as the energy required removing a unit volume of material. Knowing the depth and width of cut, the length required to create a unit volume can be easily calculated. If this process is considered over some unit interval of time, then the power required for a given volumetric removal rate is calculated.

6.3.2 Coolant/Cutting Fluid

Coolant Comparison Testing is required to help identify the economics between the optimized blade parameters and the coolant type (oil-based versus water-based), temperature, delivery, pressure, volume, maintenance and chemical properties. These tests will be performed after the Blade Endurance Testing so as to utilize this information against changes in the coolant type, delivery, pressure, volume, and chemical properties. The coolant tests may comprise of the coolant delivery system, coolant pressure, the chip removal, the coolant type, and the coolant solubility.

The proper coolant system and coolant type is important in reducing heat generated by the tool, thermal shock and increasing tool-material interface lubrication. Researching companies that specialize in optimizing coolant systems is an integral part of effective machining. The coolant must be able to control the thermal shock, increase machinability, reduce the coefficient of friction, and reduce the friction temperature collectively to help contribute to an increase in tool life. There is a need to consider the compatibility between the coolant used and the pipe's dope protection used. The cutting

fluid provides lubrication between the tool and the chip and reduces the coefficient of friction, which results in an increase in shear angle (more energy efficient cutting).

Lubricant effects vary with cutting conditions and with work material. Even flow of the cutting fluid is essential in the prevention of thermal shock and resultant fractures. For a cutting fluid to be most effective in dissipating heat, it must have a high specific heat and a high thermal conductivity. The problem is that due to high temperatures at the tool-chip interface and relatively small amount of cutting fluid reaching this zone, cutting fluid vaporizes losing some effectiveness.

The addition of an additive such as chlorine to the cutting fluid will form an iron chloride film during the cutting process at lower cutting speeds and temperatures. Iron chloride is a relatively weak solid with a fairly high melting point and therefore provides an excellent lubricant thereby reducing tool-chip friction resulting in a larger shear angle and better machinability. Sulfur added forms iron sulfide providing lubrication for higher temperatures and cutting speeds (too much sulfur activity at lower cutting speeds and lower temperatures gives rise to abrasions on the tool and the work material). The effectiveness of these iron films are limited by their melting points.

Some preliminary tests have been conducted to date with a mineral oil giving rise to better cutting through the reduction of friction and friction heat, than a water-based coolant. Further testing is required to fully determine the cutting efficiencies and variability between the oil and water-based cutting fluids.

The effectiveness of a cutting fluid in reducing the coefficient of friction and/or heat generation through type of cutting fluid is an important aspect to understand for maximizing blade use and tool-life.

Two types of cutting fluids were chosen – a mineral oil and a water-based coolant. It must be noted that dry cutting is not an acceptable practice for slotting and was eliminated from testing. The theoretical basis for the different cutting fluids is:

- mineral oil is a friction reducer but very poor at heat dissipation, and
- water-based coolant is a great heat dissipater but very poor at reducing friction

The objective of the testing was to identify which cutting fluid type produced the best tool-life results cutting low carbon steel pipe on a slotter. A ranking of the performance is displayed below in Table 8.

Table 7 - Experimental results - cutting fluid and coolant testing.

<i>Rank</i>	<i>Cutting Fluid</i>	<i>Blade</i>	<i>Average Cuts per Spindle (% increase)</i>
1	Water-based Coolant	high tooth #	507.5%
2	Mineral Oil	high tooth #	465.0%
3	Mineral Oil	high tooth #	445.0%
4	Water-based Coolant	high tooth #	437.5%
5	Water-based Coolant	high tooth #	370.0%
6	Mineral Oil	high tooth #	365.0%
7	Mineral Oil	high tooth #	257.5%
8	Water-based Coolant	high tooth #	0%

Proper selection of blade is the more important aspect to improving tool-life than the cutting fluid. After proper selection of the blade is made then the cutting fluid becomes the next important aspect to incorporate for improvement of the tool-life. This is depicted in the results above. Some blades performed better regardless of cutting fluid type. But when comparing the blades against the mineral oil and the water-based coolant the blade performed with less standard deviation and variation of tool-life when cutting with mineral oil than with water-based coolant. From these results we can infer that the more important factor, for increasing tool-life of the cutting tool (when comparing only cutting fluid types), is the reduction in the coefficient of friction between the tool-material interface. The cooling properties of the water-based coolant are of less importance than the friction reducing properties of the mineral oil. Therefore, the mineral oil improved tool-life more than the water-based coolant. The mineral oil reduces the coefficient of friction which reduces the shear cutting angle which reduces the tooth load and therefore the subsequent tool wear rate and indirectly heat generation, whereas the water-based coolant reduces the heat generation but not the shear angle or tooth load or BUE tendencies. Also, due to the cutting area limitation and the high cutting temperature within this zone, the small amount of water-based coolant entering the cutting zone is small and may even evaporate. Another reason is the width of the blades is important in determining the cutting fluid type. For blade widths greater than 0.030", a water-based coolant may be a better cutting fluid selection; and for blade widths of <0.030", a mineral oil may be a better cutting fluid selection.

Primarily, a cutting fluid must contribute in three ways to a machining process.

- 1) It must act as a lubricant - by reducing friction, it reduces the heat generated.
- 2) It must also act as an effective coolant - because frictional heating cannot be completely eliminated.
- 3) It should act as an anti-weld agent to counteract the tendency of the pipe material to weld to the tool under heat and pressure.

To perform satisfactorily as a lubricant, cutting oil must maintain a strong protective film in the area between the tool rake and flank faces and the pipe material. This film (microns thick) would assist in decreasing the friction between the chip and tool, allowing for sliding action. Besides reducing heat, proper lubrication lowers power requirements and reduces the rate of tool wear, particularly when machining tough ductile metals. If the cutting fluid performs its lubricating function, the problem of heat removal from the cutting tool, chip and pipe material is reduced. But cooling still remains an important function, and to perform this function effectively, a cutting fluid should possess high thermal conductivity so that maximum heat will be absorbed and removed per unit of fluid volume.

The main reason for applying cutting fluid in a “flood” application is to allow for maximum fluid distribution and maximize the cooling properties of the fluid. The cutting fluid provides lubrication between the tool and the chip and reduces the coefficient of friction, which results in an increase in shear angle. Lubricant effects vary with cutting

conditions and with work material. Even flow of the cutting fluid is essential to prevention of thermal shock and resultant fractures.

It is known that there are only two directions in which the cutting fluid can go: between the chip and tool face, and between the work material and the tool land. Pressurized cutting fluid delivery into either of these directions is superior to normal flooding applications. But even with pressurized delivery, not much cutting fluid will enter the two directions since both the chip and the work material are moving in opposite directions to the fluid flow that is required. Furthermore the extreme thinness of the labyrinth formed by the surface irregularities discourages copious fluid flow.

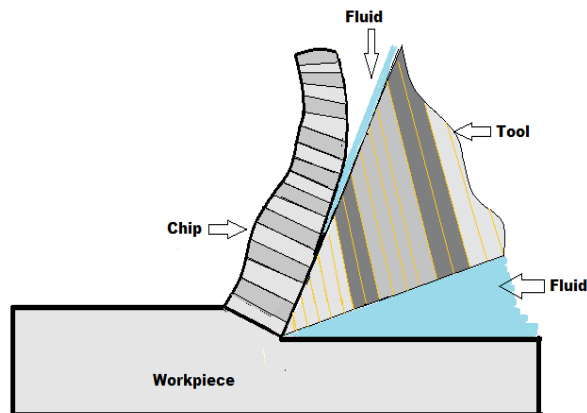


Figure 51 – Illustration showing the theoretical fluid, tool and chip optimal interface interaction where the cutting fluid is optimally placed between the slotting blades tooth performing the cut and the pipe material being cut which forms the chip and helps reduce friction and particularly heat generation.

For a cutting fluid to be most effective in dissipating heat, it must have a high specific heat and a high thermal conductivity. Oil is inferior to water in these respects but oil cooled down to 4-5°C can emulate the cooling effects of water. Water has a specific heat

of $1 \text{ J/g}^\circ\text{C}$ compared to $0.45 \text{ J/g}^\circ\text{C}$ for oil and thus water transfers heat two to three times faster than oil. Some problems associated with water are that it promotes rust, has no lubricity and little wettability (high surface tension). Therefore water must have products added to it to make it less viscous with higher wettability. A synthetic emulsion of oil and water are theoretically superior to either an oil or water-only application. The oil phase of the emulsion provides oiliness, lubricity, and anti-weld properties and the water phase provides a high thermal conductivity or transfer of heat. Water is the cooling medium and oil is the lubricating medium. The most important function of the cutting fluid is to reduce the coefficient of friction between the tool and work material. Cutting oils are far superior at reducing the coefficient of friction than water-based coolants. To perform satisfactorily as a lubricant, the cutting oil must maintain a strong protective film in the portion of the area between the tool face and the work material. This film assists the chip in sliding over the rake face effectively increasing the primary shear angle and reducing power requirement. If a cutting fluid lubricates properly, the problem of heat removal from the cutting tool, chip and work material is minimized. Straight cutting oils or neat oils are petroleum-based mineral oils reinforced with “extreme pressure” (EP) additives. The neat oils are used in conjunction with low cutting speed, large depth of cut, and high cutting pressures. They provide adequate lubricity so that the coefficient of friction is reduced and prevent pressure or temperature welding of material to the tool, which are seen as built-up edges. Important points to consider when selecting oil for cutting are:

- 1) Viscosity – the higher the better since lubrication ability increases with fluid viscosity.

- 2) Flash point – with excessive heat generated by insufficient fluid delivery and viscosity, there is a risk of fire; the flash point of the neat oil should be high enough to prevent combustion.
- 3) EP package (sulfur and chlorine additives) – depends on material and cutting parameters (may react with metals and or blade coatings when heated)
- 4) Wetting agents – to provide adequate lubricity in the cutting zone.

Sulfur added to the neat oils increases their lubricating and cooling qualities and helps prevent welding of the chip and tool. The chlorine is added to give anti-weld characteristics. Neat oils are one of the worst cooling fluids, but one of the best lubricating fluids on the market, and are generally high cost. The addition of an additive such as chlorine to the cutting fluid will form an iron chloride film during the cutting process at lower cutting speeds and temperatures. Iron chloride is a relatively weak solid with a fairly high melting point and therefore provides an excellent lubricant thereby reducing tool-chip friction resulting in a larger shear angle and better machinability. Sulfur added forms iron sulfide providing lubrication for higher temperatures and cutting speeds (too much sulfur activity at lower cutting speeds and lower temperatures gives rise to abrasions on the tool and the work material). The effectiveness of these iron films is limited by their melting points. The recommended temperature for neat oils is 20°C, for effective maximization of cooling. Keeping the oils cool also reduces oxidation and tendency to fume.

A semi-synthetic fluid which has all the inherent cooling properties of water and lubricating properties of oil may be effective in combining the cooling effects of water with the lubricating effects of oil. Figure 52 to 55 are representative of the laboratory coolant results for blades.

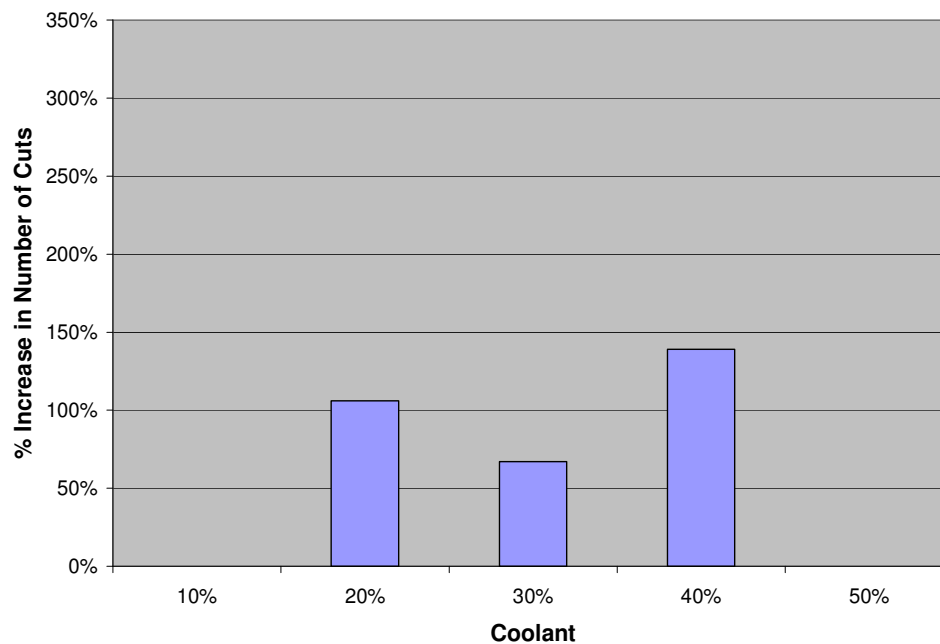


Figure 52 – Experimental results - water-based coolant test and tool-life response.

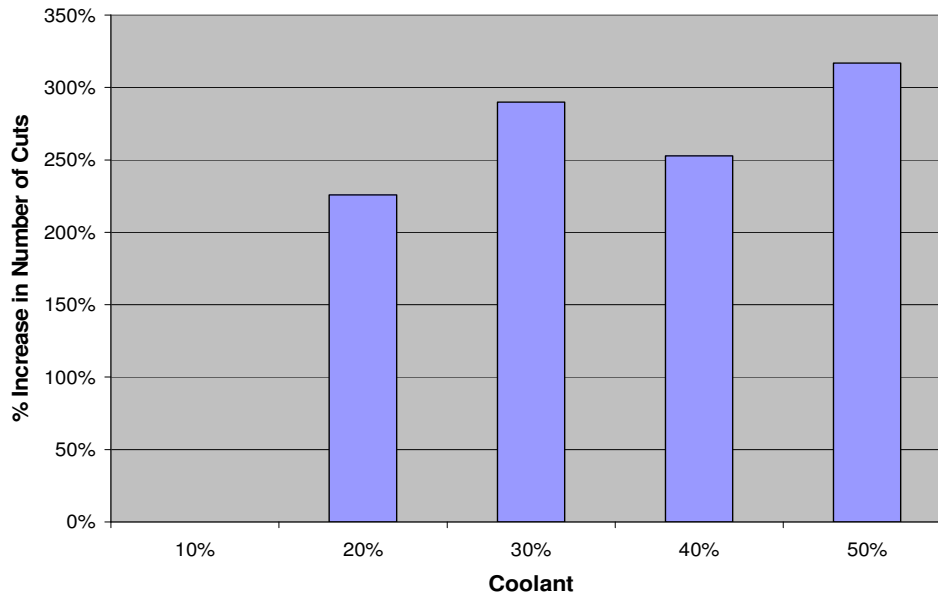


Figure 53 – Experimental results - water-based coolant test and tool-life testing results with similar pipe grade and slotting parameters.

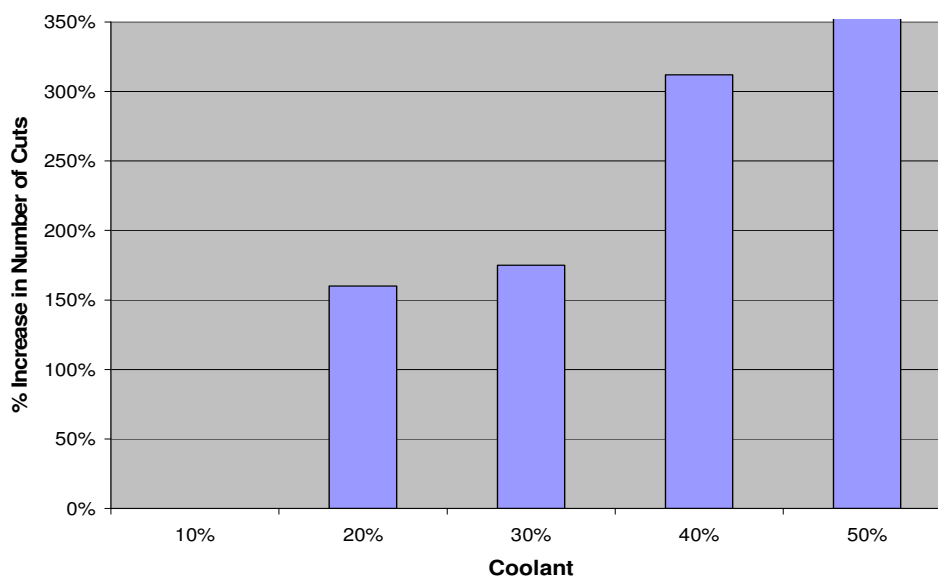


Figure 54 – Experimental results - coolant concentration tool-life tests showing that a higher additive concentration performs better than a lower additive, giving rise to the notion that the slotting process requires lubricant more than heat extraction and this can be due to the fact that the intermittent slotting process has a difficult time allowing for optimal displacement of coolant between the blade tooth and the work piece or pipe.

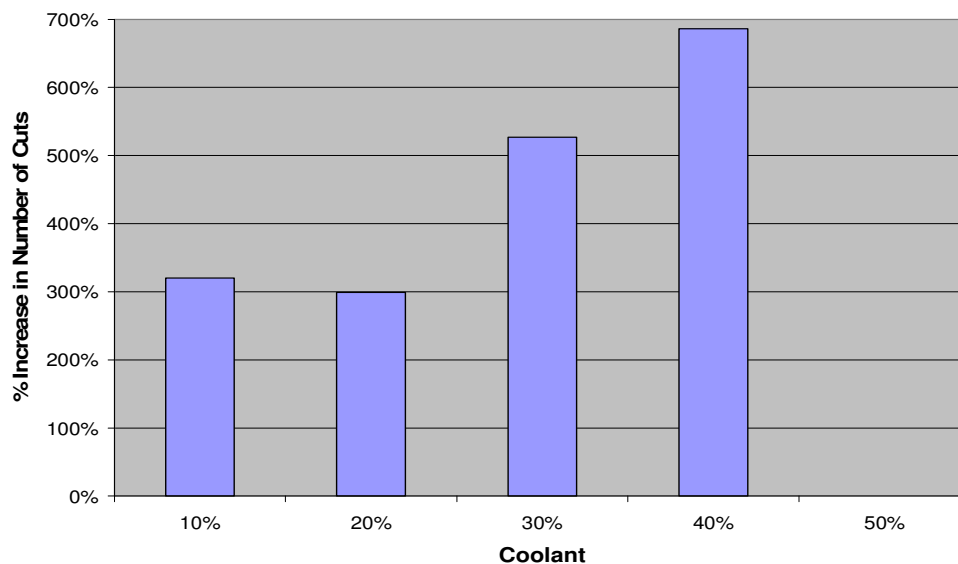


Figure 55 – Experimental results - coolant concentration tool-life tests with one pipe material grade cut.

The results displayed in Figure 52 to 55 shows that a higher coolant concentration consistently improved tool-life independent of material selection. The differences in tool-life between the four pipe materials are representative of their relative machinability. A coolant comparison for an oil lubricant may need to be investigated in the future.

A refract meter was used to measure the coolant concentration by referencing a supplier supplied conversion graph for each coolant product used. The refract meter is recommended to be used after each shift change for best coolant concentration control. The use of a pH meter is important in controlling the water-based coolant from microorganism growth and dermatitis. The range of the pH should be between 8.5 and 9.5; for optimum coolant control, a recommended reading should be conducted daily. The coolant should be kept as near to 20°C a possible to provide its optimum

effectiveness in reducing the cutting temperature during the cutting process. Some problems arise when the water-based coolant is above 32°C. A problem associated with cutting is due to the high temperatures at the tool-chip interface and the relatively small amount of cutting fluid reaching this zone, the cutting fluid vaporizes losing some of its effectiveness.

Due to the wide variety of chemicals used in cutting fluids, the risks associated with these chemicals and their concentration levels and reactivity's, must be researched to fully understand the posed health risks. Workers can be exposed to the cutting fluids through skin contact by exposure to splashes, handling coolant coated parts and equipment, and through inhalation of aerosols. Bacteria, fungi and other contaminants must also be included within the research on the health effects of cutting fluids. Safety precautions must be taken to reduce the exposure risk to employees when working with cutting fluids and specifically undiluted coolants.

6.3.3 Machinability

Machinability testing is where torque, elapsed time, distance, and cutting speed were monitored and recorded. These recorded parameters provided information on the relative machinability index of a number of different pre-selected pipe material. The results may be extrapolated into a model for prediction of other grades with respect to machinability. The mill certifications, material composition and manufacturing processes were known and created a unique identifier.

The relative machinability index is independent of tool life and only identifies the pipes measure of manipulation (i.e. slotting). With the use of a slitting saw, the relative machinability was identified through the manipulation of the cutting parameters. Machinability directly controls the economics of the cutting process and feasibility and identifies the lowest torque value, depicting the measurement of machining. The carbon equivalent percentage was calculated and used as a measure and predictor of the machinability of the pipe with little effectiveness. Testing proved that the carbon equivalent cannot be used to predict the machinability of the pipe.

Hardness and ductility are the two largest factors affecting machinability. Increasing hardness increases cutting difficulty due to tool penetrability and increasing ductility increases cutting difficulty through the formation of continuous chips (discontinuous chips are preferred). The hardness of the pipe was recorded and used as a measure and predictor of the machinability with limited effectiveness. Testing also proved that the machinability is not directly related to the hardness of the pipe (i.e. the harder the pipe the lower the machinability). Also the carbon content was used as a predictor and measure of the machinability with limited co relational success. The carbon content is closely related to the hardness of the pipe. The machinability of the pipe varied drastically with little to no variation in the carbon content.

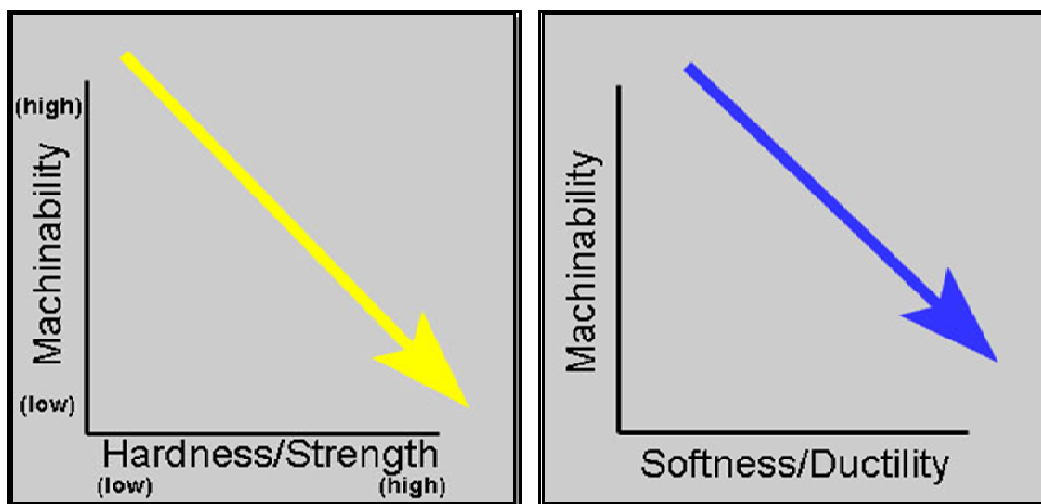


Figure 56 – The ease of material grade/pipe machinability and the pipe’s hardness and ductility (Machinability of OTCG, 1998).

To identify the machinability index tests were conducted based on up-milling and down-milling and radial plunging at various feed rates, cutting speeds and on various pipe material. The tests were conducted in the laboratory and/or the industrial settings.

Testing data shows that the following machinability holds relatively true for different grades of low carbon steel pipe: J-55 is easier to machine than K-55 which is easier to machine than L-80. It is believed that the cutting parameters and the testing methods are independent of the machinability index and that the cutting torque trend will be the same between different cutting parameters. On a highly detailed scale the best pipe grade to machine was difficult to identify due to the many criteria and manufacturing and chemical parameters having an influence on the machinability. Machinability is not a precisely defined term but it attempts to account for several factors of pipe material comparison: tool life, cutting power requirement, surface finish, and/or operational costs.

The machinability index is a relative machinability index; a comparison based on the recorded torque values (relative torque values) and the different pipe material (heat numbers). Testing concluded that the relative machinability index was potentially inconclusive and therefore further higher order testing and a revised methodology to accurately gather the required information from the testing may be required. The results were influenced greatly by too much variability within the pipe grades and too low of recorded pipe chemistry and manufacturing detail. Therefore a higher order of research was conducted on the chemical composition and the microstructure of the pipe, to identify the machinability, with some generalized conclusive results. A pipe with higher sulfur content or a pipe which has been normalized and resulfurized proved easier to machine than a pipe which was not; increased the machinability of the pipe. Also, the coarser the pearlite-ferrite microstructure was, the easier the pipe was to machine. If martensite formed within the microstructure than the pipe was very difficult to machine.

At this point, there seems to be no correlation between the hardness of the pipe, in Rockwell C (HRc), and the machinability. The qualitative measure of the pipes machinability and the hypothesis was that if the pipe was harder, higher HRc than another pipe, then the pipe would be more difficult to machine. What may offset the non-machining qualities of a harder pipe is the inclusion of the resulfurization stage in the pipe manufacturing process.

The presence of sulphide inclusions and the absence of aluminates and oxide inclusions proved beneficial to machining. The greatest factor controlling the machinability is the sulfur content (higher the better) along with the microstructure. A coarse, banded pearlite-ferrite microstructure and a microstructure with a higher amount of pearlite-bainite phases with equiaxed ferrite seemed to improve the machinability of the pipe. A fully untempered bainite microstructure is detrimental for the machinability.

Testing and research has proven that for these small width slotting saw blades, the machinability is affected by both the chemical composition (especially sulfur) and the microstructure. It must be noted that the machinability can be modified through a change in the microstructure and pipe chemistry. Changing the microstructure to improve the machinability of any pipe can be achieved by process of manufacture also, such as reheating the pipe to 890°C and then normalizing and resulfurizing.

6.3.4 Relative Material Machinability Index

The relative material machinability index (RMMI), was established by comparing torque values for various cutting modes and parameter settings. The results from down-milling, up-milling and radial plunge were combined to give the final laboratory machinability index. The criteria for calculating the machinability index was based on the exponential equation from the graphs, which are based on torque.

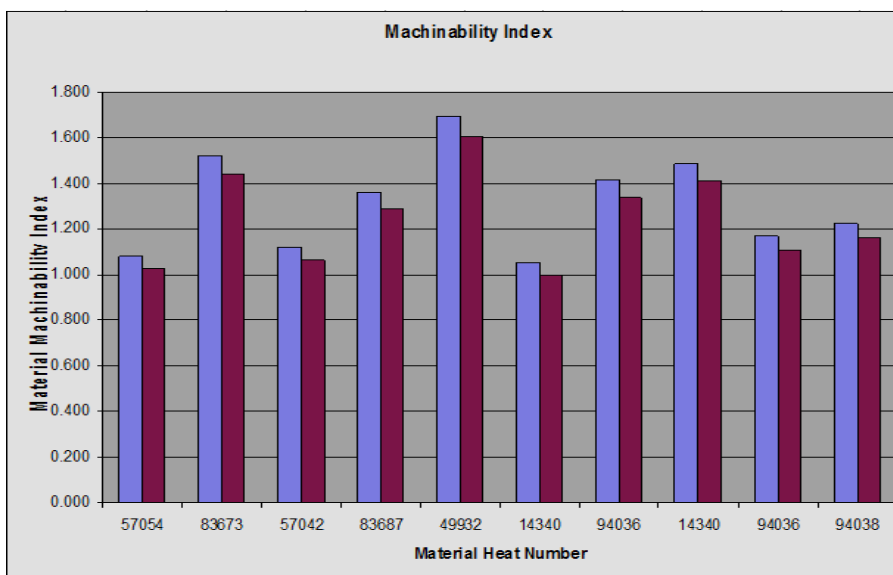


Figure 57 - Experimental results - relative machinability index graph.

Through the research and testing conducted the following formula was developed and used to calculate the RMMI:

$$RMMI = 1 + \left[\left(\left(0.1 \frac{DBI}{SPP} \right) \left(\frac{1}{CVI} \right) \right) + \left(\left(\frac{BBI}{SPP} \right) \left(\frac{1}{CVI} \right) \right) \right] \dots\dots\dots (30)$$

where CVI is the cutting volumetric indicator (inches) which is equal to the product of the internal diameter, slot length, wall thickness, and saw blade thickness, DBI is the dull blade indicator, and BBI is the broken blade indicator, and SPP is the slots per pipe.

From Figure 57 the top two pipe grade materials identified, from the RMMI calculation, is K-55 “New”. These are newly developed materials and several other machinability tests indicate this relationship and result also. Therefore, this RMMI has been verified as

being a new, novel, slotting specific calculation for machinability. The issue with this approach to identifying a pipe's machinability is that it may be a reactive measure and not a prescreening measure of machinability; therefore it may not be useful to predict the machinability before conducting any machining, but may be useful in relating the process of manufacture and the chemistry of these pipe material and relating them to other mill certifications of other pipe heats.

Several cutting modes were performed to help correlated and identify the material machinability index. The first cutting mode was Down-Milling (DM). Down-Milling is identified as having the blade rotation in the same direction as the material movement. The second cutting mode was Up-Milling (UM). Up-Milling is identified as having the blades rotate in the opposite direction to the material movement. Note: The graph below shows equal number of runs for the analysis (i.e. equal cut sequences).

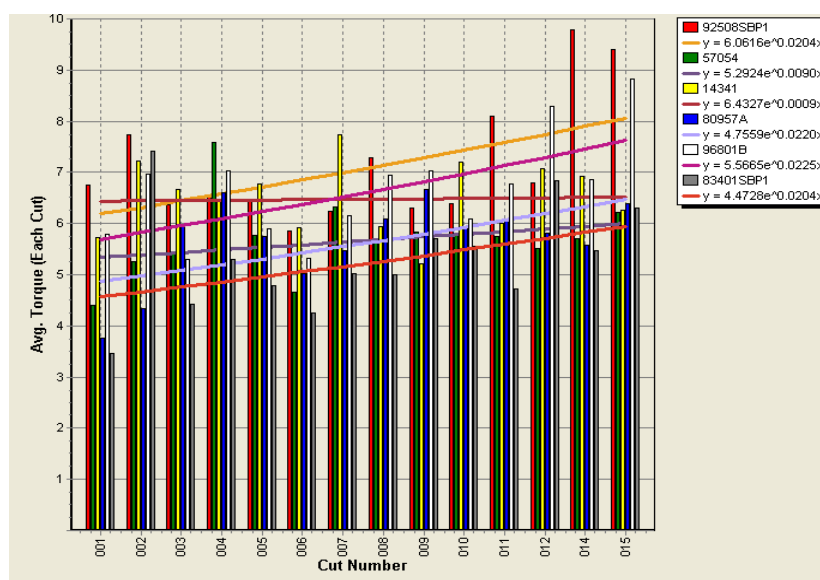


Figure 58 – Experimental results - RMMI and pipe material response with torque rating during the slotting process.

The results are interpreted as better material to machine (being equal to 1), to worse material to machine (being equal to 6), on a numerical scale from one to six. At this point we are only able to quantitatively interpret and identify a machinability index; basis being “cutting torque” and the “torque requirement pattern” for each material identified. The RMMI is identified through the extrapolation of data from the individual heat number’s equation (see legend in above graph); substituting $x = 100$ cuts. Further verification of these results is required:

Table 8 - Experimental results - Relative Material Machinability Index.

Best to Machine

<i>1</i>	K-55 “NEW”	9 5/8”
<i>2</i>	K-55 “NEW”	9 5/8”
<i>3</i>	K-55 “OLD”	9 5/8”
<i>4</i>	K-55 “OLD”	10 3/4”
<i>5</i>	L-80 “OLD”	9 5/8”
<i>6</i>	L-80 “OLD”	10 3/4”

Worse to Machine

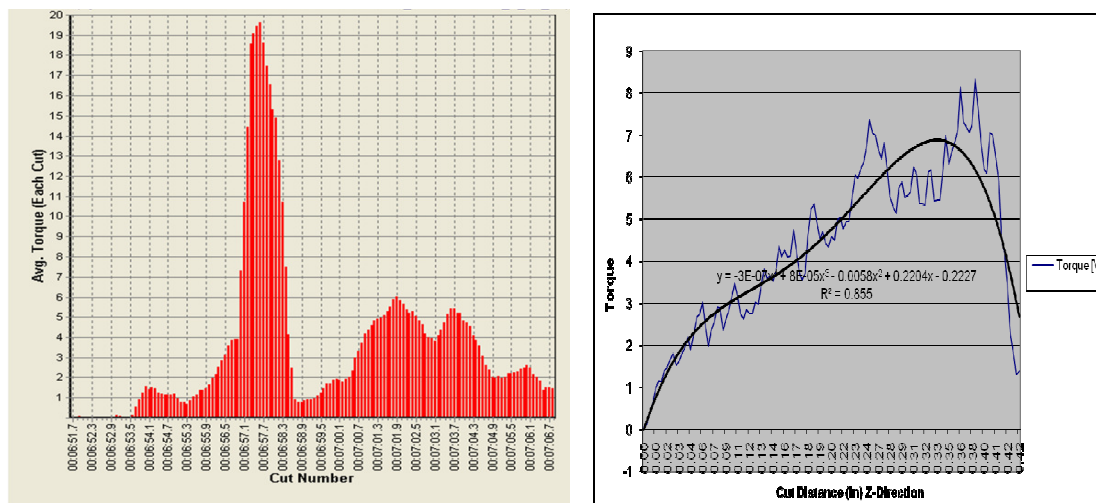


Figure 59 – Experimental results - torque graph of an individual slot and the distance into the slot creation on a pipe showing the point the blade has broken through the pipe wall thickness as the torque requirement to complete the slot is reduced.

The red spike in the data set of Figure 59 is approximately 0.200” in length and occurs for about 1.5 seconds in duration. It also seems to have no bias on the different cutting modes (up milling or down milling) as to whether there would be a spike or not. There seems to be more of a pattern for torque spikes for the older identified pipe material and not the newer identified pipe material.

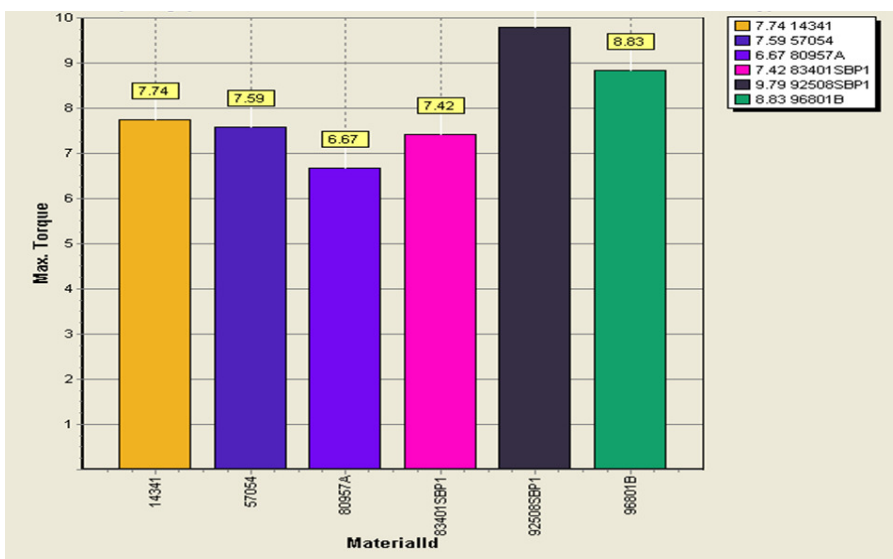


Figure 60 – Experimental results - maximum torque required per pipe material grade.

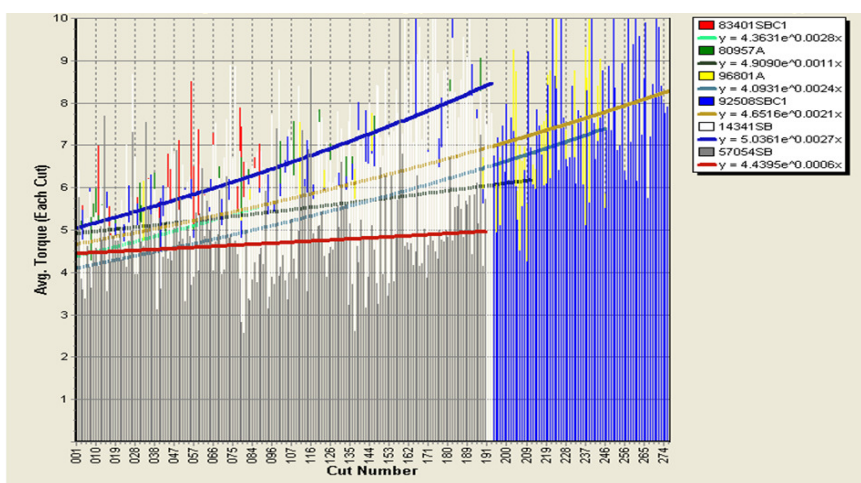


Figure 61 – Experimental results - relative machinability index according to torque or current draw during the slotting process.

The results are interpreted as better material to machine or worse material to machine, on a numerical scale from one to two. At this point we are only able to quantitatively interpret and identify a machinability index, the basis being “cutting torque” and the “torque requirement pattern” for each material identified. Therefore, the graphical presentation of the machinability index, for the maximum and average torque, for each material proves inconclusive and contradictory at times. This is due to the average being calculated based on the amount of runs and the skewness is attributed to the total number of runs. This is because as the blade wears-out the torque measurements are higher. This higher average torque does not necessarily denote a poorer machinability index, it merely states that based on that number of cuts, this is the torque required. Hence, each cut or run should be analyzed according to its sequential order of cut for the material. Also greater numbers of cuts are required to provide more confidence in this research approach.

6.3.5 OTCG Pipe Process and Manufacture

The mill manufacturer and their incorporated manufacturing process contribute to a large degree the machinability of the pipe grades. Pipe in the normalized condition, improves machinability compared with low carbon steels due to their lower ductility and it can be further enhanced with the addition of sulfur or lead if special “free machining” properties are required. Normalization of the pipe (i.e. L-80) is predicted to be of better machinability than non-normalized pipe (i.e. K-55) due to the lower ductility and microstructure uniformity with L-80 grade pipe. Ductility and impact resistance is, however reduced with normalization. Silicon and magnesium are added as deoxidizing

and desulfurizing elements during the manufacturing stage. While the quantities present are not considered to effect the mechanical properties, an indication of the quality of the steel is given by the phosphorus and sulfur content, where the lower the content, the higher the quality, but the additions of sulphur, lead and phosphorus to low-carbon steels help to break up chips, reduce built-up edge (BUE) and improve surface finish quality.

The normalizing of steel improves the grain size (coarse to fine) uniformity. The normalizing process is the heating of steel into the normalizing temperature range identified in the “Iron-carbon phase Diagram” followed by air cooling.

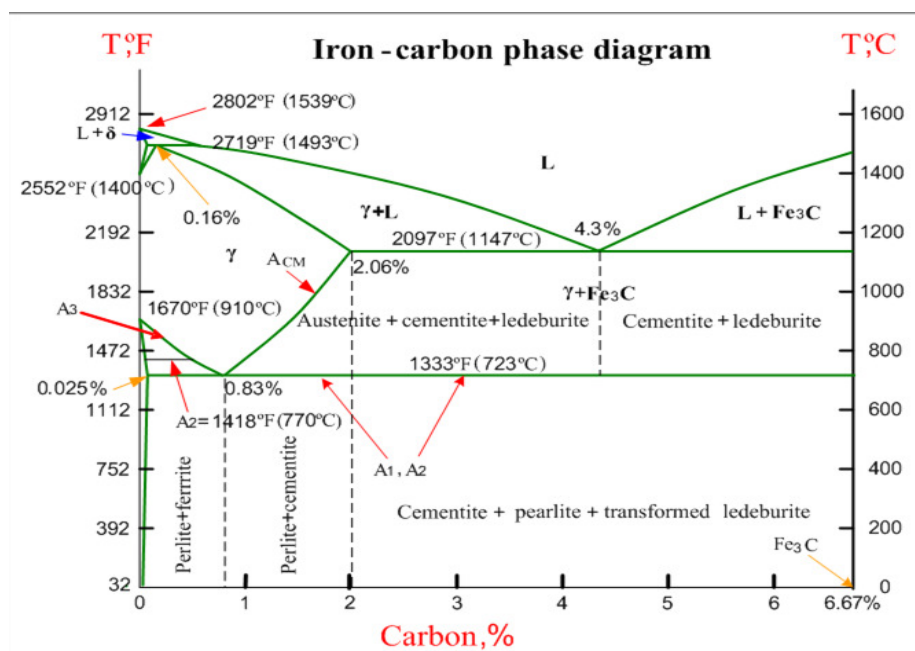


Figure 62 – A graphical representation of an iron-carbon phase diagram with changes in microstructure according to temperature and duration of heating or cooling (Subtech 2010).

The severe demands placed on steel tubular in thermal wells have been well documented in technical papers written by oil & gas operators, technical consultants, research organizations and manufacturers. In general, the design basis for thermal wells must consider the high probability that the steel tubular will be exposed to loads that will result in casing strains beyond the elastic limit of the steel casing. Strain-based design theory using Finite Element Analysis (FEA) as a tool is commonly used to model the behaviour of the casing beyond the elastic region where strength based design techniques are no longer valid. Recognizing that the standard API specification did not specifically address any of the mechanical or dimensional properties that determine how a material will perform beyond the elastic limit in a thermal well environment.

6.3.6 OTCG Hardness

The hardness of steel is largely controlled by the carbon content and the heat treatment it receives. A Rockwell hardness of 67 HRC is the maximum hardness plain carbon or alloy steel can develop. Hardenability increases in proportion to carbon content. Increased hardenability results in an increase in the likelihood of brittle structures forming. The annealing process is softening of the steel for working by heating to the hardening temperature and then slowly cooling (pearlite microstructure forms). Hardening is the process of heating the steel to the hardening temperature and quickly cooling through quenching (martensite forms).

Tempering is the process of reheating the hardened steel (martensite) to the desired tempering temperature in order to relieve stress induced during the hardening process, and to remove some hardness in exchange for toughness and ductility. Untempered hardened steel can be as brittle as glass.

Surface roughness is proportional to the cutting speed. The harder the pipe material the lower the cutting speed i.e. L-80 is harder than K-55 which is harder than J-55. A pipe's microstructure is the single most important factor in identifying the machinability of the pipe and machining. Two entirely different microstructures of a similar pipe grade can have the same hardness but give different machinability ratings. A pipe's hardness is not the best method of qualifying machinability of a pipe but when coupled with microstructure can be very helpful. As a general rule the harder the pipe material (greater the carbon content) the harder the cutting forces and increased tool wear and reduced tool-life. Any given pipe is harder to cut in a harder form than when it is in a softer condition (warm pipe versus cold pipe). Hot rolled pipe can create a hard surface finish (<0.030"), making cutting difficult. Cold working the pipe increases its hardness. It is necessary to reduce cutting speed when cutting harder material (L-80 versus J-55). Normalizing the pipe can help reduce inclusions and hardness variation among the pipe.

When machining hard pipe (L-80 and K-55), reduce cutting speed, increase feed rate and increase the coolant pressure and application (to offset the materials low thermal conductivity). You can expect less heat when cutting metals of low tensile strength.

- J-55 Yield Strength = 55,000 - 80,000 psi, Tensile Strength min. = 75,000 psi

- K-55 Yield Strength = 55,000 - 80,000 psi, Tensile Strength min. = 95,000 psi
- L-80 Yield Strength = 80,000 - 95,000 psi, Tensile Strength min. = 95,000 psi, max. hardness = 23 HRc

6.3.7 OTCG Chemistry and Carbon Content

By machinability standards, magnesium scores high on the scale for ease of machining. Rates of tool wear are very low because magnesium does not alloy with steel, and the metal and its alloys have a low melting-point (650°C), so that temperatures at the tool-work interface are low even at very high cutting speeds and feed rates. The hexagonal structure of magnesium is probably mainly responsible for the low ductility which leads to the fragile segmented chips and the short contact length on the tool rake face. The worst feature of the machinability of magnesium is the ease with which fine swarf can be ignited and the fire risk which this involves.

Steel and iron have high melting-points and therefore give rise to machinability problems. The alloying elements added to iron to produce steel and to increase its strength (carbon, manganese, chromium etc.) influence the machinability through cutting stresses (forces, tool deformation) and heat energy (temperature) generated. To permit higher metal removal rates and/or machinability and/or tool-life, it is therefore normal to heat treat to reduce the hardness to a minimum. The heat treatment often consists of annealing just below the transformation temperature (about 700°C) to reduce the cementite into its least strengthening effect.

The carbon equivalent % is calculated and may be used as a measure for machinability and as a predictor of the relative machinability. Table 10 below depicts the relative machinability ranking for the specific K-55 pipe heat numbers based on the carbon equivalent % calculation using carbon, silicon, manganese, phosphorus, and sulfur. The higher the value the better the machinability.

Table 9 - Experimental results - Relative Machinability Ranking by Carbon Equivalent - K-55.

Relative Machinability Ranking	Grade	Carbon Equivalent Calculation $C+(Si/30)+(Mn/20)+2P+4S$
<i>1 - Best</i>	"New" K-55	0.4773
2	"Old" K-55	0.4767
3	"New" K-55	0.4742
4	"Old" K-55	0.4511
5	"Old" K-55	0.4431
6	"Old" K-55	0.4431
7	K-55	0.4415
8	K-55	0.4330
<i>9- Worst</i>	K-55	0.2978

Table 11 below depicts the relative machinability ranking for the specific L-80 type pipe heat numbers based on the carbon equivalent % calculation using carbon, silicon, manganese, phosphorus, and sulfur. The higher the value, the better the machinability.

Table 10 - Experimental results - Relative Machinability ranking by Carbon Equivalent - L-80.

Relative Machinability Ranking	Heat Number (L-80 Type)	Carbon Equivalent Calculation $C+(Si/30)+(Mn/20)+2P+4S$
<i>1- Best</i>	“New” L-80	0.3882
<i>2</i>	“Old” L-80	0.2705
<i>3- Worst</i>	L-80	0.2601

Hardness and ductility are the two largest factors affecting machinability. Increasing hardness increases cutting difficulty due to tool penetrability and increasing ductility increases cutting difficulty through the formation of continuous chips (discontinuous chips are preferred).

6.3.8 OTCG Microstructure and Chemical Composition

Cutting parameters and the testing method are independent of the machinability index and the cutting torque trend will be the same between different cutting parameters. This is a relative term due to what is wanted as a result (e.g. tool life required before slot surface finish). Machinability is not a precisely defined term but it attempts to account for several factors of pipe material comparison. They may be: tool life, cutting power requirement, surface finish, and/or operational costs. Machinability is defined as “the mode of behavior of a material during cutting that can be clearly defined and which would be an indicator for the pipe material’s ease or difficulty to machining, under similar valid cutting conditions” (Brunet, 1977).

Conducting a machinability study was to identify which pipe grade material would provide the best machining characteristics and/or meet or exceed the American Petroleum Institute (API) for pipe classifications and specifications. It should be of the easiest to machine, and be used as a reference to evaluate incoming pipe material, to ensure that the selected cutting tools will not fail prematurely under the specified conditions (minimum number of cuts per blade etc.). Testing and evaluation of the pipe division - tool-life testing and comparison between the pin end, center and box end, was conducted with the results being inconclusive. There seems to be no pattern associated with the tool-life and the cut location on the pipe. In other words the pipe seems to be fairly uniform in microstructure and hardness, or the blade's tool-life coefficient of variance is greater than the coefficient of variation with the pipe. Secondary objective was to evaluate new tool geometries for establishing the machinability index for any material machined and to develop optimum blade geometries for the cutting process so as to determine the consistency of the machining characteristics or material.

It is understood that considerable differences in machinability are occurring at different cutting speeds and with different pipe materials. Testing was constrained by the material received and therefore these tests will be naturally referred to as a relative machinability index. Firstly, even if as hoped a particular test indicates that material A machines better than material B which in turn machines better than material C, in most cases there is no indication of the magnitude of the differences because the measure of machinability does not, in general, correlate on a predictable scale with, for example, the life of the cutting tool under a given set of conditions (Mills, 1983). Secondly, even if the test does attempt

to compare work pieces for a given set of cutting conditions, there is no guarantee that when the cutting conditions change the ranking will be the same (Mills, 1983). The intent was to develop a relative machinability index of the selected pipe material we received, to accomplish this through the use of non-machining and machining tests (absolute tests i.e. tool-life testing) and to develop a consistent relationship of relative machinability index ranking to pipe specifications. It is understood that this may be difficult to quantify, correlate and transfer to the commercial slotting operation/machine from the testing apparatus, and a good confidence indication of machinability of the pipe, based on machining and non-machining tests, may not exist.

An identified non-machining test is the microstructure test. This is the calculation of machinability with relation to the work pieces' microstructure. In general, Whittman et al. (1974) concluded that uniformly distributed pearlite of large interlaminar spacing was the optimum microstructure for both turning and milling; similar conclusions were drawn by Boulger et al. (1995) using their constant pressure test (Brunet, 1977). The type of microstructure and the combination of different microstructures are most important, when identifying by non-machining techniques, for the ranking order of the pipe material or heat. Machinability of the pipe is largely controlled by the combination of optimal microstructure (process of manufacture) and chemical composition (specifically sulfur content). Also seamless pipe, which is pierced and elongated, may be better at forming elongated/stretched MnS inclusions than electric-resistant welded pipe, benefiting machining/slotting.

Machinability can be determined by microstructure and hardness, as there is a close relationship between hardness and machinability but only for similar microstructures. Field and Murphy both held the opinion that tool-life is primarily dependent on the relative proportion of pearlite and ferrite and that an optimum ratio of the two exists (Brunet, 1977). Steel which contains more than 50% ferrite gives rise to good machining properties and therefore machinability, but this is subjective to the pipe structural specification and its intended use, as pearlite is hard and gives the pipe its strength and ferrite is soft and gives the pipe ductility and toughness.

If the carbon content of the pipe is increased, the amount of pearlite is increased and thusly hardness. Application of this relationship, of hardness and/or carbon content with respect to the pipe received, as a generalization that the pipe with the lowest hardness and carbon content will be ranked highest among relative machinability ratings, is possible only if the microstructures of the pipe received are similar and the heat treatments are the same among each heat and or mill manufacturer. Nevertheless, Table 12 below depicts the results of the received K-55 pipe and the corresponding average hardness (HRC) as the ranking criterion.

Table 11 - Experimental results - RMMI by pipe grade, carbon content and hardness.

Relative Machinability Ranking	Grade	C - Carbon (% wt.)	Average Hardness Value (HRC)
1 - Best	00 - K-55	0.33	7.3
2	50 - K-55	0.33	10.7
3	09 - K-55	0.32	11.5
4	44 - K-55	0.34	11.7
5	68 - K-55	0.23	12.5
6	21 - K-55	0.34	13.2
7 - Worst	34 - L-80	0.26	16.9

There seems to be a direct correlation to the hardness of the pipe and the spindle torque requirement. Figure 67 below shows a clear relational representation to the hardness of the pipe and its relative machinability ranking to the spindle torque requirements. This is significant as the laboratory results in Figure 67 are depicting the spindle torque requirements based on as few as 6 cuts. These results show correlation due to a proper selection of the blade parameters and possibly due to similar microstructures formed between the selected materials. From Figure 67 the best exponential equation relating to spindle torque was the 00 material; then 09; then 50; then 44 and finally 68. This is an interesting correlative relationship as the lowest carbon content (% wt.) is the material 68, and therefore other elements not represented within this table could be influencing the machinability.

Carbon content, as we know, influences the pipes hardness to a large degree, but doesn't identify the microstructure or the heat treatment the pipe received as readily does the pipe average hardness value. Therefore, if the average hardness value (Rockwell C or

Brinell) is known for the pipe received, then a generalization of the relative machinability index/ranking may be identifiable (maintaining similar pipe processes, heat treatments and/or microstructure).

The addition of manganese, carbon, tin and/or hard inclusions/spots and higher amounts of them gives, rise to higher tool wear rates. Hard spots can seriously degrade machining performance. Undissolved inoculants, oxides (slag), refractories, dross and burned-on molding sand are attributing factors to producing hard spots and are detrimental to machinability. Hard spots in the pipe can be reduced by the use of heat treatments such as annealing or normalizing. A machining (absolute) test is the “constant pressure test” developed by Boulger *et al.* This test is conducted with the feed force kept constant and the resultant feed rate is measured, which provides an indication of the machinability of the material. This is a simple test but an effective test for ranking pipe material on a machinability index. Research did not include this test as the slotting technique we employ is of the interrupted cut style, which has a large bearing on the changes in load on the tool, but the “constant pressure test” conducted on a small scale (milling) would be effective in identifying the relative machinability of a wider range of material, and therefore may be an area for future exploration in identifying a relative machinability index. The reason the “constant pressure test” would work in identifying a relative machinability index is simply due to the mechanics of cutting. The “constant pressure test” basically measures the chip-tool friction, which is closely related to the temperatures generated in the cutting process, which in turn will have a pronounced effect on the wear rate of the tool.

Being that machinability determination is very much process and cutting condition dependent, it is difficult to relate the results from one set of conditions to another set of conditions. This may sometimes explain why, when changing any parameter of the cutting process, the machinability results may sometimes differ.

The tool-life tests conducted as the machining or absolute testing for the material selected proved to be the best way to rank the received pipe materials to their respective relative machinability index for the interrupted cutting technique of the slotting process. It was originally thought that the cutting torque data could be gathered on several cuts under several conditions and then extrapolated to identify the torque requirements for many cuts and the maximum number of cuts for a set of cutting conditions, based on theoretical and previous knowledge of blade breaking torque values. But due to the variability within the blades, pipe material, the machine wear, and the dynamics of the cutting process and tool wear relationship we are limited to correctly identifying the minimum number of cuts required for utilization of the extrapolation theory of the data set. We recorded 1 run, 3 runs, 15 runs, then 50 runs, and eventually concluded that full life, tool-life tests were of the most valuable in ranking the machinability of the materials before extrapolation of data sets. Insufficient data was the largest factor in deducing the extrapolation theory. With sufficient tool-life data, resultant cutting torques and testing experience, the extrapolation theory would be efficient in predicting tool-life. Table 13 and Figure 64 below offer the relative machinability ranking order, with no regard for parameter changes but with respect to blade widths and their respective tool-life graphs.

Table 12 - Experimental results - blade, pipe, grade and machinability ranking.
Note: there is insufficient data for machinability ranking based on blade widths for any other blades tested.

<i>M2 Blade</i>	
Relative Machinability Ranking	Grade
<i>1 - Best</i>	"New" K-55
<i>2</i>	"Old" K-55
<i>3</i>	"New" K-55
<i>4</i>	L-80
<i>5</i>	"Old" K-55
<i>6- Worst</i>	L-80

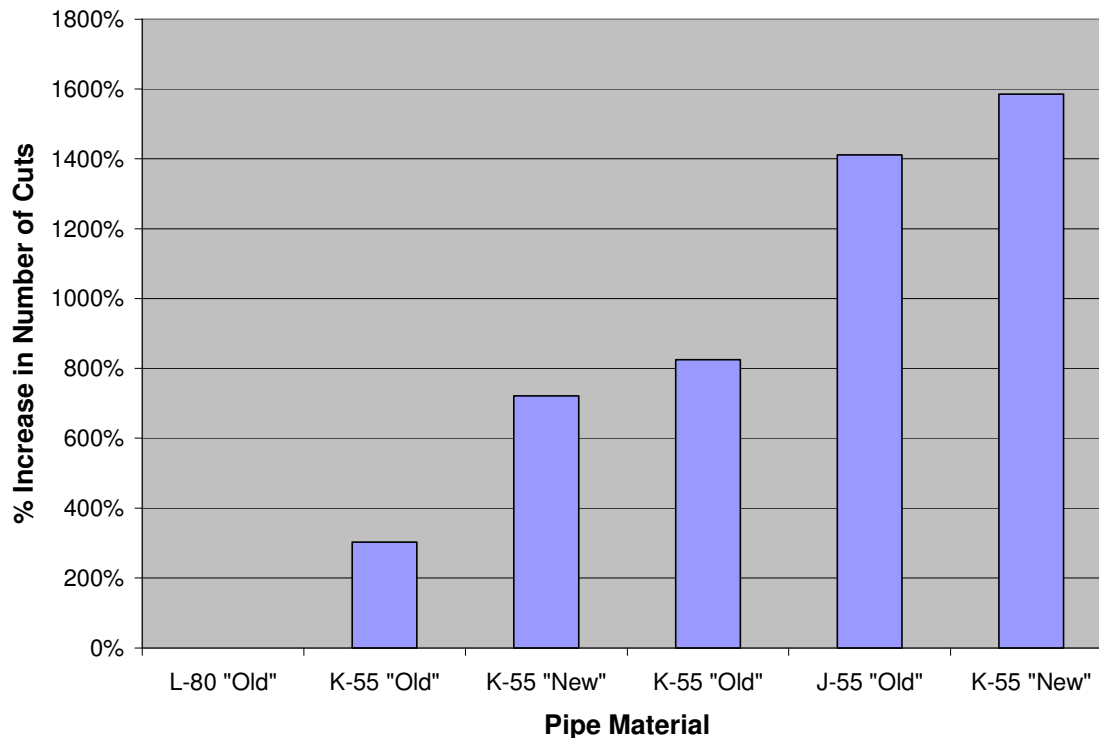


Figure 63 – Experimental results - Tool-life of a slotting blade and the machinability response.

Throughout the results of the testing, regardless of the cutting parameters, a relationship exists that the K-55 “NEW” pipe material is of the best to machine, with the J-55 “OLD”

and K-55 “OLD” heat materials interchanging between 2nd and 3rd. Therefore, the most logical approach or utilization of this machinability ranking for the K-55 “NEW”, J-55 “OLD”, and the K-55 “OLD” materials, is to maintain these results as the reference sets; used for comparison against other incoming pipe material and/or other testing criteria. An optimum cost controlling measure is to have one material pipe composition or grade for the majority of the pipe incoming for slotting. From the analysis of the testing results to date, this would most logically be a material grade or composition of similarity to K-55 “NEW” pipe.

Simplifying machinability, it can be assumed from a theoretical basis that machinability is mostly dependent on the pipe materials hardness and microstructure. Therefore, from our table of pipe material and heats, we can infer that the material with the lowest hardness and/or carbon content will have the best machinability rating, assuming proper geometric selection of the cutting tool. The higher the work piece hardness the lower the machinability and the shorter the tool-life because of heat generation and plastic deformation at the cutting edge of the tool (Milovic, 1983). As a general rule, tool wear rates increase in a consistent manner as the carbon content of the work piece is increased beyond 0.35% (Brunet, 1977). To minimize tool wear, for a given rate of production, it is important that steels are chosen which have the minimum carbon content consistent with the strength requirement of the finished product (Brunet, 1977). It is known that certain properties of the pipe material give advantages to machining and hence good machinability (low tool wear rate).

These properties are:

- 1) Low yield strength and low work hardening rate: A material with low yield strength and low work hardening rate give a lower cutting force and a lower contact pressure (machinability based on “the constant pressure tests”) resulting in lower cutting temperatures. This explains why some material can be cut at higher spindle speeds and others cannot.
- 2) High thermal conductivity: A high thermal conductivity assists heat flow away from the secondary shear zone and tertiary shear zone (tool-chip contact area and flank-material contact areas).
- 3) Low chemical reactivity with the tool or atmosphere: The material should not react chemically with the tool or the atmosphere since this can cause tool wear by either low strength tool material alloys being formed or abrasive work piece alloy particles being formed.
- 4) Low fracture toughness: A low fracture toughness contributes to easy crack formation and permeation, which results in a reduction in the difficulty of producing broken chips; long continuous chips are undesirable since they present problems of gullet entanglement, pressure and disposal.
- 5) Absent of unstable built-up-edge (BUE) forming: Unstable BUE formation causes poor surface finish, poorer dimensional accuracy of the machined pipe material and can contribute to the tool torque requirements and wear rate during the cut, as the BUE is breaking off. But, BUE can be helpful in increasing the tools tool-life if it is stable, by increasing the hardness of the rake face.

6) A satisfactory microstructure: Control and consistency of the pipe materials microstructure is particularly important on any pipe grade or hardness level, since it can be controlled, largely, through the pipe manufacturing process.

The relative machinability index is independent of the cutting conditions signifying tool-life differences with parameter changes but similar comparative tool-life trends. The “New” grade of pipe proved to help improve tool-life better than the “Old” grade of pipe. The difference between the “New” grade of pipe and the “Old” grade of pipe is that the “New” grade has been normalized and resulphurized. The manufacturing location seemed to contribute to variations in tool life regardless of “new” or “old” pipe classification. The material grade of pipe should be normalized to reduce hard spots and inclusions, and resulphurized to promote manganese sulphide (MnS) secondary phases. The carbon content should be between 0.30 and 0.33% - a carbon content value less than 0.30% decreases the pipe’s thermal conductivity and a carbon content value higher than 0.33% increases the pipe’s hardness; lowering tool-life. MnS inclusions promote micro fractures during cutting and help reduce cutting forces and torques, as long as the manganese content is greater than 1.00% to allow the sulfur to form MnS inclusions. Where machining conditions are less severe (medium to low cutting speeds using a high speed steel tool) the addition of calcium (Ca) can improve the machinability of steels killed with aluminum by reducing the abrasive effect of the alumina on the tool. (Brunet, 1977).

The chemical elements which influence a pipe's machinability are carbon (C), sulfur (S), phosphorus (P), nitrogen (N) and manganese (Mn) and silicon (Si) and aluminum (Al) if the steel has been deoxidized. Since bismuth (Bi) is closely related chemically and physically to lead (Pb), a prediction that bismuth might give rise to similar machinability properties as lead can be made. Bismuth in the presence of lead and sulfur give great improvement to the pipe's machinability. Bismuth does not affect the hot workability of the pipe, but may be costly, rare or have undesirable intrinsic properties. Selenium (Se) is a machinability enhancer and may be used as an elemental replacement for sulfur to counteract and avoid the inherent disadvantages of sulfur during the SAGD application, but also may be costly, rare or have undesirable intrinsic properties. Selenium and sulfur are most effective as single additives and when there is a limit to the % weight of 0.05% or less.

The optimum properties of the pipe material are to have a low chemical reactivity, low fracture toughness, low yield strength, consistent satisfactory microstructure and high thermal conductivity. Pipe K-55 "NEW" has most of the above stated properties required for full benefit of tool-life improvement. References should be made to the K-55 "NEW" pipe material when assessing the relative machinability of incoming pipe material heats. The most precise machinability test is the tool-life tests, but they are time consuming and costly. An easier but less precise machinability assessment is to relate the pipes hardness, microstructure, chemical composition, mechanical characteristics and carbon content to tool-life. The optimum tool-life predictability, reduction in tool-life variation between

different heats of pipe and cost effectiveness is to maintain consistent pipe material properties or a single heat for the incoming pipe material to be slotted.

Tool-life is greatly controlled by the blades fracture toughness, hardness and hot hardness. Blade dynamics and machinability are complex phenomenon which need strict testing guidelines for validity and are highly specific to the slotting machines tested on. Further study is required to fully comprehend Taylor's equation and its effectiveness in selection of parameters for the slotting industry. The tool-life data should be mathematically interpreted and statistically analyzed and the blade dynamics should be modeled and calculated for effective data interpretation, prediction and analysis.

It is clear that machining behavior or machinability is complex and cannot be meaningfully evaluated by a single test method. It is understood that machinability index identification may be difficult to quantify, correlate and transfer to a commercial slotting operation/machine from a test apparatus, and a good confidence indication or transferability of machinability of the pipe, based on machining and non-machining tests, may not exist or be easily identifiable. If a relationship exists and can be transferred to a commercial scale, then a conglomeration of machining and non-machining tests are required for relational significance of the ranking order of pipe materials, which may be costly and unrealistic.

Tool-life tests, although costly and laborious, can be useful in predicting tool-life of similar pipe material under similar sets of cutting conditions, as can metal removal rates,

and power requirements/consumption. But these cannot be regarded as evaluations of machinability for a whole range of operations, pipe or cutting conditions encountered, due to the data results of the relative machinability index being specific to a particular machining operation and/or test parameter setting. As a condensed rule, controlling the microstructure (process of manufacture which promotes coarse ferrite or ferrite-pearlite microstructure and little-to-no martensite/bainite microstructure) and the chemical composition (specifically sulfur content) helps increase the machinability index of a pipe material grade.

6.3.9 New OTCG Chemical Tolerance

Mill certifications (heat numbers), material composition and manufacturing processes are known and create a unique identifier. The material behavior is studied and represented in the mill certifications. A clear representation of the machining behavior estimates can be conducted based on the chemical composition. A relative machinability index is obtainable by key chemical elements and or alloys present in the pipe and their respective percentage content. An acceptable/optimum range based on the chemical composition is depicted below in Table 14.

Table 13 - New K-55 pipe chemical composition.

<i>% Composition</i>											
	Material Grade	Carbon (C)	Manganese (Mn)	Molybdenum (Mo)	Aluminum (Al)	Silicon (Si)	Titanium (Ti)	Chromium (Cr)	Nickel (Ni)	Boron (B)	Vanadium (V)
Min.	K-55	0.30	1.0	0.05	0.00	0.3	0.001	0.02	0.01	0.0000	0.000
Max.	K-55	0.33	1.3	0.10	0.01	0.5	0.010	0.05	0.05	0.0001	0.001

<i>% Composition</i>									
	Niobium (Nb)	Tin (Sn)	Copper (Cu)	Calcium (Ca)	Nitrogen (N)	Phosphorus (P)	Sulfur (S)	Bismuth (Bi) to replace Lead (Pb)	Selenium (Se) to replace Sulfur (S)
Min.	0.000	0.006	0.08	0.0015	0.003	0.010	0.010	0.05	0.05
Max.	0.001	0.009	0.12	0.0030	0.009	0.015	0.015	0.10	0.10

From Table 14 the elements and/or alloys color coded in yellow are controlled elements during manufacture – increasing amounts of the yellow color coded elements will increase hardness of the pipe, decreasing the machinability, with % carbon content having the greatest increase in hardness and decreasing degrees of hardness with the other elements color coded as yellow. The elements/alloys color coded in blue are uncontrolled elements which also contribute to the hardness and strength of the pipe, which decrease machinability. The elements which are not color coded, in varying ways contribute to the pipe’s characteristics which help improve the machinability of the pipe.

The two largest factors improving machinability are sulfur (S) and phosphorus (P). Although, increasing the sulfur content can be an issue for brittle pipe formation or embrittlement in the presence of H₂S gas, a possible alleviation to the “freed” sulfur and grain boundary “cracking” during high pressure and high temperature steam injection, typical with SAGD applications, might be controlled by the content of manganese (Mn). Manganese (Mn) content greater than 1.0 % will allow for stable MnS (type I and II) inclusions to form, which help improve machinability of the pipe and providing stable bonding of the sulfur element. With the increase of sulfur content care must be taken during the hot rolling process to not allow for embrittlement formations. The rolling process dictates the particular orientation (generally elongated) of the MnS inclusions in the pipe. MnS inclusions help improve the machinability of the pipe by promoting chip formation, promoting discontinuous chips during cutting, reducing cutting temperature and tool wear.

The minor element (MnS) is called a secondary phase and acts to improve the machinability index of the pipe through micro fracture promotion of the weak manganese sulfide inclusion. It is estimated that the manganese (Mn) content of the pipe must be high enough (> 1.0 % by weight) to ensure that all the sulfur is present in the form of manganese sulfide (MnS). From the information we do have, on the pipe elemental breakdown (mill certificates), we see that most of the received pipes have a minimum manganese content greater than 1.0% by weight, except for heat number 96801. This could be a limiting factor to why 96801 pipe material was not a good machining pipe.

The re-sulfurization and normalization of the pipe K-55 “NEW” help to ensure that the MnS inclusions and sulfur are present in high quantities and that during the normalization process of these pipes, the hard spots are reduced or eliminated. Certainly the presence of the sulfide [MnS] reduces the temperatures in high-speed steel tools (Trent, 1977). Control of the manganese particle shape, size and distribution can be achieved during the pipe making process. It is controlled and influenced by de-oxidation of the molten steel (liquid form) and by the hot rolling process during the pipe making process. If widespread use could be made of the de-oxidation practice employed in making those steels, at present available, which contain inclusions conferring good machinability, this would be a great advantage to machinists in terms of consistently high rates of metal removal in high speed cutting (Trent, 1977). Whether or not the ‘special de-oxidation’ practice can be generally adopted, it is certain that there is scope for adjustment of steel making practice to produce steels capable of more consistent performance during machining at high rates of metal removal, without resorting to the addition of large percentages of sulfur (Trent, 1977).

The presence of MnS inclusions promotes micro fractures which result in reduced cutting tool energy (power) requirements, lower tool forces and thinner chips; machinability is ranked as easier to machine with MnS inclusions present in the pipe material. The contact length on the rake face is shortened by the presence of MnS. Separation of the chip from the tool, to which it is bonded, requires fracture, and the weak interfaces between the sulfide ribbons and the steel form nuclei for this fracture (Trent, 1977).

Microstructure tests are not easily conducted and require specialty equipment and experienced staff to perform and make use of the information.

Phosphorus (P) is generally regarded as an undesirable impurity in the pipe due to its embrittling effect and for this reason, according to 5CT API Specifications, is limited to a maximum content of 0.030%. It increases machinability and resistance to atmospheric corrosion, hardness and strength, much akin to carbon, but it decreases ductility and toughness (impact strength).

Another element which can be added to improve the machinability is Selenium (Se). Selenium (Se) has similar chemical and physical properties to sulfur (S). With the addition of Selenium (Se) there is a modification to the shape of the MnS inclusions. Due to selenium (Se) having similar chemical and physical properties to sulfur, investigation whether this element can be used to replace sulfur, to maintain sulfurs machinability characteristics and to reduce the effects of brittleness with H₂S gas under high pressure and temperature, needs to be conducted. Calcium (Ca) is also referred to as a good machining element because it:

- 1) Treats the manganese sulfide inclusions to reduce the planes of weakness associated with MnS inclusions
- 2) Treats hard, angular, abrasive alumina inclusions in aluminum deoxidized steels, giving rise to calcium aluminate inclusions which are softer and globular thereby improving the pipe's machinability.

- 3) Acts as a deoxidizer and degasifier when added in the form calcium silicide.
- 4) Enhances ductility and toughness.

By adding calcium to the molten steel before casting we can convert the alumina inclusions (e.g. aluminum oxide), which are hard and abrasive and cause high tool wear, into calcium aluminate, often encapsulated by manganese sulfate help produce a lubricating effect for the tool tip improving machinability and tool life by the deformation of the inclusions when struck.

Other elements general characteristics are described below. Carbon (C) increases strength and hardness of the steel, with an increase of carbon content increasing tensile strength while decreasing ductility and weldability. Carbon content below 0.3% is synonymous with a high ductile material creating high built-up edges on the tool; cutting speeds should be low to prevent tearing and dragging of the metal during cutting, and heat generation. A carbon content greater than 0.33% constitutes a hard and brittle pipe, which is more difficult to machine.

Titanium (Ti) can cause work hardening, and give rise to a finer grain size. Boron (B) is hard and brittle and should be kept to a minimum or to zero due to it forming hard carbides, negative to machining. Chromium (Cr) improves corrosion resistance and at elevated temperatures resists oxidation, but is hard and reduces tool life and machinability, and increases hardenability and provides wear and abrasion resistance in the presence of carbon. Chromium also promotes carbide formations which have a

detrimental effect on machining. Copper (Cu) does not significantly affect the mechanical properties of the pipe but increases the pipes resistance to atmospheric corrosion – at elevated temperatures it can cause brittleness in the steel negatively affecting the surface quality. Molybdenum (Mo) is an alloy which increases the pipes hardenability, can reduce the risk of temper brittleness and helps reduce corrosion. Nickel (Ni) increases the toughness, hardenability and tensile strength of the pipe without having a detrimental effect on the ductility. Nitrogen (N) forms nitrides and thus is applied to the case-hardening of the steel. Silicon (Si) acts as a machinability reducer and as a deoxidizer. Generally, killed steel has higher percentages of silicon. Tin (Sn) is generally regarded as an undesirable impurity in the pipe which gives rise to temper brittleness, but has good resistance to corrosion. Vanadium (V) creates a fine grain structure, and increases hardenability.

Free machining pertains to the machining characteristics of an alloy or pipe to which one or more ingredients have been introduced to produce small broken chips, lower power consumption, improve surface finish and increase tool life; among such additions are sulfur or lead to steel, lead to brass, lead and bismuth to aluminum and sulfur or selenium to stainless steels. Chromium, molybdenum and vanadium form stable carbides (negative for machining), which do not allow for hydrogen (H_2S gas wells with high pressure and temperature) to react with the carbides to form methane gases, which can rupture the pipe if high enough pressure is obtained. Increasing the chromium, nickel, phosphorus, copper and/or silicon content will improve the pipes corrosion resistance.

6.4 Discussion

Steam Assisted Gravity Drainage is extensively used and will continue to be extensively used to exploit the oil sands of the world and in particular one of the world's largest heavy oil and bitumen reservoirs in the world located in Alberta. The heavy oil and bitumen reservoirs of Alberta are mostly unconsolidated; therefore they require some form of sand control for the horizontal wellbore schematics. Slotted liners are the most prevalently used sand control screen in Alberta. They are low cost robust thermal liner systems which can provide "keystone" slots, called seamed slots, and the small slot width apertures necessary for optimal sand control.

PSD analysis and modeling can help determine the slot specifications in relations to the reservoir sand size present. A new analytical model has been developed to help more accurately estimate the optimum slot width specifications and has been used successfully in the laboratory and has translated well to the filed applications. The slot manufacturing or slotting is controlled by many factors but the feed rate (mechanical wear influential parameter) and the cutting speed (thermal wear influential parameter) are most important. The slotting blade is very important to control the quality of the slot as well as the economics of the slotted liner manufacturing. Taylor's Tool-life equation can be utilized to estimate the pipe material response to slotting parameters and the blades tool life.

The particle size distribution (PSD) or reservoir sand sieve analysis is a necessary reservoir parameter required for initially developing an optimal sand control slotted liner

slot width. In 1937-1938, C.J. Coberly had conducted physical laboratory tests on reservoir core sand to identify the optimal sand control according to the particle size distribution. Further work has been conducted by HYCAL/Weatherford Labs for SAGD and CSS specific exploitations, and B. Meza-Diaz (University of Alberta) for cold primary exploitation, so as to refine Coberly's testing protocol for specific reservoir fluid properties, which are affected by external parameters such as steam, condensation, water pH, temperature etc. The mobility of the wetting phase induces migration of fines and clays. The heavy oil and bitumen reservoirs of Alberta are typically water-wet, and with the injection of steam which condenses, the wetting phase quickly becomes mobile; thereby creating potential sand control issues and mobility of the fines and clays within the reservoir. The most problematic clay is smectite clay as they are swelling clays. Fortunately, smectite clays are not as prevalent in the oil sand reservoirs of Alberta. Kaolinite and illite are prevalent and deflocculation of kaolinite and migration of finger-like dendritic illite clays become problematic for optimal sand control. Therefore, careful consideration of these problematic clays in the design of a slotted liner slot width and slot density should be taken.

Flow velocity to the slot is an important physical hydraulic parameter that needs to be carefully considered. All sand control screens induce a convergence skin factor as compared to a barefoot completion, which causes an increase in the flow velocity to the slot, thereby increasing pressure drops and creating a potential increase in the drag force coefficient that could cause failure of the sand in this convergence zone. This affects inflow performance and sand control. Open area is not a good measure to gauge the

convergence skin factor but slot density is. A higher slot density decreases the flow convergence skin factor to the slot, which is more beneficial for sand control and inflow performance.

Slotted liner manufacturing and slot cutting dynamics is complex and blade slot tests are sometimes difficult to translate into meaningful information which is transferable to machines. The process of slotting is one of an interrupted cut and is one of the most difficult machine dynamics of all machining. HSS blades of high hardness are used to effectively cut each slot. With any metal-to-metal cutting process, considerable heat is generated and the cutting tool must be harder and more resistant to deformation than the work piece. Also the work piece must not significantly work harden during the cutting process or difficulty in slotting will arise. Typically, stainless steel work hardens more than regular OTCG pipe of J-55, K-55 and L-80. Heat created in the cutting zone effects tool-life more than any other parameter and cutting speed directly influences the heat generation. For a given combination of work material and tool material, a 50% increase in speed results in a 90% decrease in tool-life, while a 50% increase in feed results in a 60% decrease in tool-life. A 50% increase in depth of cut produces only a 15% decrease in tool-life. (W. Knight, 2005). A triangular blade tooth form (DIN 1837-A) provides better tool-life than a curvilinear tooth form (DIN 1838-B), which is attributed to the land wear area as the blade wears out during slotting – curvilinear has more area to generate heat due to friction than the triangular tooth blade. The optimal slotting operational approach would be to lower the cutting speed or RPM of the blades and increasing the feed rate of the blades into the work piece. Work piece or pipe grade is of importance

here as with harder and higher tensile pipe, such as L-80 vs. J-55, their becomes a limit to the lowering of the RPM and increasing of the feed rate, as the fracture toughness corresponding tooth load of the blade, which is dependent on the blade material and width, may become too high for stable slotting/cutting.

Typical pipe grades such as K-55 and L-80 are used extensively in the SAGD operations of Alberta's heavy oil and bitumen reservoirs. Machinability varies widely from OTCG pipe grade, OTCG manufacturer and blade width. Relative material machinability tests can be performed to identify the optimal slotting parameters with a somewhat good transferability of results. The RMMI has identified that a normalized, re-sulphurized pipe provides improved machinability and tool-life. This is thought to be attributed to the formation of elongated sulphide inclusions in the form of manganese sulphide (MnS). These inclusions provide lubricity for the primary shear cutting zone, which may not get enough cutting fluid within this zone to reduce the coefficient of friction and provide cooling. An issue with re-sulphurization of OTCG pipe for use in-situ, is the potential for embrittlement and SSCC with the presence of H₂S. As little as 7% H₂S can become a potential issue for SSCC forming. API Specification 5CT and ISO 11960:2001, Petroleum and Natural Gas Industries – Steel Pipe for Use as Casing and Tubing for Wells, stipulates that a maximum of 0.030% content of sulphur within the OTCG grade pipe – particularly K-55. Slotting and blade tool-life can be improved by increasing the sulphur content of the pipe even by a little amount, which also is below the limit specified by API 5CT or ISO 11960:2001.

6.5 Conclusions

A properly designed cutting tool or slotting blade will have three distinct tool-life stages. The first one is the break-in region, the second is the steady state region and the third is the failure region. Taylor's Tool-life Equation has been successfully used to calculate and predict the optimum cutting speed or blade RPM and tool-life response based on similar cutting parameters for differing grades of pipe.

Mineral oil proved slightly better than a water-based cutting fluid based on mineral oil having a higher consistency of statistical tool-life results. The water-based cutting fluid showed a trend that with higher concentrations the tool-life increased. The mineral oil seemed to spread on the surface of the pipe better as well as the blade and this is thought to help reduce the coefficient of friction during the slotting process thereby directly reducing the heat generation which in turn increased the blade's tool-life. The testing seemed to show that it is better to reduce the spindle RPM as low as possible as this allows the blade to transfer its energy into slotting as opposed to transferring its kinetic energy into heat.

The greatest influence on machinability proved to be sulphur content. This was proved in the testing as well as in historical information. The pipe K-55 "NEW" had the highest sulphur content out of any other pipe grade tested. As well it had the highest carbon equivalent and one of the lowest hardness. The tool-life was recorded to be as high as 1600% more than material L-80. The microstructure as well as the hardness seemed to

play a role in the machinability differences. Also, the K-55 “NEW” pipe was normalized and re-sulphurized, which helped improve the machinability of the pipe. The best non-machining test for machinability is the microstructure test. A 50% or more microstructure content of ferrite increases machinability as this is a soft and ductile constituent. Pearlite is a hard microstructure, which reduces machinability of the pipe. Increasing carbon content increases the pearlite microstructure forming which in turn increases the hardness of the pipe. Testing has proven that the hardness of the pipe directly influences the machinability of the pipe. Bainite and martensite decrease the pipes machinability but coarse pearlite-ferrite microstructure increases the pipes machinability. Hardness showed a good trend as the hardness is linked to the microstructure.

Carbon equivalent did not correlate easily to machinability as it is thought that the sulphur and phosphorus were in quantities too low when compared to the carbon content, but when low carbon steel and higher sulphur and phosphorus are present then the carbon equivalent correlation is trendable.

The pipe's grade has somewhat of a bearing on machinability as J-55 has a lower tensile strength than K-55 which has a lower tensile strength and yield strength than L-80 pipe grade material. But the chemical composition that has higher sulphur content will generally prove to have a higher machinability. When manganese (>1.0%) content in the pipe coupled with sulphur in the pipe forms and promotes MnS inclusions that are elongated in structure when a seamless pipe is being pierced, rolled and stretched. MnS

inclusions, although is a hard constituent, is encapsulated in sulphur and during the machining process enhances the machinability by allowing crack propagation around the weakly bonded sulphur thereby reducing the work required to create a chip, slot or to machine the pipe. A new grade of K-55 pipe, that has a tighter tolerance of the 17 elements that make up the chemical composition of a typical OTCG pipe, has been identified which would fall within API standards for chemical composition as well as pipe integrity while providing for better machinability and slotting. One concern is the higher phosphorus and particularly the higher sulphur content. Although this content is still below the API specifications, the higher sulphur content could give rise to pipe integrity issues during the thermal operations of the SAGD well pair, as hydrogen sulphide can be easily present in the reservoir. Higher sulphur content in the pipe coupled with a high propensity for H₂S to form and be present in the reservoir of a SAGD well, increases the sulphide stress cracking (SSC) which is a form of hydrogen embrittlement. Also, high Temperature Hydrogen Attack can become more of an issue with a higher sulphur content pipe and thermal exploitation such as SAGD.

Machinability ranking is difficult to quantify and correlate amongst trends and transferability of results to differing machining parameters.

CHAPTER 7: CONCLUSIONS AND RECOMMENDATIONS

The conclusions of the research documented in this thesis are as follows:

- 1) Seamed slotted liners are preferred over straight slotted liners specifically for the producer wellbore of a SAGD process, due to the “keystone” profile of the slot, which provides a reduction in the plugging potential of sands, fines and clays within the slot.
- 2) The slot width model developed, which is based on the analysis of the reservoir PSD's can be very effective to identify and select a reservoir specific slot width for sand control.
- 3) As an arbitrary but effective rule, when the clay content ($\sim 5 \mu\text{m}$ particle size from the PSD) plus the fines content ($\sim 44 \mu\text{m}$ particle size from the PSD) is greater than 5.5% then a seamed slot is recommended.
- 4) There are two types of plugging that impact production in-situ: pore space plugging and sand screen (or slot) plugging. The near wellbore pore space geometry is influenced by the slot width and the $1/3^{\text{rd}}$, $1/7^{\text{th}}$ rule of producing fines (a particle which is $1/7^{\text{th}}$ of the slot width) to arching over the slot (a particle which is $1/3^{\text{rd}}$ of the slot width) creating a pore geometry which must allow free unabated flow of the fines and clays through this pore space. Particles of $\sim 44 \mu\text{m}$ and less should be produced through the pore space and the slot and from pore space geometry and the $1/3^{\text{rd}}$ rule; the slot should not be less than 0.012”.

- 5) The optimal slot density depends on the length of the wellbore, production rate variability, plugging effects, and phases produced. From observations of slotted liners, the optimal slot density, SD_{opt} , at a given liquid production rate for a minimum flow velocity and volume of fluid to the slot: $SD_{opt} = 0.505 \frac{qJ_L}{VLS_L}$.
- 6) There is an identifiable limit to a slot width being too large where no sand control is being sustained and a slot width which is too small where too much sand control is being maintained thereby inducing a higher propensity for pore space plugging of fines and clay particles.
- 7) An LPSA can be modified to simulate a wet/dry sieve analysis which is better for estimating the required slot width for sand control by re-calculating the retained weight or the percentage of particles measured for that size range and re-establishing the cumulative % for the range of sizes above 44 microns.
- 8) A reasonably high confidence model can be built around analyzing the PSD's for slot width sand control requirements that are specific to the reservoir sand intervals. This take into consideration the D10, D40, D50, D70, D90 and D95. The use of the D70 is a new development and can give an indication of the minimum slot width required for a particular sand.
- 9) When $ASW4$ converges on either $ASW1,2$ or 3 then a higher confidence in that selected slot is generated. If they do not converge then a review of the UC and the MaxSW and the MinSW will help in determining the slot width required for sand control. Also, the standard deviation is important to review for each SW.

- 10) The *PS* used to estimate the size of the slot that would be required to allow the 44 micron particle or less through the pore (based on the 1/3rd bridging rule and the 1/7th rule of production).
- 11) There is a trade-off between cutting speed and feed rate during the creation of a slot with a metal blade. Higher cutting speeds increase the thermal wear rate of the tool while reducing the mechanical wear rate of the tool and vice versa. There is an optimum combined feed and speed for every width of blade and in accordance to the material grade being slotted.
- 12) A pipe's microstructure is the single most important factor in identifying the machinability of the pipe. Two entirely different microstructures of a similar pipe grade can have the same hardness but give different machinability ratings.
- 13) The most important property of any cutting tool is that it retains its hot hardness. Hot hardness is central to resisting tool abrasions and wear resistance in respect to chemical solubility between tool-material interfaces.
- 14) According to Taylor's Tool-life Equation, ($C = vT^n$) tool life is inversely and exponentially proportional to cutting speed. From the testing and this equation the trend of materials grades to slot and the tool-life could be quickly identified.
- 15) The carbon equivalent percentage was calculated and used as a measure and predictor of the machinability of the pipe with little effectiveness. Testing proved that the carbon equivalent cannot be used to predict the machinability of the pipe.
- 16) A pipe with higher sulfur content or a pipe which has been normalized and resulfurized proved easier to machine than a pipe which was not; increased the machinability of the pipe. Also, the coarser the pearlite-ferrite microstructure

was, the easier the pipe was to machine. If martensite formed within the microstructure than the pipe was very difficult to machine.

- 17) The presence of sulphide inclusions and the absence of aluminates and oxide inclusions proved beneficial to machining. The greatest factor controlling the machinability is the sulfur content (higher the better) along with the microstructure. A coarse, banded pearlite-ferrite microstructure and a microstructure with a higher amount of pearlite-bainite phases with equiaxed ferrite seemed to improve the machinability of the pipe. A fully untempered bainite microstructure is detrimental for the machinability.
- 18) Machinability of the pipe is largely controlled by the combination of optimal microstructure (process of manufacture) and chemical composition (specifically sulfur content). Also seamless pipe, which is pierced and elongated, may be better at forming elongated/stretched MnS inclusions than electric-resistant welded pipe, benefiting machining/slotting. The RMMI has identified that a normalized, re-sulphurized pipe provides improved machinability and tool-life.
- 19) Cutting torque data could not be extrapolated to identify the torque requirements and tool-life for many cuts and the maximum number of cuts for a set of cutting conditions.
- 20) Bismuth and Selenium may be used to replace the similar machinability properties of sulphur and lead to reduce the potential concerns with sulphur and lead as elements in the pipe. Bismuth and Selenium may not be an economic alternative and should be explored further for suitability.

The recommendations arising from the results of the research documented in this thesis are as follows:

- 1) A computational fluid dynamics study should be done to understand the nature of the flow through slotted liners and the flow both upstream and downstream of the slots.
- 2) A particle image velocimetry study should be done to visualize and understand the flow both upstream and downstream of a slot and to examine in more detail arching and plugging behaviour at the slots.
- 3) Flow testing of core against selected ranges of slot widths from the slot width modeling program will give rise to calibration of the model and/or verification of model assumptions, values and calculations.
- 4) A detailed review and laboratory simulation and visualization of flow convergence into a slotted liner, based on slot density and reservoir parameters, should be focused so as to understand the dynamics of flow and pressure loss on a slot without plugging and a slot which has been plugged with sand, fines and clay particles.
- 5) Design and flow test to identify the optimal outer and inner diameter slot width differential for primary and secondary sand control as well as to provide a higher confidence on anti-plugging characteristics of the slot.
- 6) Field data is imperative to the final calibration of the slot width modeling program and this provides the ability to expand on the program to include flow dynamics and pressures.

- 7) Conduct laboratory flow testing to identify the slot plugging relationship to clay content, clay type, grain size distribution, uniformity coefficient and the larger sand particles.
- 8) Flow test to verify that the $1/3^{\text{rd}}$ and $1/7^{\text{th}}$ rule from the gravel packing theory could effectively apply to build a relationship between slot width and particles arching or producing through the pore space geometry as well as the suggestion that the minimum slot width should not be less than 0.012" (~300 μm).
- 9) Conduct blade tests to determine the machine dynamics and how different vibration types influence the slotting process and performance.
- 10) Research the potential for replacing sulphur and lead with bismuth and selenium from a chemical composition, a mechanical and an economic standpoint. Conduct blade tool-life tests to verify this new composition/grade of pipe's machinability.

BIBLIOGRAPHY

Ballard, T. J., & Beare, S. P. 2006. Sand Retention Testing: The More You Do the Worse It Gets. Paper SPE 98308 presented at the International Symposium and Exhibition on Formation Damage Control Conference, Lafayette, Louisiana, 15-17 February.

Bennion, B. 2009. Formation Damage and Multiphase Flow in Porous Media. Lecture notes on ENCH 619, University of Calgary - Schulich School of Engineering, Calgary, Alberta.

Bennion, D. B. 2002. *Improving Well Productivity by Evaluating and Reducing Formation Damage Causing Overbalanced and Underbalanced Drilling Operations*. Calgary, Alberta: The University of Alberta.

Bennion, D. B., Gittins, S., Gupta, S., et al. 2008. Protocols for Slotted Liner Design for Optimum SAGD Operation. Paper SPE 2008-186 presented at the Canadian International Petroleum Conference/SPE Gas Technology Symposium 2008 Joint Conference, Calgary, Alberta, 17 – 19 June.

Blair, Terence C. and McPherson J. G. 1999. Grain-size and Textural Classification of Coarse Sedimentary Particles. *Journal of Sedimentary Research* **69** (1): 6-19.
<http://dx.doi.org/10.2110/jsr.69.6>.

Boboulos, M. A. 2010. *Manufacturing Processes and Materials: Exercises*. Ventus Publishing ApS, ISBN: 978-87-7681-695-7

Brunet, J. 1977. *Machinability Improvement by Inclusion Control Influence on Mechanical Properties of Steels*. Ohio, USA: American Society for Metals.

Chalaturnyk, R. J. 1996. *Geomechanics of the Steam Assisted Gravity Drainage Process in Heavy Oil Reservoirs*. PhD dissertation, University of Alberta, Edmonton, Alberta (April 1996).

Chalaturnyk, R. J. and Li P. 2005. *Geomechanical Model of Oil Sands*. Paper SPE 97949 presented at the 2005 SPE International Thermal Operations and Heavy Oil Symposium, Calgary, Alberta, 1-3 November.

Clays, E. E. 2010. *Clay Chemistry & The Mystery of Healing Clays*. Eyton's Earth: <http://www.eytonsearch.org/clay-chemistry.php> (accessed 10 March 2011)

Carmeuseis 2011. *Sand, Gravel and Proppant*. www.carmeuseis.com/sand_gravel_design.pdf (accessed 10 March 2011)

Gates, I. D. 2006. *Basic Reservoir Engineering*. Lecture notes on ENPE 523, University of Calgary - Schulich School of Engineering, Calgary, Alberta.

Government of Alberta, E. 2009. Oilsands 101.

<http://www.energy.alberta.ca/OilSands/1715.asp> (accessed 27 February 2011)

Halliburton 2011. Products & Services - Wire Wrapped Screens.

<http://www.halliburton.com/ps/wws> (accessed 28 February 2011)

Isehunwa, S. and Farotade, A. 2010. Sand Failure Mechanism and Sanding Parameters in Niger Delta Oil Reservoirs. *International Journal of Engineering Science and Technology*. **2** (5): 777-782. <http://dx.doi.org/1350712>.

Jean-Louis Bantignies, C. C. 1997. Clays and Clay Minerals. *Geo-Science World* **45** (2): 184-193. <http://intl-ccm.geoscienceworld.org>

Johnston, N. 1955. Role of Clay in Oil Reservoirs. *Clay Technology in the Petroleum Industry*. Bull. 169: 305-312. <http://www.clays.org/journal/archive/volume%201/1-1-306.pdf>

Kasier, T. M., Wilson, S., and Venning, L. A. 2000. Inflow Analysis and Optimization of Slotted Liners. *SPE Drilling & Completions* **17** (4): 1-12. SPE 80145-PA. <http://dx.doi.org/10.2118/10.2118/80145-PA>.

Knight, G. B. 2005. *Fundamentals of Machining and Machine Tools*. Slovakia: Taylor & Francis.

Larter, S., Adams, J., Bennet, B. et al. 2006. The Controls on the Composition of Biodegraded Oils in the Deep Subsurface. SPE 2006-045. Presented at Canadian International Petroleum Conference, Calgary, Alberta, 13 – 15 June.
<http://dx.doi.org/10.2118/2006-045>

Leet, L. D. 1982. *Physical Geology*, 6th Edition. Englewood Cliffs, NJ: Prentice-Hall.

McRory, R. E. 2010. *Oil Sands Fact Sheet*. Oil Sands Discovery Center
http://www.oilsandsdiscovery.com/oil_sands_story/pdfs/oilsands.pdf (accessed 10 March 2011)

Meza-Diaz, B., Tremblay, B. and Doan, Q. 2002. Mechanism of Sand Production Through Horizontal Well Slots in Primary Production. *Journal of Canadian Petroleum Technology*, **42 (10)**: 36-46. SPE 03-10-04. <http://dx.doi.org/10.2118/03-10-04-PA>

Mills, B. 1983. *Machinability of Engineering Materials*. London: Applied Science Publishers Ltd.

Milovic, R. 1983. *The Machining of Low Carbon Free Cutting Steels with High Speed Steel Tools*. Ohio: American Society for Metals.

Sweeny, G. 1971. *Vibration of Machine Tools*. New York: The Machinery Publishing Co. Ltd.

Trent, E. M. 1977. *Metal Cutting*. Canada: Butterworth & Co. Ltd.

Tronvoll, J., Larsen, I., Li, L., et al. 2004. Rock Mechanics Aspects of Well Productivity in Marginal Sandstone Reservoirs: Problems, Analysis Methods and Remedial Actions. Paper SPE 86468 presented at the SPE International Symposium and Exhibition on Formation Damage Control, Lafayette, Louisiana, 18-20 February.
<http://dx.doi.org/10.2118/86468-MS>.

Weatherford 2011. Sand Production Weatherford EP-Solutions. http://www.ep-solutions.com/Solutions/Consult/Sand_Production.htm (accessed 28 February 2011).

Wentworth 1922. Udden-Wentworth Grain-size Classification Scheme.

Wong R. C. K. 2003. Sand Production in Oil Sand Under Heavy Oil Foamy Flow. *J. Cdn. Pet. Tech.* **42** (3). SPE-03-03-06. <http://dx.doi.org/10.2118/03-03-06>.

Wong R. C. K. 2001. Strength of Two Structured Soils in Triaxial Compression. *Int. J. Numer. Anal. Meth. Geomech.*, **25** (2): 131-153. SPE-03-03-06. <http://dx.doi.org/10.1002/nag.122>.

Wong R. C. K. and Du J. 2010. Numerical Modelling of Geomechanical Response of Sandy-Shale Formation in Oil Sands Reservoir During Steam Injection. *J. Cdn. Pet. Tech.* **49** (1): 23-28. SPE-132638-PA. <http://dx.doi.org/10.2118/132638-PA>.

Wong R. C. K. and Yeung K. C. 2002. Borehole Stability in Oil Sands Under Drilling. *J. Cdn. Pet. Tech.* **41** (1). SPE-02-01-05. <http://dx.doi.org/10.2118/02-01-05>.

Xiang W. and Wang P. 2003. Application of Bridging Theory on Saucier Gravel to Examine the Sand Control Effect. Paper SPE 80450 presented at the SPE Asia Pacific Oil and Gas Conference and Exhibition, Jakarta, Indonesia, 9-11 September. <http://dx.doi.org/10.2118/80450-MS>.